A study of geo-chemical problems by gas-analytical methods

Reasbeck, Philip

Acknowledgements

I wish to express my thanks to Professor F.A. Paneth, F.R.S., under whose direction this work has been carried out, for his invaluable advice and many useful discussions.

I also wish to express my gratitude to K.F. Chackett, B.Sc. Ph.D for his guidance and expert help during the first two years of this work.

I wish to thank Mr. G.R. Martin, B.Sc. A.R.C.S. F.R.I.C. for his continued help and guidance with the theoretical interpretation of the results.

Appreciations are extended to Mr. L.M. Jones, of the University of Michigan, and his co-workers for their co-operation in the upper atmosphere work; to Dr. Clifford Frondel, of the University of Harvard Mineralogical Museum for the valuable specimens of "Carbo; to Dr. M.H. Hey, of the British Museum for several meteorite specimens, and to Dr. E. Hellner, of the Mineralogical Institute of the University of Marburg a.d. Lahn for the specimens of Treysa.

Finally, I would like to acknowledge with gratitude a Further Education and Training Grant for the first two years of the work, and financial assistance rendered later by the Gassiot Committee of the Royal Society.

Philip Reasbeck

" A STUDY OF GEO-CHEMICAL PROBLEMS BY GAS-ANALYTICAL METHODS "

+=+=+=+

T H E S I S

presented in candidature for the degree of

DOCTOR OF PHILOSOPHY

of the

UNIVERSITY OF DURHAM

by

PHILIP REASBECK, B.Sc.

+=+=+=+

The work described in this thesis was carried out in the Londonderry Laboratory for Radio-Chemistry, University of Durham, between October, 1949, and September, 1953, the first two years work being under the supervision of K.F.Chackett, B.Sc., Ph.D.

+=+=+=+

SUMMARY.

The thesis is concerned with two separate problems, but each problem involves the application of the same technique of micro-gas analysis, and the extraction, purification and measurement of micro-quantities of helium and neon is common to both problems.

Earlier work in the field of helium and neon analysis is briefly reviewed, and a full description of the modern helium apparatus is given in the last chapter.

The first problem involved the chemical analysis of upper atmosphere air samples from heights ranging between 50 kms. and 94 kms. obtained in the U.S.A. by means of V-2 and Aerobee rockets. These samples were analysed for their helium, neon, argon, nitrogen and oxygen contents. It has long been thought that, if a completely still region of the atmosphere exists, some diffusive separation of the lighter from the heavier gases ought to take place. In the present work, it was found that, in all the samples from above about 60 kms. height, a definite enrichment in helium and neon had taken place, while a deficit in argon was observed. In the case of the highest sample, the increase in the proportion of helium was nearly 300% compared with the proportion at ground level, the increase in the proportion of neon was 40%, and the decrease in the proportion of argon was 18%. At first sight, it seemed as if diffusive separation might have been proved, but a full consideration of all the available data does not confirm this view. The diameter of the

intake tube of each bottle was made large (3cms) compared with the mean free path of the gas molecules at the relevant heights, in order to avoid mass discrimination and effusive separation. However, it appears that a mathematical treatment based on an effusive separation process having taken place in the neck of the bottle gives a much better fit to the observed results than a treatment based on a diffusive separation process. The fact that the bottles did not even fill with air to the ambient pressure of the outside atmosphere during the 5 second sampling interval, let alone the much higher ram pressure, thus indicating that air must still have been flowing into the bottles at the time of sealing the intake tube, was the salient point in indicating that an effusive separation might be taking place, since the expected filling time should be about one-tenth of a second. It is possible that some aerodynamic "choking" of the intake tube at the supersonic speeds concerned has taken place. The conclusion must be drawn that there is no evidence to indicate any onset of a diffusive separation of the gases in the earth's atmosphere up to the highest point reached (94 kms) in these experiments.

The second problem was the investigation of the ^{3}He and ^{4}He content of iron meteorites, in order to determine whether cosmic radiation on meteorites in outer space produces any appreciable part of their helium content by disruption of the iron nuclei. Also, an investigation of several iron meteorites of varying sizes was undertaken in order to look for any variation in the helium content at different depths in the same meteorite, since

it is to be expected that the rate of helium production by cosmic radiation should decrease with increasing depth, that is, with increasing "absorber thickness".

The $^{3}He/^{4}He$ ratios, and the total helium content of fourteen different meteorites was determined. The "Depth Effect" was clearly demonstrated with the large meteorite "Carbo". A mathematical treatment of the theoretically expected helium production by cosmic radiation at varying depths in different sizes of iron spheres has been fitted to the results obtained, and found to be in good agreement. A theoretical treatment has also been fitted to the measured variation in the $^{3}He/^{4}He$ ratio with increasing depth in "Carbo". The final conclusion which can be drawn is that the major part of the helium in meteorites is produced by cosmic radiation, and, in conjunction with determinations of the uranium and thorium contents of the meteorites carried out in these laboratories, probable ages have been calculated by the "Helium Method". It seems that the maximum age of meteorites is very much lower than the previously accepted maximum age of 7000 million years, and, in fact, less than the present value for the age of the earth and of the universe.

+=+=+=+

I N D E X

CHAPTER I — Page.

Section 1 - Introduction. 1.

Section 2 - Historical Background. 2.

Section 3 - Introduction to the Modern Helium Apparatus. 4.

Description. 5.

Improvements in the Apparatus: 7.

CHAPTER 2. - Chemical Analysis of the Stratosphere.

Section 1 - Introduction. 9.

Section 2 - Method.

(a) Collection of Samples. (Undertaken in New Mexico, U.S.A. by the University of Michigan). 13.

(b) Analysis of Samples:

(i) Transfer of Air from Steel Bottles to Apparatus. 15.

(ii) Measurement of Amount of Air and therefore Pressure in Steel Bottle. 16.

(iii) Contamination Monitoring by Active Carbon Dioxide. 17.

(iv) Air pipette. 17.

(v) Estimation and Removal of Oxygen. 18.

(vi) Transfer, Fractionation and Measurement of Helium and Neon. 20.

INDEX (continued).

CHAPTER II (contd). Page.

(vii) Argon Determination. 22.

(ix) Sealing Off, and Retunn of Residue of Samples. 24.

Section 3 - Results. 24.

Section 4 - Discussion. 28.

Conclusion. 34.

CHAPTER III. - Helium Content and Age of Meteorites.

Section 1 - Introduction.

(a) The Origin of Meteorites. 36.

(b) Age Determination in Meteorites. 37.

(c) Recent Studies on the ^{3}He and ^{4}He content of Meteorites. 39.

Investigation No. 1 40.

Investigation No. 2. 40.

Section 2 - Experimental Procedure.

Measurements of Helium Contents for "Depth Effect" Investigation.

(a) Method of Dissolution and Removal of Bulk of Hydrogen. 41.

(b) Removal of Water Vapour and Remainder of Hydrogen. 42.

(c) Estimation of Helium. 43.

Section 3 - Investigation of "Depth Effect" with Treysa Meteorite. 45.

Investigation for "Depth Effect" with the available samples of Toluca (British Museum) and Toluca (Durham). 46.

INDEX (continued).

		Page.
CHAPTER III (contd)	Investigation of the "Depth Effect" in "Carbo".	48.
Section 4 -	Determination of ^3He and ^4He ratios in Meteorites.	
	(a) Method of Dissolution.	50.
	(b) Measurement of Helium Content.	51.
	(c) Transfer to Sample Tube, Addition of Carrier Gas, and Sealing Off.	51.
Section 5 -	Results.	
	(i) Clarendon Laboratory Spectrometer.	
	(a) Calibration Samples.	54.
	(b) $^3He/^4He$ Ratios in "Carbo" meteorites.	54.
	(c) $^3He/^4He$ Ratio in 14 Meteorite Samples.	54.
	(d) Neon Measurements.	55.
	(ii) Tritium Method.	56.
Section 6 -	Discussion of Results for "Depth Effect" in Carbo.	
	(i) Calculation of Cosmic Ray Production of Helium.	57.
	Evaluation of parameters in expression.	62.
	Interaction cross section of iron for protons and pi mesons.	64.
	Mean Yield of Shower Particles per Interaction.	64.
	Mean Number of Evaporation Particules per Interaction.	65.
	Conclusion.	70.

INDEX (continued). Page.

CHAPTER III (continued)

Interpretation of $^3He/^4He$ ratio Curves. 71a.

α Particle Interactions with Iron Nuclei. 76

Transfer to Spherical Body. 77

Conclusion. 80.

Investigation of the Helium, Uranium, and Thorium Contents of a Representative Range of Meteorites. 81.

Summary. 90.

CHAPTER IV.

Section 1 - The Helium Apparatus.

Introduction.

(1) Pirani Gauges. 91.

Calibration. 93.

Scale Calibration. 94.

(2) Separation of Helium and Neon and Purification from other Gases. 96.

Operating Procedure. 100.

(3) The Circulating System. 103.

(4) Production of Pure Oxygen. 104.

Section 2 - Specimen Experimental Calculation. 106.

INDEX (continued).

APPENDIX. Page.

Special Investigation of the Bethgelart Meteorite.

(a) Introduction. 109.

(b) Separation of Stone and Iron Phases. 110.

(c) Helium Determination on Iron Phase. 111.

(d) Helium Determination of Stone Phase. 111.

Results. 112.

Explanation of Figure 34. 115.

Summary of Results. 116.

BIBLIOGRAPHY: 119.

+=+=+=+=+

CHAPTER I.

Section I. - Introduction.

The basic operation involved in the problems investigated during work for this thesis is the extraction, purification, and measurement of extremely small quantities of helium, usually of the order of 10^{-7} ccs. to 10^{-6} ccs. In one problem, small quantities of neon and argon were also measured.

The first investigation was concerned with the helium content of meteorites, firstly, in conjunction with uranium and thorium measurements, to determine the ages, or to check previous values and, secondly, to clarify the position with regard to the possible production of helium in meteorites by cosmic rays.

Two methods of investigation were tried. The first was to find out if any ^3He was contained in meteoric helium samples, since it was expected that ^3He as well as ^4He would be among the products from iron nuclei disrupted by cosmic radiation. The second was to look for any decrease in helium content with increasing depth below the surface of meteorite samples, since it was expected that the cosmic ray flux would decrease with increasing absorber thickness.

The second problem was the analysis of stratosphere air samples obtained in the U.S.A. by means of V2 and Aerobee rockets at altitudes up to 100 kms. In this case, the percentages of helium, neon, argon, nitrogen and oxygen were determined, in order to investigate the possibility of gravitational separation

of these gases in the earth's atmosphere.

The earlier work in these two fields is briefly reviewed.

Section 2 - Historical Background.

In 1928, Paneth and his collaborators had constructed apparatus which, by spectroscopic means, was capable of detecting quantities of helium and neon down to 10^{-10}ccs (1). Briefly, all the gases present in air except helium, neon, and hydrogen, were adsorbed on charcoal cooled in liquid air. The hydrogen was then removed from the helium-neon mixture by burning it to water in a palladium furnace in the presence of excess oxygen, the remaining oxygen adsorbed on charcoal cooled in liquid air and the helium-neon mixture compressed in a McLeod gauge capillary tube, which served to measure the absolute amount of the gases. The proportions of helium and neon in the mixture were then determined by comparing the relative strength of the characteristic spectral lines, using the McLeod capillary as a spectroscope tube.

For determinations of meteoric helium the chief addition was that the larger quantities of hydrogen generated by acid dissolution of iron meteorites was mainly removed by heated calcium metal, the small proportion remaining then being treated in a palladium furnace. The accuracy of the method was such that about 10^{-7} ccs. of helium could be measured with an error of $\pm$ 50%. The method had several disadvantages, probably the

greatest being that the walls of the capillary tube and the mercury itself would soon become dirty due to the electrical discharge used to produce the spectral lines. Also, under the influence of a discharge, considerable quantities of hydrogen are driven out of glass under vacuum, and there is the danger of a large proportion of the helium and neon being "mopped up" due to the discharge driving them into the glass walls.

In 1930, a hot wire manometer (Pirani gauge) was first used to measure the helium and neon mixture instead of the McLeod gauge. The quantities of helium and neon mixture which were measured varied from 1×10^{-8} ccs. with an error of 50% to 1×10^{-4} ccs. with an error of 1%. (2)3).

Between 1939 and 1942, with about the same accuracy, more analyses were done on iron meteorites, and also the figures for the uranium and thorium contents of the meteorite samples were obtained. From these, by the "Helium Age Method", which is more fully explained later (Page 86), it was concluded that the age of the meteorite samples investigated fell between seven thousand million years and one hundred thousand years (4).

A Fractionation column for the separation of helium and neon was first constructed about 1939, and the amount of these gases then measured on a pirani gauge. With a much improved apparatus (5) Glückauf investigated the composition of ground level air by means of samples obtained from many parts of the world, and found that the proportions of helium and neon were geophysical

constants. From air samples taken by means of sounding balloons it seemed that a slight increase in helium content from heights between 20 and 30 kms. had been found, but in view of more recent results, this effect may probably be ascribed to helium being released from the glass walls of the sample vessels. By this time, the accuracy had also much improved, so that samples of 10^{-6} ccs. of helium and neon could be measured with an error of less than 1%. Usually, about 20 ccs. N.T.P. of an air sample were available for analysis.

In 1949, when two samples of stratosphere air from heights of 50 and 62 kms. were analysed on the same apparatus as that mentioned above, no difference in helium, neon or argon percentages compared to those at ground level were found (6)7).

Wilson also investigated the helium contents of several meteorites with the same apparatus in an endeavour to find if any variation in helium content existed with increase in depth from the surface of the meteorite. He found no evidence of this effect (8).

Section 3 - Introduction to the Modern Helium Apparatus.

For the sake of compactness in presentation, and ease of reading, a very brief description of the apparatus is given here, accompanied by a "block schematic" diagram, and a complete accoun of the design and operation of the apparatus is given in the last chapter.

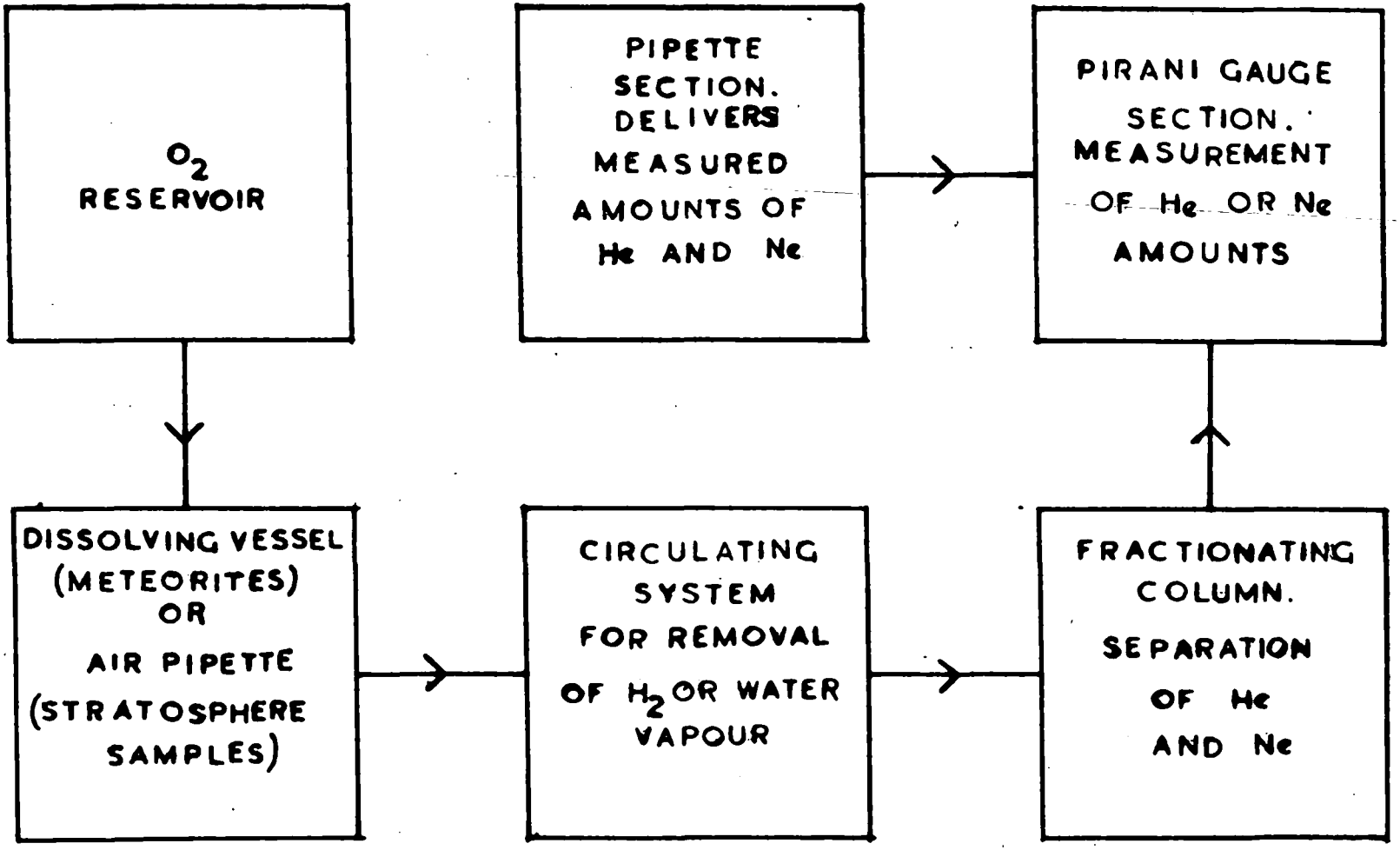

FIG. 1

BLOCK SCHEMATIC DIAGRAM OF APPARATUS

Description.

For meteorite work, the first section of the apparatus consists of a dissolving vessel, in which up to 10 grms. of an iron meteorite can be dissolved in potassium cupri-chloride solution, which has previously been freed from dissolved atmospheric gases, in order to release the helium from the iron. In stratospheric air investigations, this vessel is replaced by a pipette which will deliver accurately measured portions of the given air sample.

The pure oxygen carrier gas is stored in a reservoir, and is used to flush the extremely small quantities of helium to be measured from the dissolving vessel or air pipette, whichever is being used, into the circulating system.

The circulating system consists of a gas circulating pump, a palladium furnace, a water vapour trap, and a charcoal U-tube into which the oxygen can be adsorbed to facilitate the transfer of gases from the dissolving vessel past a non-return valve.

The palladium furnace removes any hydrogen which may be present (in excess of oxygen) from the dissolution of the meteorite, or from the air sample, and the water vapour present is trapped in the water trap. The remaining gases are then töplered into the fractionating column, which is designed to separate micro-quantities of helium and neon by a gas chromatographic method usøing hard nut charcoal cooled in liquid nitrogen.

The fractionating column consists of 15 such charcoal tubes, each containing about 0.8 grms. of charcoal, connected, in series by töpler pumps. The operation of the column has been made automatic. The oxygen carrier gas, along with any nitrogen or argon that may be present in the case of stratospheric air samples, is retained in the first charcoal tube. As the helium and neon are then töplered through the successive charcoal tubes, the two gases are separated, and the helium fraction, containing only about one half of one percent of neon, emerges from the end of the column first. The neon fraction can be obtained in a similar state of purity by further töplering.

The next section comprises the measuring arrangement. Two pirani gauges, one the measuring instrument and the other, exactly similar, but remaining under vacuum the whole time to act as a compensatory arm, form two arms of a Wheatstone net. The gauges are deeply immersed in liquid nitrogen for increased sensitivity and stability. The other two arms are formed by resistances, one fixed, the other variable to allow of adjustment When the helium or neon is admitted to the measuring gauge, the deflection of the galvonometer light spot on the scale gives a measure of the amount of gas present. Immediately after the unknown amount of helium or neon has been pumped out of the gauge an accurately known amount of helium or neon, according to which is being measured, is put into the gauge from a carefully calibrated pipetting system, and, from the observed galvonometer-spot deflection, the unknown amount of helium is measured absolutely.

For the argon measurements, the amount of an air sample is first measured in the air pipette. Then the oxygen, together with any traces of hydrogen, is removed by a heated copper spiral in the air pipette, and the remaining gas amount, containing nitrogen, argon, helium, neon, krypton and xenon, is re-measured to determine the decrease due to oxygen loss. These gases are then transferred into a barium furnace, where the nitrogen is removed as barium nitride by heating barium metal in the furnace to about 800°C. leaving the argon unaffected. The argon is then transferred to the McLeod gauge section by adsorption on charcoal cooled in liquid nitrogen, and the remaining helium and neon pumped off while the argon is retained on the charcoal. The amount of krypton and xenon present is so small as to be unmeasurable on this arrangement. The argon is then released, and measured in the McLeod gauge.

Improvements in the Apparatus.

(i) Accuracy and Reproducibility of Results.

While the accuracy of the results quoted in Chapters II and III of this thesis is about the same as that given by Glückauf for similar work (5), it should be pointed out that very much smaller amounts of air samples have been handled. Whereas Glückauf had amounts of air of the order of 10 to 20 ccs. N.T.P. available, helium and neon determinations have been carried out on air samples as small as 6×10^{-3} ccs N.T.P. in the present work, with little sacrifice in accuracy.

10^{-7} ccs. of helium or neon can be measured to an accuracy of better than 1%. 10^{-8} ccs. can be measured to an accuracy of 1 or 2%.

The volume of the fractionation column was made smaller, and the number of units increased from twelve to fifteen in order to improve its efficiency in separating helium and neon.

The pipetting system which delivers accurately measured amounts of helium and neon to enable the pirani gauge to be calibrated during each experiment was entirely re-designed, the range of volumes which it would deliver was increased, and its accuracy much improved.

(ii) Speed of Operation.

The fractionating column was made automatic in order to save the time previously devoted to manual operation, and allowed other work to be carried on in the interval. Distinct improvement was achieved in the dissolution of meteorite samples, in that quantitative dissolution was achieved, and that, whereas, with the potassium cupri-chloride reagent, 36 hours were taken for dissolving 20 gramme samples of iron meteorites (9), in the present work the same weight of meteorite could be dissolved in 5 to 10 minutes. The pirani gauge was also modified so that the filament which had previously been fixed was now demountable for repair, removing the necessity of making an entirely new gauge.

(iii) Convenience.

Finally, the apparatus was built so that all the separate sections were brought together in one unit, in order to facilitate ease and accuracy of handling.

+=+=+=+

CHAPTER 2.

Chemical Analysis of the Stratosphere.

Section 1 - Introduction.

Investigations into the chemical composition of the Earth's atmosphere began nearly two centuries ago, and the names of many great chemists, Scheele, Priestly, Lavoisier, Cavendish, Gay-Lussac, to mention only a few of the earliest ones, have been linked with this work. Since the beginning of this century, it has been realised that we have to distinguish at least two different regions of the atmosphere, and probably more.

The composition of the lower region, the troposphere, in which all meteorological changes take place, is well established and uniform with the exception of water vapour. The only changes are minor and local, such as withdrawal of oxygen by plants, animals and industrial activities, emission of carbon-dioxide by plants, and other gases by factories.

However, the main fact of tropospheric chemistry is the uniformity of composition of dry air all over the earth's surface [5], and the constituents are given in Table 1.

TABLE 1.

Gas.	% in air by vol.	Density. (air = 1.000)	Mol.Wt (O=16)
Nitrogen.	78.09	0.967.	28.016.
Oxygen.	20.95	1.105.	32.000.
Argon.	0.93	1.375	39.444
Carbon-dioxide	0.03	1.529.	44.01.
Neon	1.82×10^{-3}	0.695	20.183.
Helium.	5.24×10^{-4}	0.138	4.003.
Krypton.	1×10^{-4}	2.868	83.7
Hydrogen.	5×10^{-5}	0.0695.	2.016.
Xenon.	8×10^{-6}	4.525	131.3
Ozone I	1×10^{-6}	1.624	48.000
Radon 11	6×10^{-18}		

I Variable ___ increasing with height.

II Variable ___ decreasing with height.

When it was first observed that, above about 11 km.height, (in our latitudes) the temperature remains steady at about 219°K(-54°C) with increasing height, it was supposed that no large scale mixing could occur in such a region without temperature gradient, and the supposedly calm layer was called the stratosphere. We now know that this steady temperature only extends up to about 25 km., and from that height onwards, the temperature rises again to about 280°K at 50 km., falls to a minimum of about 190° K at 80 km. and finally rises steadily to more than 1000°K (18).

We also know that there is still large scale turbulence well above 11 km. height sufficient to ensure thorough mixing of the atmospheric gases, as previous analyses of air samples up to

about 60 kms. height show that there is no gravitational separation of the heavier gases from the lighter ones (7).

If it is importance in many fields of physics and meteorology to know the composition of the atmosphere to as great heights as possible.

For example, the explanation of the temperature changes outlined above, presents a very difficult problem for the meteorologist and theoretical physicist. A knowledge of the chemical composition at the various heights is necessary, since the effect of solar radiation depends on the nature of the gases present.

The height of maximum density of the ozone layer at 20 to 25 kms. with its probable production by photo-decomposition of oxygen molecules; the predominance of atomic oxygen over molecular oxygen at heights of about 100 km. to 120 km; the presence of atomic sodium and nitrogen and the existence of some oxides of nitrogen at higher levels have been shown by spectroscopic methods, or the light emitted by the aurora and the night sky. (11). But for an accurate determination of most constituents chemical analysis is very necessary.

In this connection, it may be remarked that while a preponderance of lighter gases may be expected at great altitudes evidence of spectroscopic data of the Aurora shows no trace of either helium or hydrogen, but mainly oxygen and nitrogen in atomic or molecular form. A publication by Herman, however (12),

suggests that a number of bands in the night sky may equally well be attributed to a superimposition of helium on a nitrogen spectrum as to a metastable nitrogen spectrum.

It is not known whether helium or hydrogen are expected to emit light under conditions of auroral excitation. Further, since the thermal diffusion of helium atoms in the upper atmosphere at temperatures of 1000°K will be very large, there will be a continual escape of helium from the top of the atmosphere into outer space. Indeed, a simple calculation shows that over 98% of the helium emitted by rocks at the surface of the earth during geological time, has been lost from the atmosphere, This effect might seem to oppose any tendency for a helium enrichment to occur in the upper atmosphere.

Maris and Epstein have calculated the rate of separation of various constituents at various heights, assuming the air to be thoroughly mixed and then left undisturbed for a certain time. Equilibrium will be attained more rapidly at greater heights where pressure is lower. Table 2 summarises their results (13).

T A B L E 2.
Time for 50% Segregation.

Height (km).	He.	A.	CO_2
200	2 min.	12 min.	8 min.
180	26 min.	2.3 hrs.	1.6 hrs.
160	4.8 hrs.	25 hrs.	17 hrs.
140	2.8 days.	14.8 days.	10.4 days.
120	34 days.	180 days.	130 days.
100	1.2 yrs.	6.4 yrs.	4.5 yrs.

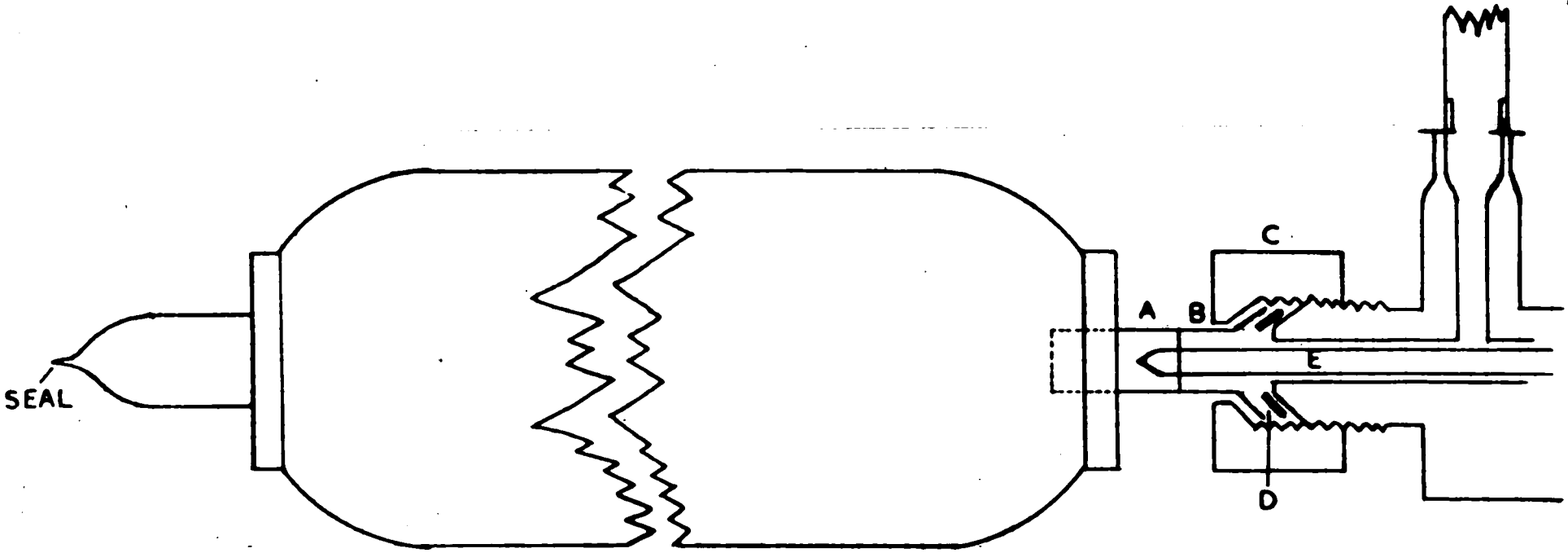

FIG 2

STEEL BOTTLE AND JOINT

These figures would indicate that, unless there is a very long lasting stillness of the upper atmosphere in regions below 150 kms we should have to obtain air samples from at least this height to observe any gravitational separation of gases. Thus, the investigation of gravitational separation of the gases in the upper atmosphere, as well as the study of the photochemical processes, the mechanisim of the temperature changes, the production of aurora by solar particles, and many other problems show that a determination of the chemical composition of the upper atmosphere is a basic necessity for their understanding.

Previous chemical analyses have been done on air samples, obtained by sounding balloons, from heights between 9 to 30kms. at close intervals, and by rocket flights from heights of 50 and 62kms., which showed that no gravitational separation of gases occurred up to this last height (5)7). The present work is chiefly concerned with samples obtained above 60kms. height with a few samples from lower heights to check the previous results. All these samples were obtained by rocket flights, since rockets afford the only way of collecting samples above about 30kms. height.

Section 2 - Method.

(a) Collection of Samples. (Undertaken in New Mexico, U.S.A., by the University of Michigan.)

The steel bottles, capacity 8½ litres, one of which is shown in Fig. 2 , were initially pumped for four or five days and heated to 340°F to de-gas them. They were mounted in the war

head of a V2 or Aerobee rocket with the wide copper tube pointing into the airflow and, 5 seconds before sampling, the nose cone of the rocket was blown clear of the body by a small explosive charge leaving the copper tube pointing directly into the airflow and ahead of the body of the rocket. The air samples were taken towards the end of the upward flight, and after the rocket motors had cut out. The sampling device opened the tube by means of an explosive charge, which forced up a pivoted bar welded to the top of the tube, thus tearing the end of the tube completely off. The closing mechanism consisted of a hammer and anvil, with the hammer pyrotechnically driven against the anvil with the tube between, and since the tube had been previously annealed to make it soft, this device produced good seals in a large proportion of samples. However, in spite of the cold welding technique, large and varying percentages of oxygen were found to have been removed from the samples and the reason may be that the copper was so well cleaned and de-gassed initially, that the fairly large copper surface presented to the air sample was sufficient to take out the oxygen in the cold; or alternatively, the air friction during flight warmed the copper enought to take out the oxygen shortly after the sample was sealed in.

After the samples had been collected, the bottles were returned to earth by parachute, and the sealed copper tube was covered over with Glyptal wax immediately on recovery from the desert.

In order to make sure that the air in the bottle did not come from a quantity of ground-level air carried up inside the envelope of the rocket, and released into the bottles during sampling, a container of radio-active carbon-dioxide was mounted in the compartment just behind the bottle assembly. The carbon-dioxide was released 5 seconds before sampling commenced, so that, if gas were carried up and released into the bottle, radio-active contamination would be observed, perhaps allowing a correction for ground level air contamination to be made, or at worst, indicating the sample to be untrustworthy.

(b) Analysis of Samples.

The samples were then flown to,this country, and analysed in Durham by the following method.

(i) Transfer of Air from Steel Bottles to Apparatus.

The narrow copper tube A, Fig. 2, was soft soldered on to another short piece of copper tube B, which had been reamed out at the other end to give a conical shape, with a complimentary shaped nut C already in place over the copper tube. A thin rubber gasket D was fitted over the end of the socket E, and the nut screwed tightly into place. At first, it was found that gaskets could easily be made from sheet rubber which would hold a high vacuum indefinitely, but later so much trouble was experienced with rubber gaskets degassing for several weeks under vacuum, and neoprene and plastic gaskets leaking, that the bottle opener had to be entirely redesigned to obviate this need for a gasket. When the whole of the bulb and side tubing

had been rigorously evacuated, the taps T_1 and T_3 (Fig. 3), were shut, and the discharge colour with a Tesla coil just below tap T_1 was noted. The large wheel was then rotated, compressing the bellows C by means of an advancing screw, and, the end of the sharpened steel rod A being attached to the end of the bellows, this advanced and pierced the copper diaphragm, releasing the air sample up to tap T_1. Tap T_1 was incorporated to guard against those bottles which had ground-level pressure inside them. In normal cases, the discharge colour was again taken to make sure the diaphragm had been pierced, and then, with liquid nitrogen round the U tube to remove any carbon dioxide and water vapour present, the sample was töplered into the storage space E between the mercury valve of the töpler pump, and the tap T_3.

(ii) Measurement of Amount of Air and therefore Pressure in Steel Bottle.

When the mercury was now raised so that the tip of the meniscus just touched the tip of the pointer sealed inside the bulb E, the gas was then compressed into a volume which had been accurately calibrated, and thence, reading the pressure differenc from the mercury levels in the bulb E, and the side arm F, the absolute volume of air was easily determined. Since the volume of the large steel bottles was 8.2 litres, the initial pressure in these bottles could then be determined, forming a useful check on the pressure measurements taken by other instruments in the rockets.

FIG. 3

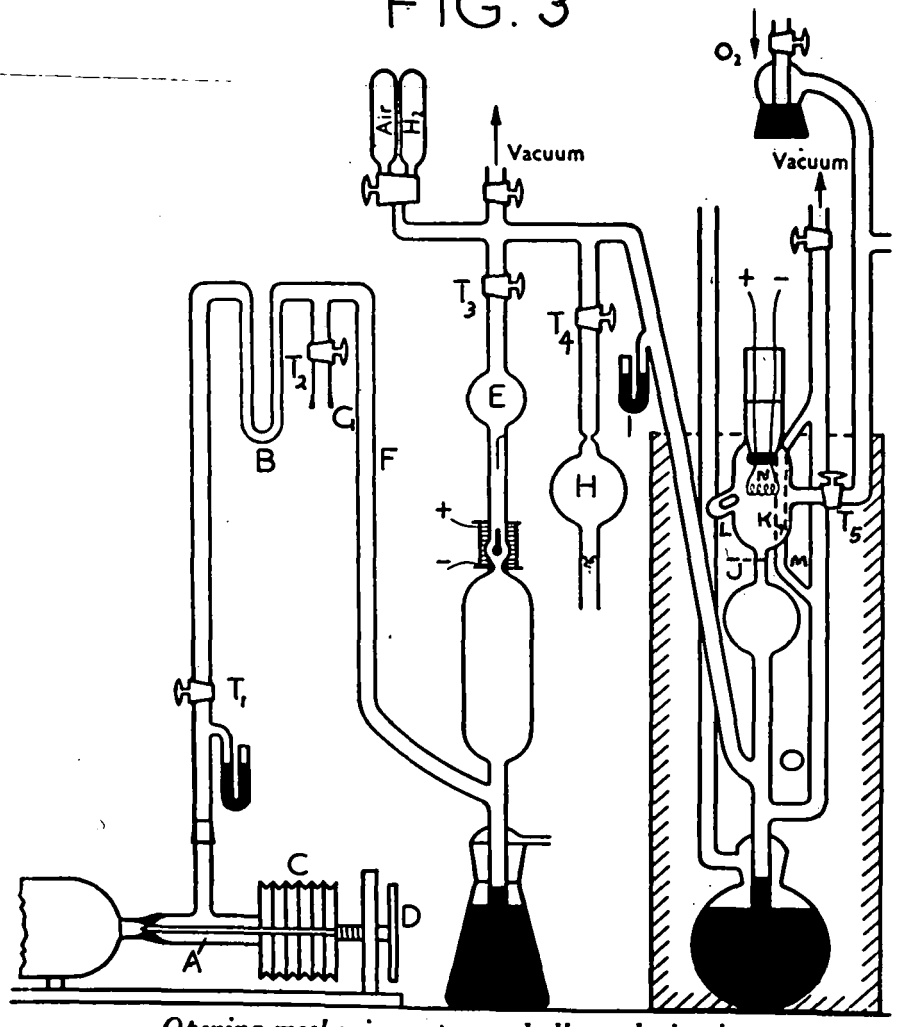

Opening mechanism, storage bulb, and air pipette.

(iii) Contamination Monitoring by Active Carbon Dioxide.

Before the release of the stratosphere air from the steel bottle, a tube containing about 1 cc.N.T.P. of carbon dioxide accurately measured was attached at the ground joint G, and the air in the dead space ℅ pumped away. After the air had been töplered into the storage space E, the mercury was kept well above the cut-off of the töpler pump, and, the U tube B being kept cooled in liquid nitrogen, the carbon dioxide from the attached tube was condensed into it by opening taps T_2 and T_6. The dewar on B was then removed, and the carbon dioxide and any radio-active carbon dioxide from the sample condensed back into the attached tube by cooling it in liquid nitrogen. After 20 minutes, the taps T_2 and T_6 were closed, the dewar removed, and the tube containing the carbon dioxide detached, to be investigated for C^{14} activity in a gas filled Geiger counter. Results of this radio-active carbon-dioxide monitoring are quoted later.

(iv) Air Pipette.

The air pipette and combustion chamber K, Fig.3, is used in essentially the same way as a McLeod gauge, the whole being immersed in a thermostat bath at a temperature of $19^{0}\pm0.10$ C. It is necessary to know accurately the volume of the bulb K, with the tip of the mercury meniscus just up to the etch mark J in the narrow tube below the bulb, and the tap T_5 closed. The KOH pellet in the side arm L and the copper spiral N were already in position. At first it was attempted to calibrate this by means of a gas expansion method, but it was found that so many

errors were introduced by this method, due to such effects as change in apparent pressures with change in room temperature, mercury meniscus height, changes due to slightly dirty mercury, and so on that, after more than a month's work, the volume could not be determined with a mean probable error of less than ± 0.2%.

Later, it was decided that the accuracy was still not good enough, so the combustion chamber was cut off, the KOH pellet was removed, and the chamber weight-calibrated with distilled water, the copper spiral being in place, and allowance was made for the bolume of the KOH pellet by weighing it immediately before insertion into the side arm. This gave a very consistent figure for the volume of the chamber at last.

(v) Estimation and Removal of Oxygen.

The operation of the air pipette was as follows. First, after ensuring that the mercury of the Töpler pump was raised above the cut-off, the non-return valve of the Töpler pump was raised by means of the solenoid, releasing the whole of the air sample into the large Töpler bulb, enabling much finer control of the amount of air allowed into the air pipette to be achieved. The tap T_3 was then opened, and the height of the mercury in the large Töpler bulb adjusted to give the required pressure on the manometer I. The mercury in the air pipette was then raised to the etch mark, and the pressure difference between the mercury in the two limbs was read. From this, the absolute amount of air taken could be calculated, generally between 0.1

and 0.05 ccs. N.T.P. The mercury was then lowered below the second bulb, so as to lower the gas pressure as much as possible, and the copper spiral heated. The best temperature for the copper spiral is said to be 160°C, (14) The spiral was first heated for 10 minutes, then the current switched off and the chamber allowed to cool to bath temperature before the mercury was raised to the etch mark and the pressure difference re-read. This process of re-heating the copper spiral was then repeated for 5 minutes at a time, until no further decrease in volume took place when the whole of the oxygen had been removed and the oxygen percentage could be obtained. After about 3 air samples had been treated in this way, the copper spiral had to be reduced again by heating in an atmosphere of hydrogen, introduced from the reservoir shown.

Any small traces of hydrogen initially present in the air sample would be burned to water at the copper spiral and removed by the KOH pellet, but since hydrogen is normally only present in air to the extent of $2 \times 10^{-4}\%$ (15) its removal would not affect the accuracy of the oxygen measurement at this stage. Only in one of the earlier experiments on rocket samples was any difficulty with hydrogen experienced, and in this case some hydrogen emerged from the column along with the neon fraction and invalidated the neon measurement. The presence of very much larger amounts of hydrogen than usual in this sample was confirmed by mass spectrometric measurements (16), and one possible source of its origin may have been in the exhaust gases from the rocket.

since this particular sample was taken at a low altitude, probably when the rocket motor was still running.

(vi) Transfer, Fractionation, and Measurement of Helium and Neon.

The gases remaining in the combustion chamber, namely nitrogen, argon, helium, neon, krypton and xenon , were now released into the connecting tube to the circulating system by opening the tap T_5 at the back of the combustion chamber, and, with the mercury in the front and back of the fractionating column raised, the charcoals cooled in liquid nitrogen, tap J (Fig. 30), closed and tap R (Fig. 29), opened, about 99.5% of the gases could be transferred to the first charcoal tube by 8 strokes of the Töpler pump. The tap in the connecting tube was then closed and about 5 mms. pressure of pure oxygen from the reservoir let into the combustion chamber via the mercury bubbler J, Fig. 3, to act as a carrier gas. The tap was then opened, and the oxygen plus traces of the air sample transferred to the first charcoal tube by six more töpler strokes. This flushing process was repeated 5 times as this was found by experiment to give 100% transfer of the sample gases into the first charcoal tube.

The column was then set for 15 operations, and, at the end of these, the mercury in the large compression bulb was raised and the tap the measuring Pirani gauge opened.

Since no helium from the sample should come through the column until operation 16 (the extra operation due to the presence of the mercury ventil at the end of the column), this measurement

showed, if there was no deflection of the gavlo spot, that there was no air left in the column originally after evacuation, or if a deflection was obtained, that the succeeding helium and neon measurements would be unreliable due to contamination by air remaining in the column. In practice, no deflection was ever observed from operations 1 to 15.

The column was then set to perform operations 16 to 36 inclusive, when a quantity of gas equivalent to 100% of the helium, but being composed of 99.3% helium plus 0.7% neon, was obtained in the compression bulb. The mercury in the bulb was then raised, when more than 99% of it was compressed into the measuring Pirani space. The apparently inevitable zero creep of the Pirani gauge galvonometer set-up was obviated by taking readings of the position of the galvo spot on the scale every minute until a steady drift was observed, opening the tap allowing the helium into the measuring pirani exactly on the minute, measuring the spot position until the drift was steady again, then opening the tap to vacuum on the minute and measuring the spot position untilthe drift was steady again. In this way, both the zero creep and the slow approach to equilibrium of the gauges on admitting and removing gas (about 3 minutes) could be allowed for.

Immediately after this measurement was done, an accurately measured amount of helium was admitted to the Pirani gauge, via the same compression bulb and with the same dead space. This was done at least twice to give calibration readings to determine

the sensitivity of the Pirani gauge at that particular time.

The column was then reset to another 25 operations, with the dewar flasks lowered or removed progressively as explained in Chapter 4, to facilitate the speedy collection of the neon, and the whole measurement and pirani calibration for neon sensitivity was repeated as for the helium. This concurrent calibration of the piranis obviated any uncertainty due to day to day fluctuation in the Pirani sensitivities, which could be caused by small changes in the various components of the measuring system.

During a series of measurements on a particular air sample, each stratosphere sample experiment was done alternately with a ground level air experiment, commencing with a ground level air experiment so that, in effect, a control of the experimental conditions and efficiency of the apparatus was kept the whole time.

(vii) Argon Determination.

For the argon determination, it has been convenient up to now to introduce a fresh sample of stratosphere air into the air pipette rather than to determine helium neon and argon on one and the same aliquot portion of air. In the event of analysing samples of stratosphere air from very high altitudes, over 100km. the smallness of the absolute amounts of air collected even in the large bottle (c.a.35 litres), would probably only be of the order of $10.^{-3}$ cc N.T.P. so that later, the apparatus may have to be modified to measure the helium, neon, and argon from one and the same sample.

FIG. 4

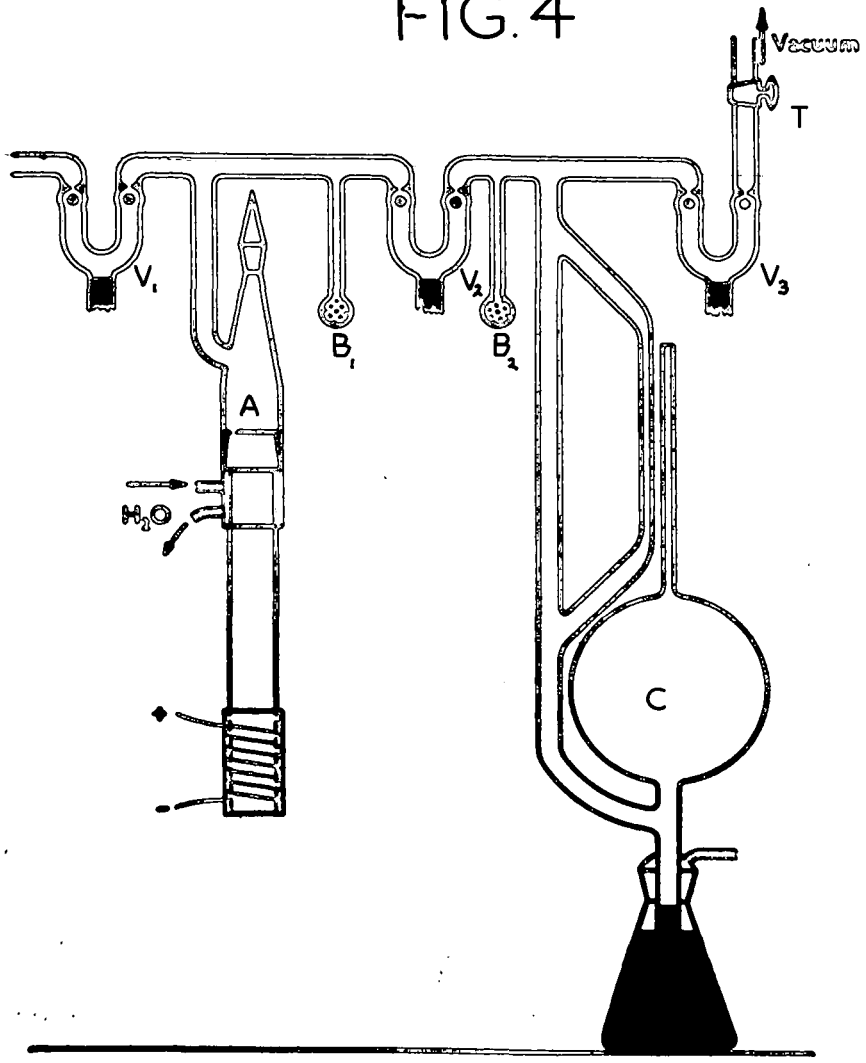

Barium furnace and McLeod gauge.

In the present work, another portion of air was introduced into the air pipette, reduced as before with the % volume decrease measured, the back tap T_5 (Fig. 3), and the ventil V_1, Fig. 4) are opened, and the nitrogen and argon in the sample adsorbed quantitatively on the small amount of charcoal (0.1gram) in tube B_1. A large proportion of the helium and neon would be left behind in the side tubing, but it was desired to remove it in any case.

After cooling the charcoal in liquid nitrogen for about one hour, thus ensuring quantitative transfer of the nitrogen and argon, the ventil V_1 was closed and the liquid nitrogen removed from the charcoal, which was allowed to warm up to room temperature. When the gases were completely de-sorbed, (10 to 20 mins. room temperature), the barium metal in the bottom of the steel furnace A was heated to 850° C. for 20 minutes, removing the nitrogen as barium nitride, leaving the argon unaffected. It was found that none of the argon was removed by capture in the thin film of barium metal which deposited on the wall of the furnace, as might have been expected. The argon was then condensed on charcoal in tube B_2 after opening ventil V_2, the charcoal remaining cooled in liquid nitrogen for one hour. The tap T and ventil V_3 to vacuum were then opened, for about one minute, which was sufficient to remove the remaining traces of helium and neon. The tap and ventil were then closed again, the liquid nitrogen remoged, and the charcoal allowed to come to room temperature again and stand until the gases were completely de-sorbed. The argon volume (usually about 10^{-3} ccs.) was then

read on the McLeod gauge C, the dead space in the side tubing having been previously calibrated by an argon expansion method from the McLeod bulb.

(ix) Sealing Off and Return of Residue of Samples.

It was usual to do two, at least, and preferably three, experiments for the determination of helium and neon, two or three determinations of the argon content, unless the initial amount of air sample was so small as to preclude this. Any of the air sample which was left in the storage space after all the determinations had been completed was then introduced into the previously evacuated sample bulb H (Fig.3), by raising the mercury in the side arm of the air pipette, opening Taps T_3 and T_4, and raising the mercury in the Topler pump up to tap T_3, to cut down the dead space as much as possible. The sample bulb was then sealed off at the constriction, and returned to the U.S.A. for other investigations, notably the N^{14}/N^{15} isotopic ratio determination by McQueen (17).

Section 3 - Results.

During the course of these experiments, each set of stratosphere air determinations were "monitored" by doing a determination on laboratory ground level air immediately before and afterwards, in order to check the accurate working of the apparatus. A résume of these ground level results is given below.

T A B L E 3.

He (p.p.m. in ground air).	Ne (p.p.m. in ground air).
5.253	18.11.
5.311	18.15
5.448	18.18
5.214	18.39
5.290	18.42
5.364	18.28
5.274	18.10
5.411	18.51
5.154	18.24
5.290	18.28
-	18.13
5.218	18.03
5.283	18.24
5.290	18.28
5.393	18.21
5.228	18.23
5.186	18.15
Mean 5.285 ± 0.010	Mean 18.23 ± 0.020.

It can be seen that these figures compare very well with Gluckauf's figures [5]. (He 5.239 ± 0.004, Ne 18.21 ± 0.04), although the present determinations were done on 10 to 100 times less air than Gluckauf used.

T A B L E 4.

Results on Stratosphere Air Samples.

No. of sample	Height (km)	Amount of Gas in Bottle C) (cc. N.T.P.)	Ratio to ground level air.			O_2 %
			He	Ne	A.	
25D	50.4-53.3	8.6	0.981	1.003	0.398	15.75
19D	54.7-583	2.04	1.013	1.450@	1.009	0
B-13	55.56-58.18	6.78	0.998	1.005	1.001	10.46
B-15	58.18-60.35	5.15	1.035	1.008	0.996	0.2
C-11-B	57.0-64.3	0.398	1133	1.040	0.962	15.3
B-6	64.3-67.0	0.415	1.445	1.080	0.929	1.875
C-5	64.3-71.0	0.204	1.570	1.232	0.90	0.
B-8	67.0-69.6	0.218	2.019	1.177	0.886	6.8
B-9	69.6-71.8	0.535 (0.185 corr.)	2.41	1.20	0.85	0.7
C-1	84.4-89.0	0.015	2.943	1.395	0.82	0
C-3	89.0-93.2	0.0032	-	-	0.82	0.

@ unreliable because of contamination by H_2 in original sample, confirmed by mass spectrometry (16).

C) corrected for loss of oxygen.

In addition, four control bottles, as far as possible the same as those used for stratosphere sampling, were filled with small amounts of ground level air in Michigan, U.S.A. and analysed in Durham.

T A B L E 5.

Results for Control Bottles.

Bottle No.	Amt. gas in bottle (cc.N.T.P.)	Ratio to ordinary laboratory air.			O_2%	Bottle pressure (mmHg) as measured in Durham.	Bottle pressure (mmHg) of air put in at Michigan.
		He.	Ne.	A.			
B-17-P	0.151	0.994	1.001	1.00	0	0.0189	0.0185
B-18-P	0.134	0.997	1.003	0.99	0	0.0165	0.0165
B-20-P	0.120	1.259	1.032	0.92	0	0.0150	0.0202
B-21-P	0.130	1.359	1.083	0.92	0	0.0162	0.0174

It can be seen that two of these bottles show no difference from ordinary air, while two show marked deviations. Bottle B-17-P was filled by breaking a glass vial containing a small amount of ground level air inside a vacuum chamber attached to the sampling tube, and sealing the copper sampling tube a few seconds later by the usual method, as was to simulate stratosphere

collecting conditions as closely as possible. This sample showed no separation. The other three bottles were filled by breaking off a sealed glass vial inside the steel bottles after the bottle had been evacuated and sealed. The first of these shows no separation, but the other two do. It may be pointed out that B-20-P and B-21-P were filled on the same day, some weeks later than B-17-P and B-18-P, and were both made by sealing off a long narrow capillary tube open to the air, which was attached to a small bulb, by use of an alchohol flame. It is felt that this technique is not entirely satisfactory, as thermal diffusion effects may occur. It is also noteworthy that whereas the bottle pressures measured in Durham compare very closely with those obtained in Michigan from the amount of air put in for B-17-P and B-18-P, that the corresponding pressures for B-20-P and B-21-P do not.

It seems unlikely that adsorption of Nitrogen and Argon on the steel walls of the bottles B-20-P and B-21-Pcould account for the observed separation (18).

However, more experiments are to be done shortly in an effort to clear up the anomolous results from these bottles.

Results for Radio-active Carbon-Dioxide Monitoring.

T A B L E 6.

Bottle No.	c.p.m.	Activity found in bottle compared to activity released from CO_2 container.
c-5	160.	1 part in 4×10^6
c-1	800.	1 part in 10^6
c-3	10.	-
c-11-B	360.	1 part in 2×10^6
C-7-B	5.	-

From Table 6, it is apparent that the radio-active carbon dioxide released in the rocket sampling compartment a few seconds before each batch of three sample bottles was opened, was adequately swept away. This would indicate that no contamination of the samples by air carried up with the rocket occurred.

Section 4 - Discussion.

When the data for samples B-6, B-8, and B-9 were first obtained, it seemed for a short time that the figures were at last a clear demonstration of the long sought for effect of gravitational separation of the atmospheric gases, which has been presumed to take place at some height ever since Dalton's Law of Partial Pressures was enumerated (19). Further consideration, however, of these and later results, showed that for several reasons, gravitational separation did not seem likely to be the cause of the observed enrichment of He and Ne, and the deficit of Argon.

Perhaps the most obvious reason for doubting the onset of gravitational separation at the heights investigated is that

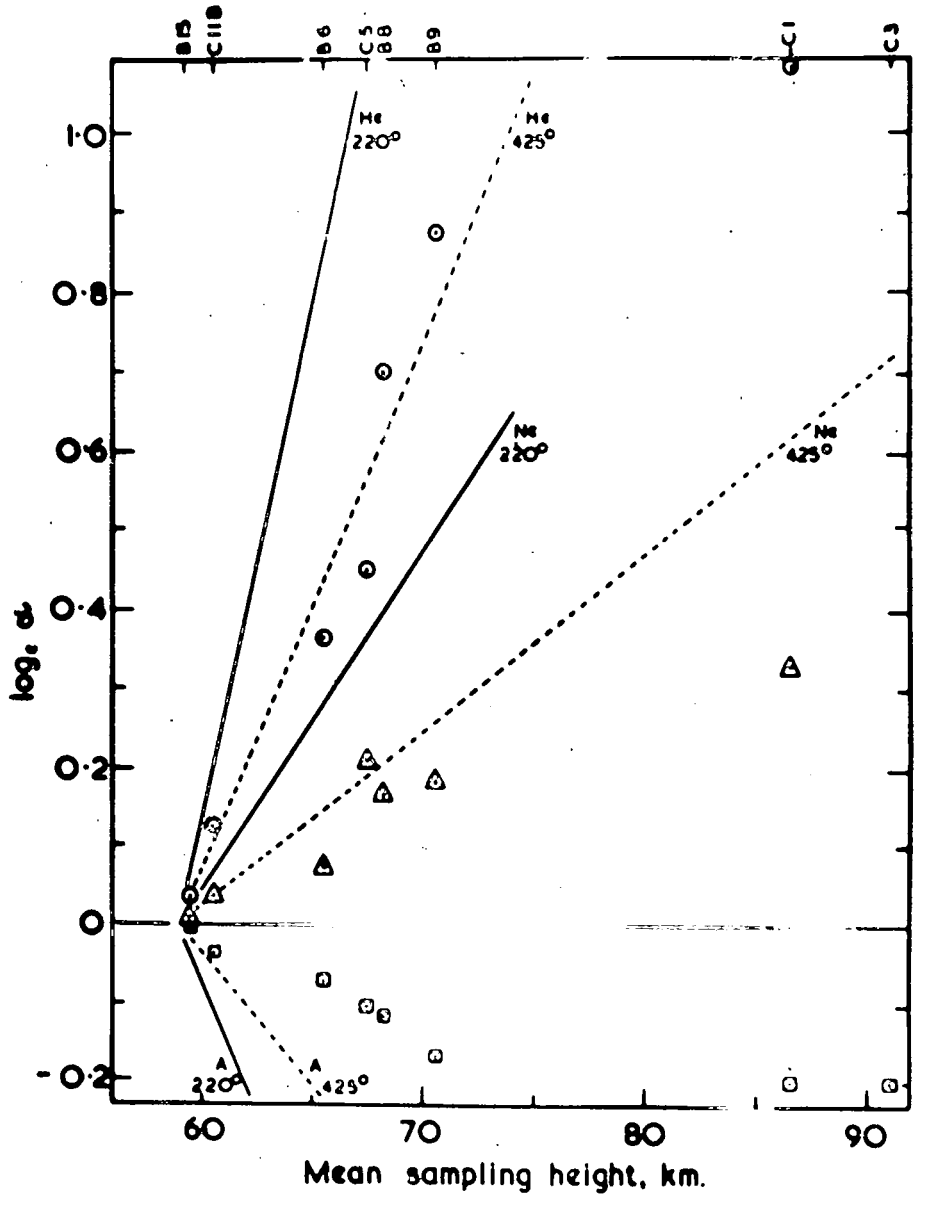

Experimental points: ⊙ helium; △ neon; ⊡ argon.

Theoretical lines calculated from: $\alpha = \exp(-\Delta M g h / RT)$.

$$\alpha = \frac{(p/p_{N_2})_{\text{argon}}}{(p/p_{N_2})_{\text{atm.}}}$$

FIG. 5

almost the whole height range over which these samples were taken is one of falling temperature with increasing height. According to the latest available data (10), the temperature decreased to a minimum of about 205°K at 80 km. It is to be expected that this will give rise to atmospheric instability and turbulence. This doubt is particularly obvious if the tendency towards instability is taken in conjunction with the results of Epstein (13) who calculates that the relaxation times for He and Argon at these heights is of the order of one and six years respectively. Further, if the "best fit" lines are calculated from the relationship to be expected on the basis of gravitational separation namely:-

$$\alpha = e^{-\frac{\Delta mgh}{RT}}$$

where

$$\alpha_{He} = \frac{\left(\frac{PHe}{PN_2}\right)_{Strato}}{\left(\frac{PHe}{PN_2}\right)_{normal.}}$$

it can be seen from Fig. 5 that the lines obtained using a temperature of 220°K (the measured temperature in this region) (10) are nowhere near the experimental points. In order to fit the observed He separation, a temperature of about 425°K would be necessary with even higher temperatures for Ne and A respectively.

Another very important discrepancy in the observed results is that the amount of air collected in the bottlesis in all cases not as much as would be theoretically predicted from the Rayleigh pitot tube formula. In most cases only 1/10th or less

of the expected amount was collected.

T A B L E 7.

Bottle No.	Mean Mach. No.	Mean ram. factor f	Ambient press. at closing height (10). Pc.	Ram press at closing height. Pc f	Bottle pressur Pb.
B-13	1.54	3.57	321	1150	628
B-15	1.38	2.78	182	541	477
C-11-B	3.30	14.50	105	1522	37.1
B-6	1.77	4.54	72	327	38.5
C-5	3.20	13.67	38	519	18.9
B-8	1.73	4.36	48	209	20.2
B-9	1.49	3.37	36	121	21.6
C-1	2.69	9.48	2.2	21.	1.4
C-3	2.36	7.67	1.2	9.2	0.3

All pressures in microns Hg.

Table 7 gives a comparison of the ram pressure operating at the closing height of each sample with the measured bottle pressure. Now, since the pumping speed of a tube of 3 cms. diameter and about 23 cms. length, such as that used in the collection of the samples, is of the order of 10 litres per second, and the capacity of the bottles is 8.2 litres, this result is somewhat surprising and leads to the conclusion that the bottles have not filled to equilibrium as expected, but that air must still have been flowing in when the sample tubes were closed. Moreover, an effective sampling orifice of only about 1/10th of the actual orifice would be needed to explain the observed bottle pressures, and since the mean free path of an "air molecule" at 64 kms. height seems to be about 0.5 mms. conditions would then be suitable for the onset of effusive separation.

It is then fruitful to consider what results are to be expected if effusive separation has taken place in the sampling tube. In this case, the degree of separation achieved would be expected to vary in a manner related to the square roots of the mass ratios of the two gases involved. Thus :

$$\alpha_{He} = (1-x) + x\left(\frac{M_1}{M_2}\right)^{\frac{1}{2}}$$

where x may be regarded as the fraction of the total amount of helium which has entered the bottle by molecular flow, and (1-x) the fraction entering by viscous flow. x will vary from 0 at high pressures where the flow is entirely viscous to 1 at very low pressures where all the gas will enter under molecular flow conditions.

An approximate treatment may then be attempted by applying Knudsen's semi-empirical formula for the quantity (q) of gas flowing along a tube under all conditions from viscous flow to molecular flow.

$$q = (P_1 - P_2)\left[\frac{\pi}{128\eta}\frac{d^4}{l}Pm + \frac{1}{3\sqrt{\rho}}\left(\frac{1 + \frac{\sqrt{\rho}}{\eta}d\,Pm}{1 + 1.24\frac{\sqrt{\rho}}{\eta}d.Pm}\right)\right] \quad \text{---(1)}$$

where $(P_1 - P_2)$ is the pressure difference between the ends of the tube ,

η is the viscosity of the gas,

where d and l are the diameter and length of the tube respectively.

Pm is the mean pressure (dynes/cm^2)

ρ is the density of the gas at a pressure of 1 dyne/cm^2, and the prevailing temperature, and

v is a factor related to the diameter and length of the tube which makes allowance for "end effects" of th tube.

In Table 8 below, C_1 is the term : $\frac{\pi d^4}{128 \eta l} P_m$

from Poiseuilles' formula for viscous flow :

$$q = (P_1 - P_2) \frac{\pi d^4}{128 \eta l} P_m$$

C_2 is the term $\frac{1}{v\sqrt{\varrho}}$ from Knudsen's formula $q = (P_1 - P_2) \cdot \frac{1}{v\sqrt{\varrho}}$ for molecular flow, and C_3 is the combined term in the square brackets of (1) above.

T A B L E 8.

d = 3cms. l = 23cms.

P_m(mms.Hg)	C_1 (visc.)	C_2 (molec)	C_3 (combined)
10	6.3×10^6	1.21×10^4	6.344×10^6
1	6.3×10^5	1.21×10^4	6.471×10^5
10^{-1}	6.3×10^4	1.21×10^4	7.74×10^4
10^{-2}	6.3×10^3	1.21×10^4	2.04×10^4
10^{-3}	6.3×10^2	1.21×10^4	1.47×10^4
10^{-4}	6.3×10	1.21×10^4	1.41×10^4

There is agreement between C_1 and C_3 down to 10^{-1} mms.Hg pressure, that is, the flow must be entirely viscous and there will be no separation of gases. There is agreement between C_2 and C_3 at 10^{-3} mms.Hg pressure and below, so that, below 10^{-3} mms.Hg pressure the flow must be all molecular and complete effusive separation of gases will take place with a tube of the

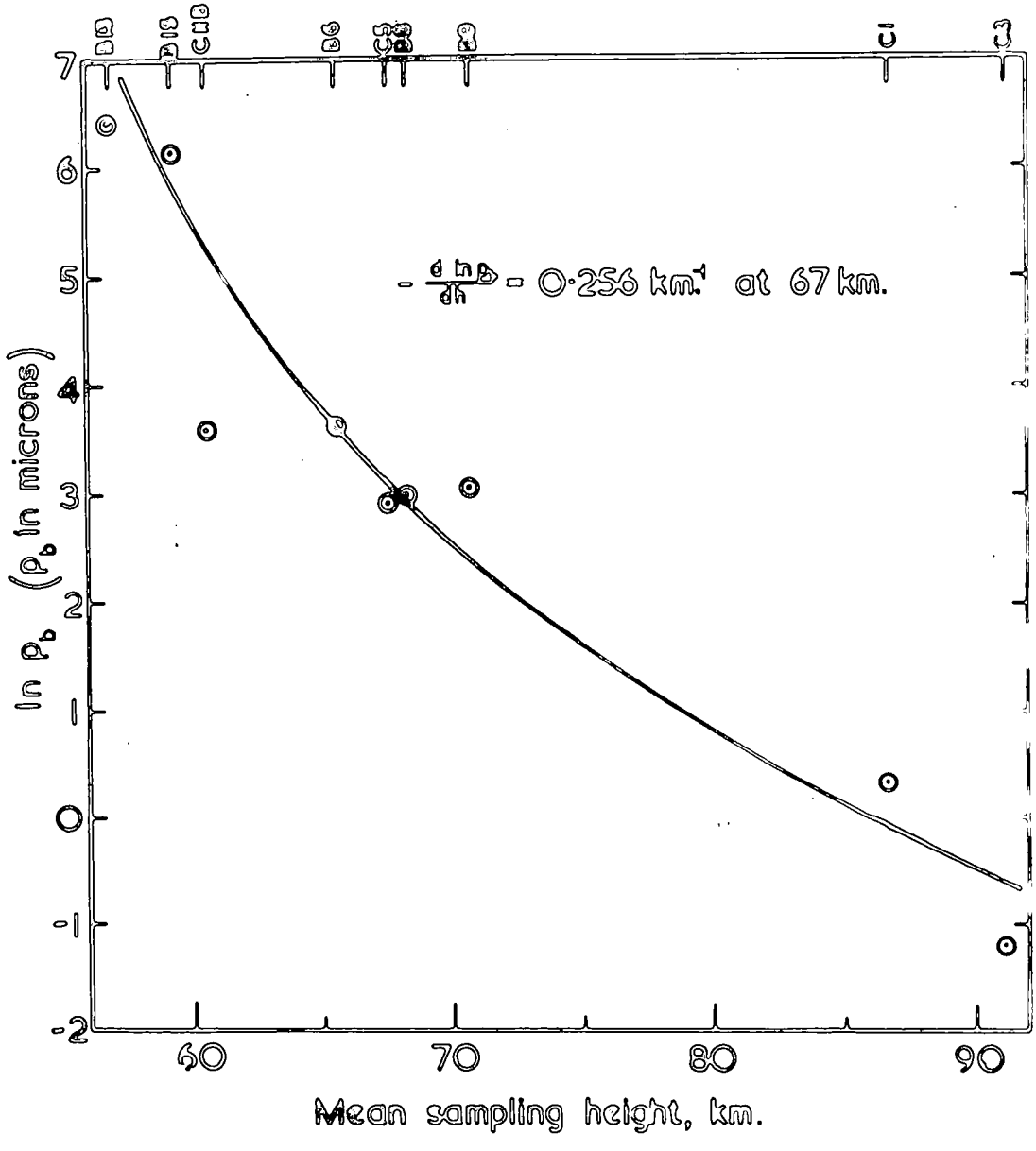
$-\frac{d \ln \rho_b}{dh} = 0.256$ km.$^{-1}$ at 67 km.
ln ρ_b (ρ_b in microns)
Mean sampling height, km.
60
70
80
90
7
6
5
4
3
2
1
0
-1
-2

FIG. 6

dimensions concerned. Between 10^{-1} mms.Hg pressure and 10^{-3} mms.Hg pressure the flow will be semi-molecular, and partial effusive separation will take place.

Now, from Fig. 6 where measured bottle pressures are plotted against height, it appears that samples below 55-60km. height should show no separation, samples above 80-85 kms.height should show complete separation, and samples between these two limits should show partial separation. The position and slope of the theoretical ^{He}/line for the region of partial separation can be fixed by the following treatment. Taking a stplified form of the Knudsen formula, that is, ignoring Kundt and Warburg's correction for slip, which is small under all conditions,

$$q = (P_1 - P_2)\left(a P_m + \frac{1}{z}\right)$$

$$\alpha = (1 - x) + R(x) = (R - 1)x + 1,$$

where $R = \sqrt{\frac{M_1}{M_2}}$ and $x = \frac{\frac{1}{z}}{a P_m + \frac{1}{z}}$

$$\frac{d \ln \alpha}{dh} = \frac{1}{\alpha} \cdot \frac{d\alpha}{dh}$$

$$= \frac{-P_m (R-1) \frac{1}{az}}{\left(\frac{R}{az} + P_m\right)\left(\frac{1}{az} + P_m\right)} \times \frac{d(\ln P_m)}{dh}$$

$\frac{d}{dp}\left(\frac{d \ln \alpha}{dh}\right)$ is a maximum when $P_m = \frac{1}{az}\sqrt{R}$

that is, when Pm = 41.7 dynes/cm^2 or 31.3 microns.Hg

From Fig. 6, when Pm = 31.3 microns, h = 67 kms. and

$$\frac{-d(\ln P_m)}{dh} = 0.256 \text{ km}^{-1}.$$

Also $\frac{d}{dh}\left(\frac{\ln\alpha}{}\right) = -\frac{(R-1)}{(1+\sqrt{R})^2} \times \frac{d\ln Pm}{dh} = 0.061$ at 67 km. height for He.

Similarly, the theoretical lines for Neon and Argon may be obtained, as in Fig. 7.

It can now be seen that the agreement between the theoretically expected separation and measured separation is good.

It must be stressed that this comparison is only the best approximation, for it treats the mixture of gases as though the behaviour of one were independent of the presence of the others. There is, for example, insufficient information on the collision cross-section of one gas in the presence of excess of another gas. There is some evidence (20)(21) to suggest that the "corners" of the theoretical curves of Fig.7 are sharper than those given by the Knudsen formula, and for this reason, these portions of the curve have only been filled in with dotted lines.

Conclusion.

For the four highest samples, it can be seen that the separation is slightly greater than that ideally predicted, which may represent the onset of a genuine gravitational separation, or it may simply reflect the greatly increased difficulties of working with so little gas (3×10^{-3} ccs N.T.P.) air in the highest case, which contains only 1.5×10^{-8} ccs. of helium).

However, from the above considerations, one is led to prefer a mechanism for separation depending upon the square root of the masses rather than upon exponential $\left(-\frac{\Delta mgh}{RT}\right)$.

Consequently, it seems likely that the observed separations can better be accounted for by an aerodynamic phenomenon in the sampling tube itself, perhaps some "choking" of the mouth of the tube due to supersonic shock-wave effects rather than by gravitational separation in the atmosphere, so that up to the maximum heights reached in this investigation there is no strong evidence to suggest an onset of gravitational separation of the lighter gases from the heavier.

It is proposed to carry out a rocket flight during which air samples will be collected at the peak altitude of the rocket, about 80 kms. height, whilst the sampling tubes are travelling at sub-sonic speeds, and with different diameters of sampling tube for each sample bottle. This experiment may well clear up these uncertainties outlined above, but it is not expected, at the time of writing, that it will be possible for the rocket flight to be carried out for several months.

CHAPTER III.

Helium Content and Age of Meteorites.

Section 1 - Introduction.

(a) The Origin of Meteorites.

It is generally believed today, from such evidence as can be collected, that meteorites have their origin in the solar system and are not of cosmic origin, as was formerly postulated Such evidence - though it is far from conclusive - includes the fact that meteorites seem to have elliptical orbits, suggesting an origin in the solar system, and not hyperbolic orbits, which would show an origin in outer space; also, the preponderance of afternoon falls over morning falls indicate that meteorites move in the same direction round the Sun as the Earth for, if they originated in outer space and approached in random directions, the half of the Earth which is leading the sweep through space - that is the half on which the time is between 12 midnight and 12 noon - would be expected to "collect" most meteorites, Further, Professor C.C.Wylie showed that the Pultusk meteorites, as well as several other "fireballs" moved in elliptical orbits, resembling those in the small asteroids in their eccentricities, inclinations to the ecliptic, periods of revolution and mean distances from the Sun, which would seem to connect them with the theory which attributes the origin of the asteroids to the disrupting force of Jupiter on a primeval planet. (62)

Geological and chemical studies also show that the composition of meteorites and the abundance and distribution of the trace elements amongst the main constituents is what might

be expected if we assume that the original scource was the same as that of the Earth, with only some difference in the highly volatile elements and compounds, e.g. hydrogen, inert gases, methane, ammonia and water, which might have escaped during the evolution (63), (64), (66). No difference in isotopic composition of the various elements has been found. (65)

Since these meteorites then seem to originate in the solar system, and are at present the only extra-terrestrial material available for examination, an investigation of the age of this material should help towards obtaining more information about the age of the solar system itself, and possibly the mode of formation of meteoric bodies, by helping towards differentiation between the several theories. It should be noted that "Age" in this connection is taken as the time since the body under consideration last solidified.

(b) Age Determination on Meteorites.

Iron Meteorites are very good objects for age determinations by the Helium method, since they retain helium so well that all the helium produced within them will be quantitatively retained providing they are not appreciably heated at some stage in their history (22). Experiment has shown (see page 115) that even on heating at 1000°C in vacuo for 3 hours, only about 5% of the helium content of an iron meteorite is released and, since it appears that the heating effect of the rapid flight through the atmosphere only penetrates to a depth of about 1 mm from the surface of recovered pieces, to judge from the Widmannstätten figures, the bulk of the meteorite remaining will not be affected However, whether or not a meteorite has been re-

heated at any time since its original solidification, either as part of a large parent body, or by close approaches to the Sun, cannot yet be stated.

The pioneer work of Meteoric Age Determinations has been extensively conducted by Paneth and his collaborators since 1928. (23,(4)(24). The assumption made was that all the helium was of radio-genic origin, and that if the helium, uranium, and thorium contents of meteorite samples could be determined, the age of the sample could be obtained, knowing the decay constants of the members of the uranium and thorium series.

Up to 1942, a large number of meteorites had been analysed for their Helium, Uranium and Thorium contents, and a few of the results are given in Table 9 below (4).

T A B L E 9.

Name.	Uranium 10^{-8} g/g.	Thorium 10^{-8} g/g	Helium 10^{-6}cc/g.	Age in millions of years.
Cape York(Savik)	0.7	4.0	< 0.0002	< 0.11
Cape York (Ahnighito)	0.7	4.0	< 0.001	< 0.55
Bethany(Goamus)	1	4.0	0.15	60.
San Martin	0.6	8	1.6	500.
Bethany (Amalia)	1.0	4	3.0	1100.
Thunda	0.8	4	28	6100.
Mount Ayliff.	0.4	2	40	7600.

From these results, it seemed that the maximum age of

meteorites must be about 7×10^9 years. Further, meteorites with varying ages from this maximum value right down to only a hundred thousand years old were represented. This seemed to indicate that the age of the solar system could not be less than 7000 million years. Since the age of the Earth is now geologically established as about 3500 million years, if we accept this as representative of the age of the solar system, we must turn to some hypothesis to account for the "excess helium" in meteorites which would lead to high age values.

The study of cosmic ray "star" production has shown that cosmic rays by their impact on matter produce helium. This led to a hypothesis put forward by C.A.Bauer (25)(26); H.E.Huntley (27) and others, to account for the high age values by cosmic ray helium. From a study of the figures obtained by plotting helium contents against log mass in kilograms, Bauer arrived at the conclusion that it was possible for the total helium content of any meteorite, up to the ones containing the largest amount of helium (40×10^{-6} ccs/grm) to be accounted for by cosmic ray production well within the time assigned as the age of the Earth.

(c) Recent Studies on the ^3He and ^4He content of Meteorites.

It seemed best to investigate the possibility of helium production by cosmic rays in meteorites by two methods:

(i) A determination of the amount of ^3He present in meteoric helium, since cosmic rays would be expected to produce this isotope as well as ^4He.

(ii) A determination of any variation in the helium content of the meteorites with increasing depth from the surface since the He production by cosmic rays would decrease with increasing depth.

- Chapter III -

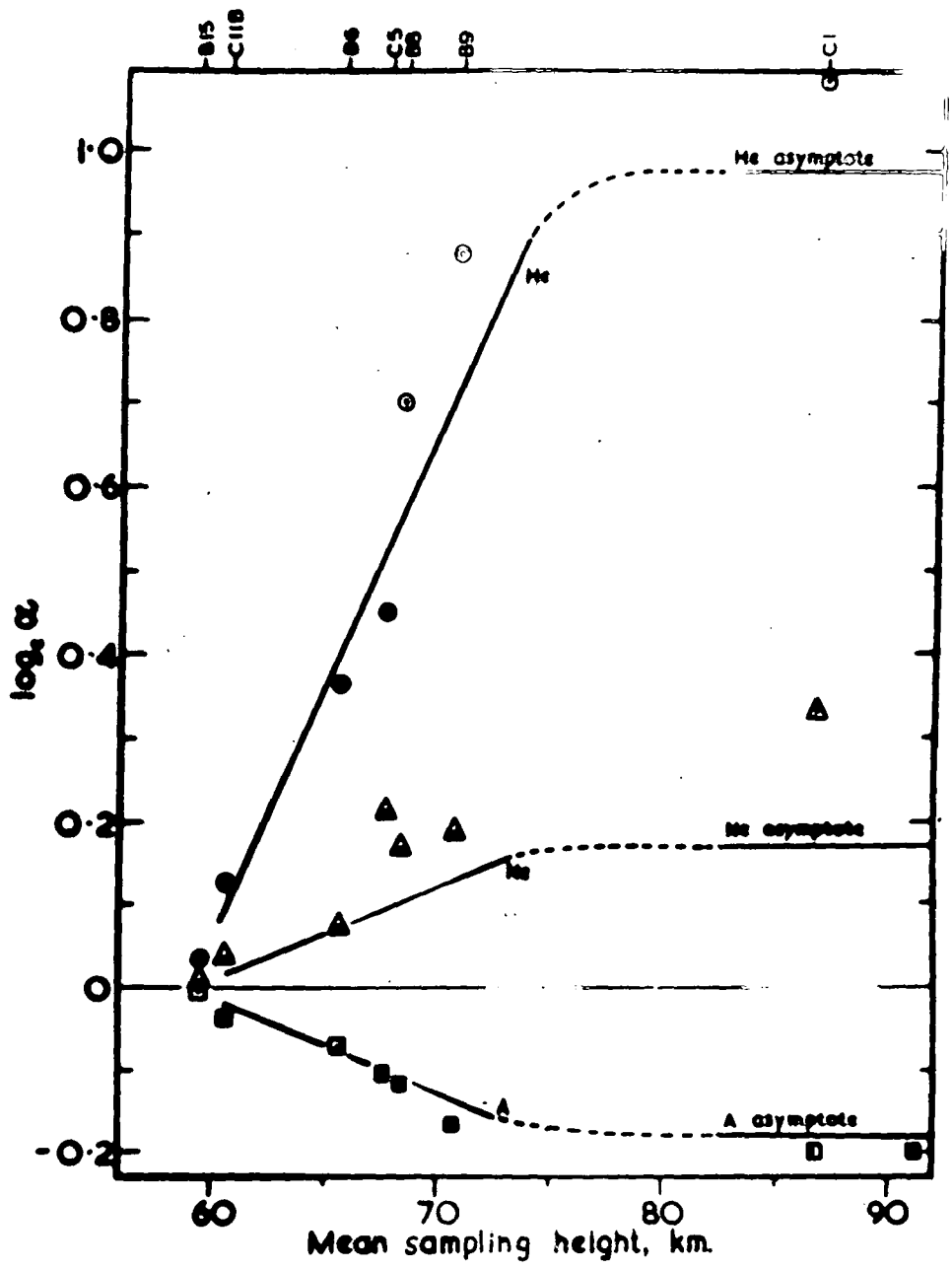

Experimental points: ⊙ helium; △ neon; ⊡ argon.
Theoretical lines deduced on the basis of Knudsen formula

FIG. 7

The second of these two methods was investigated by Dr. E.J.Wilson in the Durham laboratory, notably with the meteorite "Sacramento Mountains". (8). Samples from places up to 60 cms. apart were used, and he concluded that no significant differences in helium content were founds. However, due to the fact that this meteorite is roughly cylindrical in shape, of length 60 cms. and maximum diameter about 16 cms., it is extremely difficult to orientate it with regard to its probable position in the pre-atmospheric mass, and hence to form an estimate of what variation in helium content would be significant.

However, the present work was intended to investigate further the above two methods of approach.

Investigation No.1

It was decided to extract and purify samples of meteoric helium of the order of 10^{-4} ccs. N.T.P. from as many meteorites as possible, and to investigate their ^3He content by two methods -

(a) By mass spectrometric measurements.

(b) By irradiating the helium samples with neutrons in the Harwell pile, so that any ^{3}Helium present would be converted to tritium by the reaction.

$$^3_2He + n \longrightarrow {}^3_1H + P.$$

The tritium was then to be counted, and having an accurate knowledge of the volume of helium put into the sample tube, the proportion of ^{3}Helium to ^{4}Helium could be calculated.

Investigation No.2.

It was also decided to obtain samples from different sized

FIG. 8

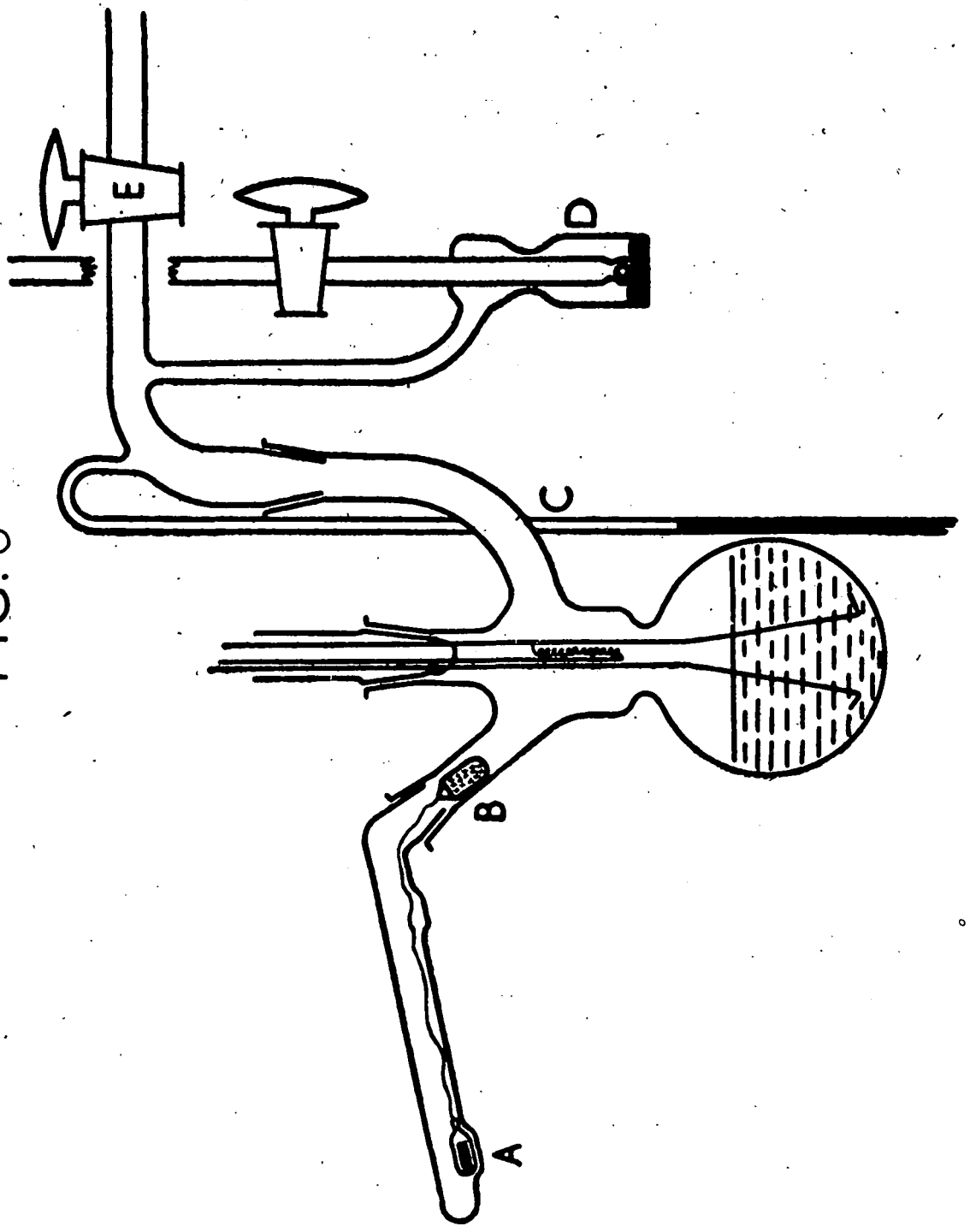

meteorites, taken at intervals along a radius of the present masses, in order to look for any decrease in helium content with increasing depth. Meteorites as nearly spherical as possible were chosen, or at least massive rather than flat slabs, or ones with ill-defined shapes, in order to obtain samples as many centimetres as possible from the nearest surface.

Section 2. Experimental Procedure.

Measurements of Helium Contents for "Depth Effect" Investigation.

(a) Method of dissolution and removal of bulk of hydrogen.

A dissolving vessel was made as shown in Fig.8.

The meteorite shavings were weighed by difference into the glass bucket B, which was kept in the neck A until the initial degassing was complete. About 30 milligrams of meteorite were generally used. The re-agent was 2N H_2SO_4, saturated with $K_2S_2O_8$. It was found by experiment that H_2SO_4 of strength 2N was quickest and most effective for dissolving iron meteorites, and $K_2S_2O_8$ was added to prevent the iron from becoming "passive". By using this re-agent with a warm bath at about 40°C round the dissolving vessel, the whole of the meteorite sample could be brought into solution in about one hour.

The dissolving vessel was evacuated via tap E until the re-agent was effervescing freely, when tap E was closed and a small electrolysing current applied across the two platinum wires which dipped into the reagent. The hydrogen and oxygen produced served to flush out the dissolved air from the reagent, and when about 5 mms pressure of gas, measured on the manometer C

had been produced, the electrolysis was stopped, and the tap E to vacuum opened again for about one minute. The tap E was then closed again, and the whole flushing process repeated six times. This flushing in batches was found to be much more effective than continuous pumping and electrolysing, since with the latter the partial pressure of helium is only reduced very slowly owing to its speed of back diffusion. After the whole of the dissolved air was flushed away, the Tap E was closed, and the meteorite sample lowered into the reagent. Any shavings of iron which were not lifted out of the bucket by evolved hydrogen could be withdrawn under the solution by means of a magnet.

When the meteorite sample was completely dissolved, about 2 cms. pressure of pure oxygen was let into the dissolving vessel via the mercury bubbler D, and the platinum spiral carried on the second and the third platinum wires was heated to bright red heat, the whole of the vessel being cooled in water. When no further decrease in pressure on the manometer could be detected, a further small amount of oxygen was let into the vessel, and the spiral again heated. If no pressure decrease took place the bulk of the hydrogen had been removed.

(b)Removal of Water Vapour and Remainder of Hydrogen.

The charcoal U tube G (Fig. 30) and the water trap M were then cooled in liquid nitrogen, the mercury in the ventil F lowered until it was just above the bend to act as a non-return valve, and the tap E opened. The majority of the helium and Oxygen in the dissolving vessel then bubbled past the mercury into the circulating system. When bubbling ceased, tap E was

shut, the electrolysis repeated, about one cm. pressure of pure oxygen let into the dissolving vessel and tap E opened again. This flushing was repeated six times, which was found by experiment to be sufficient to carry the whole of the helium into the circulating system. The ventil F was then closed, the liquid nitrogen removed from the charcoal U-tube, and the circulating pump H set in operation, after having lifted the töpler valve. The palladium furnace L was then heated for 20 minutes to remove the remainder of the hydrogen, and the water vapour was trapped out in the liquid nitrogen trap. The circulating pump was then stopped, the tap J closed, the tap R opened, and, with the mercury in the column raised, and the column charcoals cooled in liquid nitrogen, the oxygen carrier plus helium töplered into the first charcoal tube.

(c) Estimation of Helium.

The column was then set to do 15 operations. Next, the mercury in the large compression bulb was raised, and the tap to the measuring pirani opened. Any deflection observed indicated imcomplete preliminary evacuation of the column while baking the charcoals, and invalidated the experiment. In practice however, only once did this happen. The column was then set to do operations 16 - 36 and the amount of helium collected in this interval was measured on the pirani gauge. This represented 99.3% of the total helium. At least two calibration readings were then taken with pure helium as indicated in Chapter 4, Section I.

The column was then set for operations 37 - 42, when the

remaining 0.7% of the helium should come through. The deflectio for operations 37-42 were measured, and the column set for operations 43-48. If any deflection were observed, it would be due to neon, and would indicate either a leak in the dissolving vessel or circulating system or else incomplete preliminary flushing of the dissolving vessel and reagent. This criterion was always applied in earlier work, and in the present work until the presence of ^3He was definitely confirmed. When ^3He was found in meteoric helium, meteoric Neon was then looked for, and in fact a small amount of meteoric Neon was observed in some samples from meteorites with high helium contents. The amount of neon was about 170 times smaller than the amount of helium.

Many of the helium samples prepared for mass spectrometric analysis were of the order of 10^{-4} ccs. N.T.P. which meant that the pirani gauge had to be set to its lowest sensitivity to be able to measure such a comparatively large amount. When all the helium had been brought through the column, the pirani gauge was then set to a very high sensitivity, more than 100 times higher than before and the amount of neon measured. The results are given later.

With the older method, when the pirani sensitivities were much lower, the sensitivity range used for the helium measurement was already the best possible, and an amount of neon 100 times smaller than the helium would pass undetected. Only then, in the cases where the amount of neon was of about the same order of magnitude as the helium, was the above-mentioned correction for atmospheric helium contamination applied.

FIG. 9

"TREYSA"

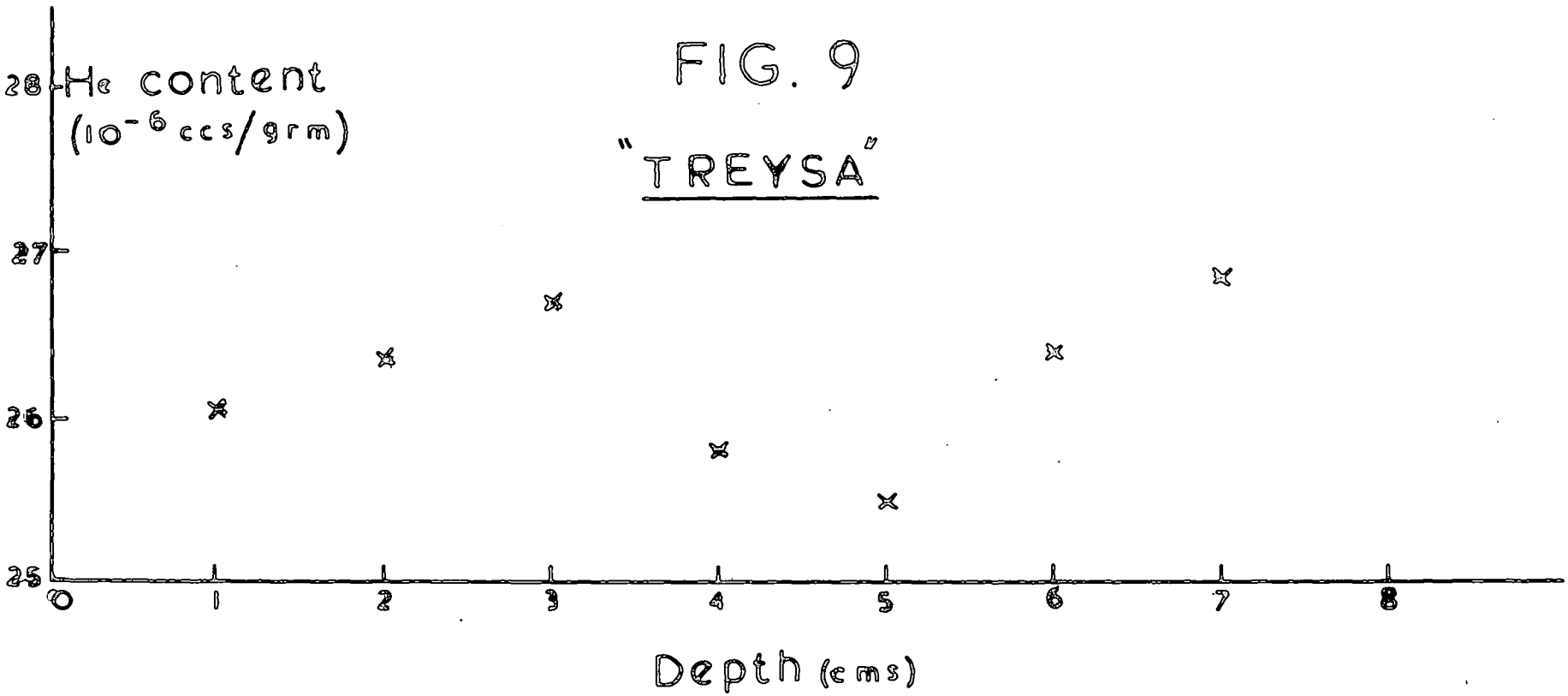

In this case, it would be necessary to bring the rest of the neon through the column by completing the operations up to 61, measure it, and then obtain a correction figure by calculating from the amount of neon present the amount of atmospheric helium present in the meteoric helium sample. Again, in practice, this was never necessary as no comparable amount of neon was found to come through the column during an ordinary meteorite experiment designed solely to measure the helium content, where only 10^{-6} ccs. of meteoric helium were used.

Section (3). Investigation of "Depth Effect" with Treysa Meteorite.

By courtesy of the authorities of the Mineralogical Institute of the University of Marburg, a series of special drillings were obtained from the Treysa meteorite, which is roughly spherical and of radius 12 cms. The samples were taken at one cm. intervals from one to seven cms. in depth.

Results:

TABLE 10.

Depth, in cms.	Series I.	Series 2.	Repeat.	Mean.
1	26.07	Spoilt by air leak.	26. 03	26.05
2	Spoilt by air leak.	26.43	26.27	26.35
3	26.91.	26.47		26.69
4	25.13	26.32		25.73
5	25.55	24.77	26.18	25.50.
6	26.42	26.42		26.42
7	26.86	26.86		26.86

At the time of carrying out the above determinations, it was not known at what depth the decrease in helium content would be detectable, and since the results were so close together, e.g. the helium content at 2cms. is almost exactly the same as at 6cms they were taken to indicate that no depth effect was to be found and that therefore no appreciable cosmic ray influence was apparent. As will be shown later, this was erroneous.

Investigation for "Depth Effect" with the available samples of Toluca (British Museum) and Toluca (Durham).

Samples of the meteorite "Toluca" were available for investigation. A flat slab of Toluca, the property of Professor F.A.Paneth, is kept at Durham, and another flat slab of Toluca in the British Museum. It seemed likely, from the orientation of the Widmannstätten figures with respect to the remains of the outer crust, that these two slabs had been fairly close together in the original mass before cutting.

It therefore appeared worth while to investigate samples from these, although the data on the positions of the drillings taken, with respect to the original mass, was somewhat uncertain.

Results: Toluca (Durham) Slice. T A B L E 11.

Position.	Helium Content ($\times 10^{-6}$ ccs/grm.)
Centre (C)	19.82. 19.63. Average: 19.72.
Top Edge (E)	19.67 19.32 Average: 19.50.

The distance between B and C is 15 cms.

Toluca (British Museum) Slice.

T A B L E 12.

Position.	Helium Content (x10^{-6} ccs/grm.)
Edge (Outer Slice) (A)	19.14 19.19. Average: 19.16
Edge (Inner Slice) (b).	20.07 20.59 20.04 Average: 20.24
Centre (Inner Slice) (C).	19.23 19.14 Average: 19.18.

The distance between A and C is 18 cms.
The distance between B and C is 14 cms.
The distance between A and B is 14 cms.

Since the position of the above samples, within the original mass, were so ill-defined, it is impossible to say whether or not the small differences in helium content represent any significant "depth effect".

In addition, a further sample of Toluca was investigated.

Toluca (Hamburg, Suess).

T A B L E 13.

Determination No.	Helium content (x10^{-6}ccs/grm.)
1. 2.	0.17 0.15 Average: 0.16

Again, although it is thought that the Hamburg (Suess) specimen came from the same fall as the Durham and British Museum

FIG. 10 – SKETCH OF "CARBO"

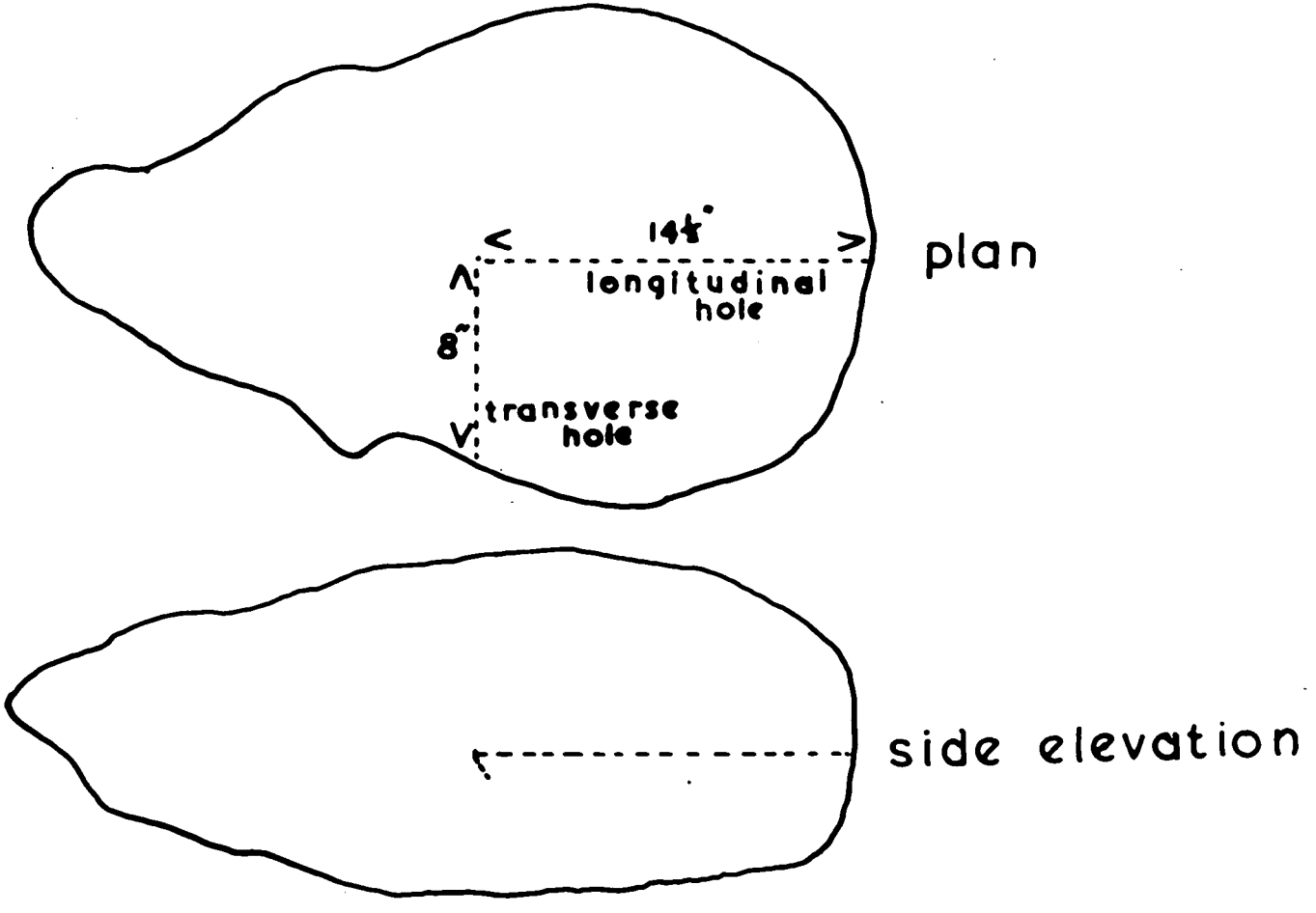

specimens (28), the evidence that they were part of the same original mass is so scanty that the large difference in helium contents cannot be taken as evidence of a depth effect.

Investigation of the "Depth Effect" in "Carbo".

The meteorite "Carbo" seemed a particularly promising specimen for an investigation of the depth effect, since it was a large though rather irregular mass of about 450 kg. Its shape was not spherical, but rather conical, as shown in Fig.10, but at least it offered the possibility of obtaining samples at much greater depths from the nearest surface than had hitherto been available.

At first, samples of a few milligrams were dissolved for investigation by the method given in Section 2 of this chapter, but later it was found possible to measure both the absolute helium content and the ^3He and ^4He ratio on one and the same sample, so that samples of 5 - 10 grms. were then used as described in Section 4.

Samples from two bore-holes, at right angles to each other, were available, the inner ends of the bore holes being only a few cms. apart.

Results:

T A B L E 14.

Longitudinal Hole.		Transverse Hole.	
Depth (cms)	He content (x 10^{-6} ccs/grm)	Depth (cms)	He content (x 10^{-6} ccs/grm)
0	23.03	0.5	19.45
0.5	22.30	3	20.25
1.5 c	21.70	5.5	19.24
2.5 - 3	21.06	6	19.01
3	20.81	12	18.64
6	19.50	18.5	17.50
9.5	18.53		
13	17.60		
17	17.24		
21	17.04		
28.5	16.83		
36	17.13		

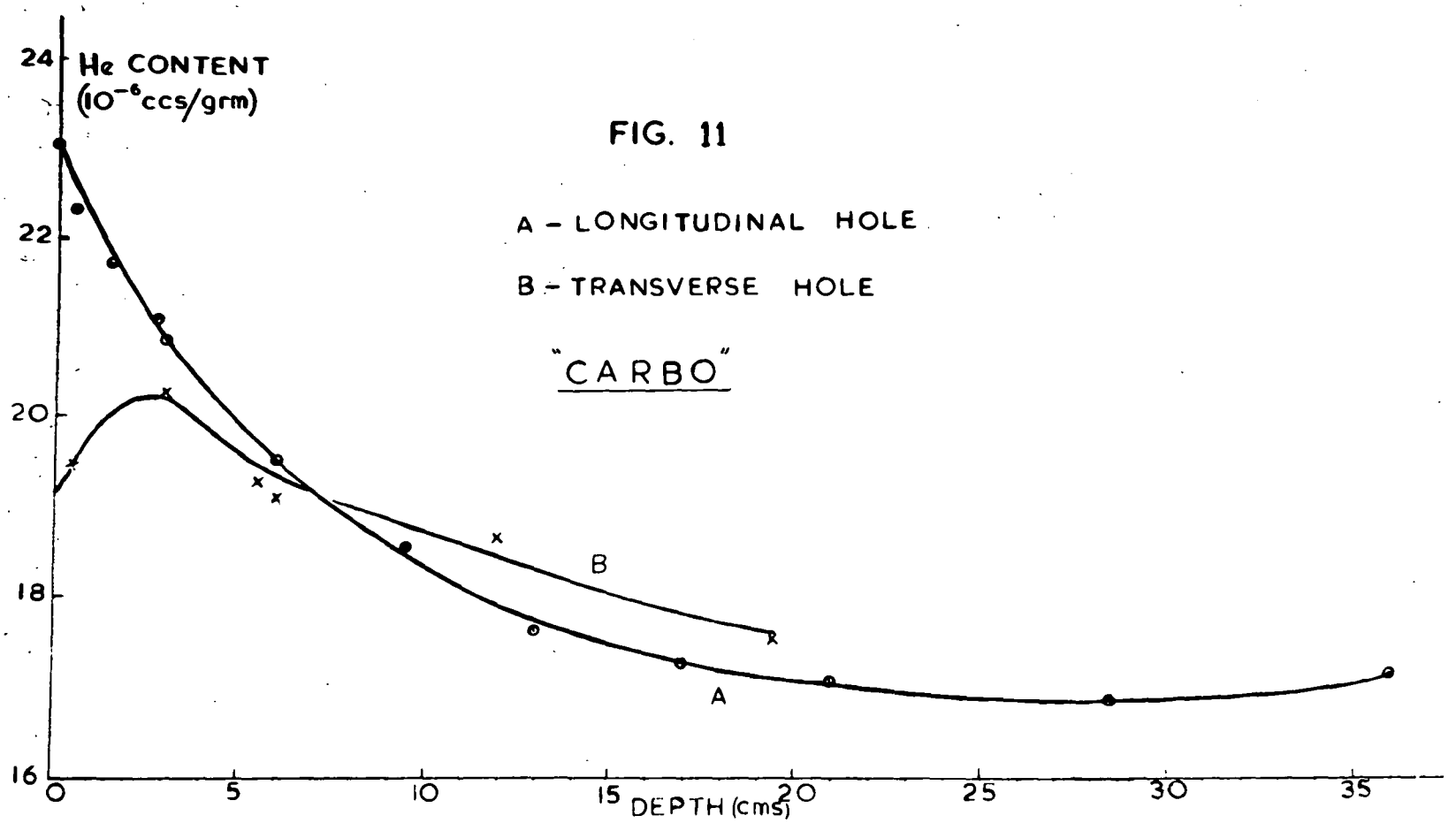

FIG. 11

A – LONGITUDINAL HOLE

B – TRANSVERSE HOLE

"CARBO"

Many of the figures quoted in the above table are the mean of at least two determinations, and the error is thought to be very small. Thus, for example, two determinations were done at the point 28.5 cms. along the longitudinal hole, and gave the figures 16.83 and 16.84 x 10^{-6} ccs/grm. respectively.

From Table 14, and Fig.11, it can be seen that at last a very clear demonstration of the "depth effect" in a meteorite is obtained. The curve for the longitudinal hole is extremely smooth, decreasing continuously towards the centre. It appears that this bore-hole goes past the "pre-atmospheric centre" of the meteorite, since a definite increase in helium content is observed between 28.5 and 36 cms. depth, so that the "true" centre appears to be at about 28.5 cms. along the longitudinal bore hole. The irregularity in the helium figures for the transverse hole seem to be accounted for by the fact that there is a hollow in the surface of the meteorite at a point above the 3 cms. depth position of the transverse bore-hole. In fact, the meteorite had never been moved from its stand in the Harvard Museum, the drillings being obtained in situ. The helium contents of the samples were then measured, and the irregularity noted in the transverse hole. When the figures were sent to the Museum authorities, Dr. Clifford Frondel had the meteorite turned

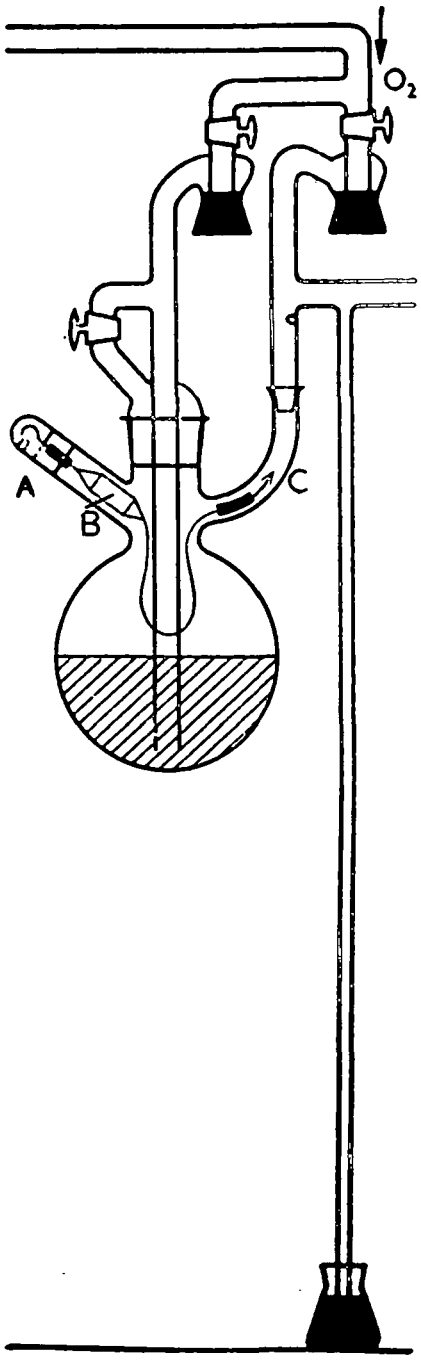

Meteorite-dissolving vessel.

FIG. 12

over, and the above-mentioned hollow was then found.

A discussion of the implications of the curve obtained for the longitudinal hole is given later in this chapter.

Section 4 - Determination of ^{3}He and ^{4}He ratios in Meteorites.

(a) Method of Dissolution.

Since it was desirable to have as large a quantity of helium as possible for mass spectrometric measurements, and in fact usually 10^{-4} ccs. was obtained with 10^{-5} ccs. in one experiment, and 10^{-6} ccs. in another, these last two being specimens with low helium contents, it was necessary to dissolve about 10 grms. of meteorite for each determination. This necessitated a much larger dissolving vessel than previously used, and to obviate the production of large quantities of hydrogen by acid dissolution cupric-potassium chloride solution was used (29), which gave no hydrogen evolution.

The dissolving section was designed as in Fig. 12. The bulb was about 600 ccs. volume. The meteorite shavings were kept in the glass bucket B in the side arm A until the reagent had been freed from dissolved air by bubbling through with pure oxygen about twelve times. The bucket was then lowered magnetically into the reagent, the shavings extracted, and the bucket and attachments lifted clear of the reagent, into the side arm C, to allow the reagent to be magnetically stirred. By this means, the meteorite shavings could be dissolved within 5 to 10 minutes. If this stirring is not carried out, the meteorite shavings tend to become covered with a layer of displaced copper, which stops further reaction.

(b) Measurement of Helium Content.

The transfer of the helium content to the circulating system was the same as described in Section 2 (b), except that O_2 was bubbled through the solution to remove dissolved helium, instead of electrolytic flushing. About 2 or 3 ccs. of water were removed in the cold trap, and as a precaution the gases were circulated through the palladium furnace for 20 minutes to ensure that if any hydrogen had been generated it would be removed. The fractionation of the helium was then carried out as before, and the helium amount measured on the pirani gauge.

(c) Transfer to Sample Tube, Addition of Carrier Gas, and Sealing Off.

The proportion of ^{3}Helium to ^{4}Helium was to be measured by two independent methods.

(i) By means of a mass spectrometer specially built to work in this mass range by Mr.K.I.Mayne, in the Clarendon laboratory, Oxford.

(ii) By neutron irradiation in the Harwell pile and measurement of the radio-activity of the tritium produced from the ^{3}Helium.

For method (1) it was necessary to dilute the meteorite helium with sufficient gas of a different mass to facilitate the gas handling operations in the spectrometer. Argon was chosen as most suitable for this purpose, and the arrangement of the Töpler pump S was as shown in Fig.29 . Two sample tubes at a time were sealed onto the leads from the two way tap. The meteoric helium sample was introduced into the measuring Pirani, and after measurement of the amount was töplered into a sample tube.10^{-2}ccs. argon was then töplered from the pipetting system

into the tube, the mercury raised nearly to the constriction, and the sample tube sealed off at the constriction.

For method (ii): Hydrogen was the most suitable filler gas, since it is isotopic with tritium and was therefore the best "carrier", and secondly it was feared that the small amount of tritium produced in the tube after irradiation would be partly taken up by chemi-sorption on the glass walls of the tube, and hydrogen would tend to prevent this. Since the temperature of the tubes probably rises during irradiation to about 100° C., it was necessary to fill the tubes only to about one-third of an atmosphere pressure. Special sample tubes had to be made, of thin-walled soda glass (about $\frac{1}{2}$mm. thickness) with the sample tube, break off septa, and sufficient tube left above the septa to seal on to the counting apparatus only about 5 cms long altogether. Also, it was necessary to know accurately the amount of helium which was actually sealed off in the tube, in order to be able to calculate the $^3He/^4HE$ ratio from the tritium activity. Thus, cylinder hydrogen was streamed into a reservoir through a large charcoal U-tube cooled in liquid nitrogen to trap out any traces of more adsorbable gases. A glass bulb was then made with two taps attached in series, and the space between them was calibrated by filling with mercury and weighing. The bulb and taps were then attached to the hydrogen reservoir, and the bulb filled to a pressure of 6.25 cms.which ensured that 10^{-1} ccs, of hydrogen were delivered by the pipette giving one-third atmosphere pressure in the sample tubes. The hydrogen was found to be free from helium by

putting a sample through the column in the normal way. The bulb and taps were sealed into place on the tube leading from the fractionating column to the large compression bulb. The meteoric helium sample was then obtained in the usual way, measured on the pirani gauge, töplered into the sample tube, and one pipette-full of hydrogen also töplered into the sample tube. The mercury was then raised right up into the constriction and the sample tube sealed off very carefully with a specially made small gas jet. The position of the mercury inside the constriction was fixed by a scratch mark on the glass, the end of the tube broken off, and the dead space volume measured by filling with mercury to the scratch mark and weighing. This volume was in each case only about 1×10^{-3} ccs. The volume of the sample tube was obtained by measuring carefully with calipers, and the dead space volume left behind was always $\leq$ 0.5% of the sample tube volume.

In each of the above two methods, sample tubes containing only argon or hydrogen respectively were also made up to serve as "blanks", and sample tubes were made up containing accurately measured amounts of a $^3He/^4He$ mixture obtained from Harwell of known ^3He ratio, to serve as calibration standards, with the appropriate filler gas added.

FIG. 13 _ "CARBO"

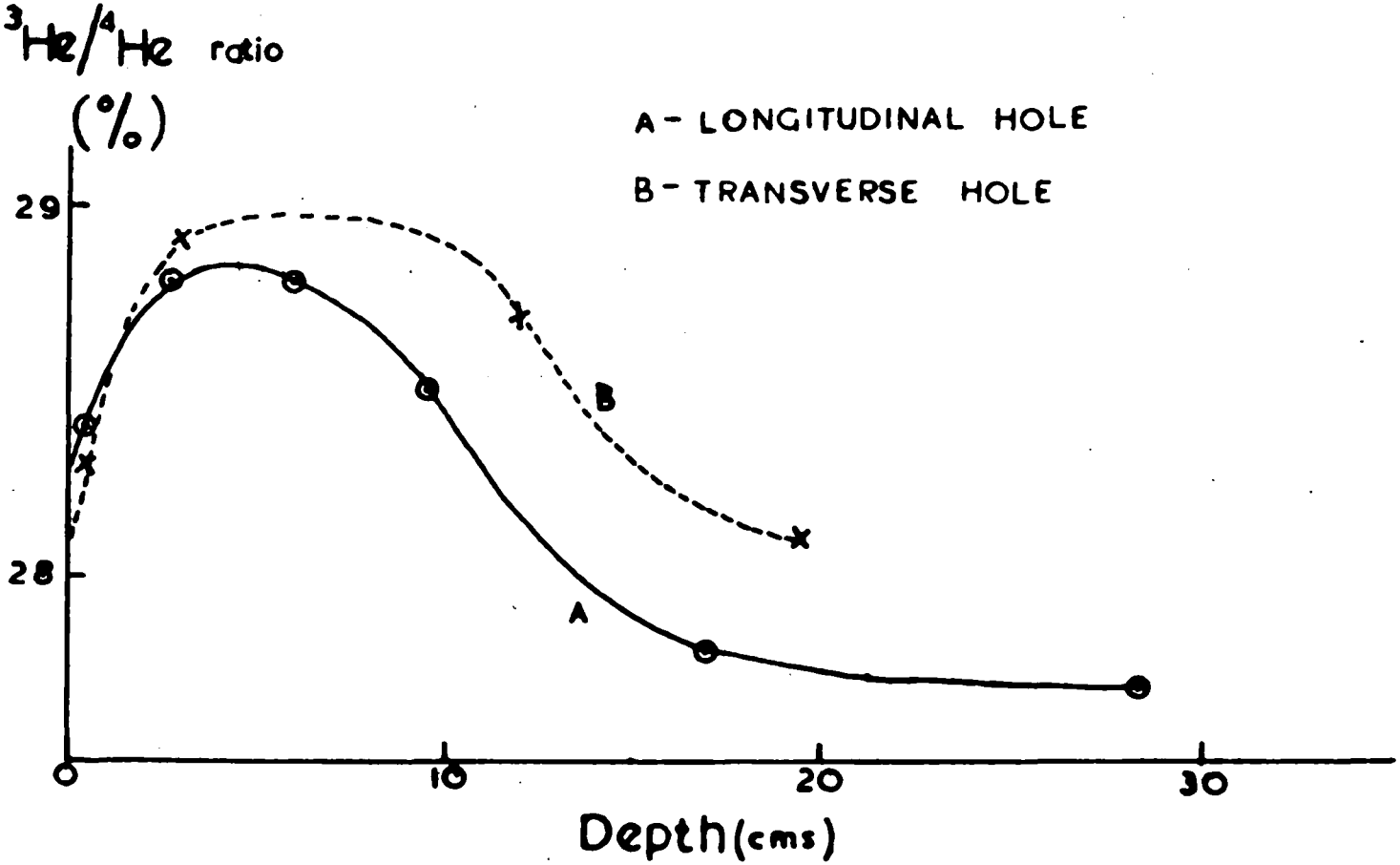
$^3He/^4He$ ratio
(%)
A - LONGITUDINAL HOLE
B - TRANSVERSE HOLE
29
28
A
B
0
10
20
30
Depth (cms)

Section 5. Results.

(1) Clarendon Laboratory Spectrometer.

(a) Calibration Samples.

TABLE 15.

No.	Argon Filler. x 10^{-1} ccs.	$^3He/^4He$ mixture. ccs. N.T.P.	$^3He/^4He$ ratio.	Remarks.
1	1.0	0	-	Blank sample for argon purity test.
2	0.96	1.04×10^{-2}	$3.71 \pm 0.02\%$	-
3	0.98	1.05×10^{-3}	$3.74 \pm 0.03\%$	-
4	0.73	1.27×10^{-4}	$3.73 \pm 0.05\%$	-

(Harwell spectrometer gave 3.91%. $^3He/^4He$ ratio.)

(b) $^3He/^4He$ ratios in "Carbo" meteorite.

TABLE 16.

Longitudinal Hole.		Transverse Hole.	
Depth (cms).	$^3He/^4He$. ratio (%).	Depth (cms)	$^3He/^4He$. ratio (%).
0.5	28.4	0.5	28.3
2.5-3	28.8	3.	28.9
6	28.8	12.	28.7
9.5	28.5	19.5	28.1
17	27.8		
28.5	27.7		

TABLE 17.

(c) $^3He/^4He$ ratio in 14 meteorite samples.

Name.	Total Helium Content. ($\times 10^{-6}$ccs/grm).	$^3He/^4He$ ratio (%).
Mount Ayliff.	36.8	31.5
Tamarugal.	23.59	30.9
Carbo.	22.0	28.6
Toluca (Durham)	18.9	29.7
Sacramento Mts.	11.21	30.75
Arispe.	5.32	27.2
Bethany (Amalia).	3.4	27.8
San Martin.	1.76	16.8
Henbury.	0.88	25.4
Negrillos.	0.46	19.0
Bethany (Harvard).	0.36	17.8
Coahuila.	0.20	23.3
Uwet.	0.17	11.0
Toluca (Hamburg).	0.16	19.6

TABLE 18.

(d) Neon Measurements.

Name.	He. content ($\times 10^{-6}$ccs/grm).	Ne. Content ($\times 10^{-6}$cc/grm.)	He/Ne ratio.
Toluca (Durham)	18.6	11.4	164.
Carbo (0.5 cms)	22.36	13.2	169.
Carbo (3 cms)	20.94	12.3	171.

It must be stressed that these neon measurements were carried out incidental to experiments which were really designed to obtain helium for $^3He/^4He$ ratio determinations, and that therefore the highest degree of accuracy was not attempted in the measurement of the neon. However, it seems certain that meteorites do contain some neon, probably of cosmic ray produced origin, and that the neon content is about 170 times smaller than the helium content.

(ii) Tritium Method.

The counting of the tritium in the sample tube after irradiation in the pile was undertakem by Dr. K.F. Chackett, and Dr. E. Barrett at the University of Birmingham.

Four calibration samples, containing 1×10^{-3} ccs. of 3% $^3He/^4He$ mixture, one tube with 1×10^{-1} ccs. of atmospheric helium, two tubes with 1×10^{-4} ccs. of meteoric helium, were used, all these being filled in addition with 1×10^{-1} ccs. of pure hydrogen, and one tube containing 1×10^{-1} ccs. of pure hydrogen alone to act as a "blank" was used.

It was shown that the gaseous activity was due to tritium by an investigation of the shape of the β spectrum by means of a proportional counter.

It soon became obvious that several difficulties had arisen.

(1) The difficulty of releasing the tritium quantitatively from the irradiated ampoule.

It was observed that, after the ampoule had been broken, an

the gas inside taken into the counting apparatus, more tritium was released from the walls of the ampoule.

(2) Adsorption effects on the walls of the geiger tube, probably due to the discharge itself, driving ions containing tritium into the walls, and making decontamination between runs almost impossible.

(3) The ^3He content of the samples, and hence the counting rate, was too high. (Up to 100,000 c.p.m. were recorded from a sample which had contained 4×10^{-5} ccs. of ^3He).

Because of these difficulties, and since the quantity of ^3He in meteorites was found to be quite large enough to handle accurately by mass spectrometric means, it was decided to discontinue the tritium method.

However, it should be pointed out that if it is necessary later to investigate the $^3He/^4He$ ratios of meteorites with very low helium contents, this method - due to its high sensitivity - may well offer an advantage over the mass spectrometric method.

Section 6 - Discussion of Results for "Depth Effect" in Carbo.

I- Calculation of Cosmic Ray Production of Helium.

Bauer's Picture : An isotropic flux of cosmic ray particles in free space of 1.5 parts/cm^2/sec --- exponential absorption with absorption m/f/p of 150 g/cm^2 in iron and producing an average of one He nucleus per disruption.

This picture was totally altered by the discovery (30) of pi mesons. Pi mesons, produced in substantial numbers by primaries, themselves strongly interact with nucleons, and consequently a "transition effect" in the number of interactions with increasing depth is to be expected.

New Picture. High energy primaries disappearing as a result of collisions will give rise to low energy evaporation particles (some of them He nuclei) but also to pi mesons and secondary protons and neutrons sufficiently energetic to initiate further star production - so called shower particles - and a proportion of these secondary particles will be sufficiently energetic to initiate further "showers".

In the calculations undertaken to determine the depth dependence of helium production in meteorites by cosmic rays (31) it has been assumed that the direction of motion of the primary particles is preserved by particles of subsequent generations, and from considerations of conservation of momentum, this will be sufficiently near the truth for the high energy particles and only in these would any variation be important.

The calculations are confined to iron meteorites, and since the only impurity present in these to any significant amount is nickel (up to 15% in some) the treatment is applied to an infinite slab of iron.

Since the energies of the star producing particles are well above the Coulomb barrier, and it seems that in this case the interaction cross section is almost independent of the nature and

and energy of the incident particle, the number of primaries will be attenuated exponentially so that, at any depth x, the residual intensity of primaries will be given by :-

$$J_1 = J_o \, e^{-\mu x}$$

where $= \frac{Na\rho}{A}$ (absorption coefficient)

where N is the Avogadro Number

a is effective cross section of the iron nucleus.

ρ is the density of iron.

A is atomic weight.

Jo is the intensity of flux in free space

The rate of interaction per unit volume of iron will be

$$I_1 = \mu J_1 = Jo\mu e^{-\mu x}$$

and rate of production of "evaporation" particles by the primary radiations at this depth will be

$$N_1 = I_1 \cdot Y_1 = Y_1 \cdot Jo\mu e^{-\mu x}$$

where Y_1 is the mean yield of evaporation particles per interaction.

These interactions will also produce secondary particles at a rate given by :

$$S_1 \cdot Jo\mu \, e^{-\mu x}$$

Where S_1 is the mean shower particle yield from the interaction of a primary particle with an iron nucleus.

The flux of the "first generation" secondary particles at any given depth can be obtained by solving the differential equation representing the difference between the rate of formation of secondary particles, and the rate of their disappearance

by nuclear interactions, the latter given by: $I_2 = \mu J_2$

So that $\frac{dJ2}{dx} = S_1 Jo\mu e^{-\mu x} - \mu J2.$

Integrating, and inserting $J_2 = 0$ at $x = 0$.

$J_2 = S_1 Jo\mu^2 x e^{-\mu x}$

This flux of secondaries will give rise to interactions at a rate of I_2 equal to: $\mu J_2 = S_1 Jo\mu^2 x e^{-\mu x}$

and will produce evaporation particles at a rate :

$$N_2 = I_2 Y_2$$

$$= Y_2 S_1 Jo\mu^2 x e^{-\mu x}$$

where Y_2 is the mean yield of evaporation particles per interaction of a secondary with an iron nucleus (the energy spectrum being that appropriate to the secondary particles).

Similarly, the flux of the third generation of high energy particles with a mean shower particle yield S_2 can be obtained if the energy spectrum of the secondary particles is known.

In general, the flux of the nth generation of energetic particles is:

$$J_n = \frac{1}{(n-1)!} Jo\mu^{n-1} x^{n-1} e^{-\mu x} S_1 . S_2 \cdots S_{n-1} \quad (n > 1).$$

and the corresponding number of evaporation particles will be :

$$N_n = \frac{1}{(n-1)!} Jo\mu^{n} x^{n-1} e^{-\mu x} Y_n . S_1 . S_2 \cdots S_{n-1}.$$

Thus, the total rate of helium production at depth x will be given by the sum of all such terms, multiplied by α , the fraction of the evaporation particles which yield helium, i.e. those particles initially ^3H , ^3He, or ^4He.

The helium yield per gram of iron at depth x, is:-

$$H(x) = \frac{\alpha}{\rho} \cdot \sum N_n$$

$$= \frac{\alpha}{\rho} J_0 \mu e^{-\mu x} \left[Y_1 + \mu x \cdot S_1 Y_2 + \frac{\mu^2}{2!} \cdot x^2 \cdot S_1 S_2 Y_3 + \frac{\mu^3}{3!} x^3 S_1 S_2 S_3 Y_4 + \ldots \right] \quad \text{---- (i)}$$

The energy spectrum of the secondary particles is more or less independent of the energy of the incident radiation (32). Thus the mean yield of evaporation particles and the mean shower yield will be the same for successive generations after the first and hence we can put: $Y_2 = Y_3 = Y_4 - - - = Y_n$

and

$$S_2 = S_3 = S_4 - - - = S_n$$

Hence equation (i) can be rewritten :

$$H_{(x)} = \frac{\alpha}{\rho} J_0 \mu e^{-\mu x} \left[Y_1 + \frac{S_1 Y_n}{S_n} \left(e^{\mu S_n x} - 1 \right) \right] \text{ atomsHe/gFe/sec/sterad - - - (2).}$$

The effect of the heavier cosmic ray mesons has been neglected in this derivation, since their yield is so small as to give no appreciable effect. The production of neutral pi-mesons has also been neglected, since their lifetime ($\sim 10^{-14}$ sec) is so short that they will almost all decay before interacting, and the resulting particles, μ mesons, electrons, high energy photons, etc. do not give strong interactions with nucleons.

The charged pi-mesons, on the other hand, which normally decay in the atmosphere before interaction, with a lifetime of 2.54×10^{-8} sec(33) corresponding to a mean decay length of 10^3 cm. will almost certainly undergo a nuclear interaction in iron and have hence been included in the above treatment.

Evaluation of parameters in expression (2).

The primary cosmic radiation appears to be composed of positively charged nuclei of very high energy. It seems that about 85% of the primaries are protons, and almost all the rest ^{4}He nuclei, with heavier nuclei only contributing about $\frac{1}{2}$ to 1% (34)(35). Since, at the very high energies concerned, the nuclear interactions of the primaries are more or less independent of their "chemical" nature, they have all been treated as protons, which assumption should not give rise to any significant errors.

In deducing an empirical expression for the energy or momentum spectrum of the primary radiation, three energy regions have to be considered:

(i) The very high energy region where geomagnetic effects are of little value in analysing the spectrum. A consideration of the size distribution of extended air showers (36), and absorption of radiation underground (37) has led to general agreement on a power law spectrum of the form: $F(E)\,dE \propto \frac{dE}{E^{2.67}}$

This method has only been applied between the energy limits 50 B.e.v. to 5×10^3 B.e.v. leaving a large gap between 50 B.e.v. and the maximum 15 B.e.v. of the spectrum deduced from geomagnetic effects. The consequent uncertainty will not be very important, since the number of particles with energies in this region is comparatively small.

(ii) The spectrum of the lower energy end has been investigated by measuring the energy flux or number flux of the primary radiation as a function of geomagnetic latitude. Thus Van Allen and

/Singer

(38) obtain:

$$J\ (>\xi) = \frac{0.48}{\xi^{1.1}}$$

ξ is magnetic rigidity $\left(\frac{pc}{ze}\right)$ of particle in 10^9 volts.

The form $F(E)dE = \frac{0.0480E}{E^{\frac{2}{3}}(1+0.09E^{\frac{4}{3}})^{\frac{3}{2}}}$

(E is particle Energy in B.e.v.)

is due to Neher (39) and the form :

$$J\ (>E) = \frac{0.30}{E^{0.90 \pm 0.05}}$$

is due to Winkler et al (40) (where the primaries are assumed to be all protons).

(iii) There appears to be no particle of energies less than about 1 B.e.v. At latitude above about 56°N, where the permitted access of particles of energies less than this value would be expected, no such increase in flux is found. Janossy (41) has suggested that the cut off is due to the magnetic field of the sun, but von Kluber (42) found no evidence for such a magnetic field. The suggestion has also been made that particles of energies of less than 1 B.e.v. may be stopped by interstellar matter.

For the region 1 to 15 B.e.v. a form of the spectrum similar to Van Allen and Singer's and also Winkler et al has been adopted, but with Jo (the absolute flux) half way between the value 0.144 parts/sec/cm^2/sterad obtained by Nehers ionisation current measurements and the value 0.29 parts/sec/cm^2/sterad obtained by Winkler and Van Allen and Singer by counter telescope methods, namely: Jo = 0.22 parts/sec/cm^2/sterad.

This gives: $J \quad (> E) = \frac{0.22}{E^{0.95}}$

or

$$F(E)dE = \frac{0.21\,dE}{E^{1.95}}.$$

Thus the differential energy spectrum for the whole range will be given by:

$F(E)dE = 0 \quad (E < 1.0$ B.e.v.)

$= \frac{0.21dE}{E^{1.95}} \quad (1.0 < E < 15.^0$ B.e.v.)

$= \frac{2.57dE}{E^{2.67}} \quad (E > 15.0$ B.e.v.)

Interaction cross section of iron for protons and pi mesons.

For high energy particles, the heavier elements show a cross section which is more or less independent of the energy and nature of the particle, and is only a little smaller that the "geometrical" cross section of the nucleus. Taking the value of $r = 1.5 \times 10^{-13} A^{\frac{1}{3}}$ cm. for the nuclear radius due to Bethe, and allowing a 20% "transparency" consistent with recent determinations for the heavier elements (43)(44), a value for the nuclear cross section of iron of : 0.86×10^{-24} cm^2 is obtained. This corresponds to an interaction mean free path of 108g/cm^2 or 13.5 cms. of iron, and gives a value of 0.074 for μ

Mean Yield of Shower Particles per Interaction.

Camerini et al (45) gives a representation of the relationship between incident particle energy and "shower particle" multiplicity of the form :

$$S = 0.47\,(E_1 - 0.5),$$

E_1 the incident particle energy in B.e.v.

obtained from photographic plate experiments, and which will therefore probably make no allowance for neutron production. On the basis of the usual assumption of the charge independence of nuclear forces, a neutron component about as large as the proto component is allowed for, assuming 20% of the shower particles to be protons (32) the estimated multiplicity must then be increased by 1.20 to allow for the neutrons.

The mean yield of shower particles per interacting primary particle is then given by:

$$S_1 = 1.20 \times 0.47 \frac{\int_1^\infty (E - 0.5)\, F(E)dE}{\int_1^\infty F(E)dE}$$

and, using the assumed energy spectrum, the value :

$S_1 = 2.89$ is obtained

Similarly, using the form of energy spectrum suggested by Camerini et al (33), and assuming that this is valid for all generations of secondaries, the shower multiplicity of the secondary particles, Sn is obtained, giving : $Sn = 0.252$ $(n>1)$

Mean number of Evaporation Particles per Interaction.

Camerini, Lock and Perkins (46) give a graphical representation of the yield of evaporation particles as a function of the energy of the incident particles, which follows a law of the form

$Y(E) = 7.0\, E^{0.36}$ (E in B.e.v.)

Integrating the product of Y(E), and the assumed primary energy spectrum function gives the mean yield of evaporation particles per interaction for the primary radiation, or:

$$Y_1^H = \frac{\int_1^\infty Y(E)\ F(E)dE}{\int_1^\infty F(E)dE)}$$

which gives $Y_1^H = \underline{10.73}$.

But this Y_1^H makes no allowance for the presence of neutrons and since (47) the grey particles (protons) make up about 25% of the total heavy tracks, an addition of 25% will have to be made to allow for neutrons not included in the above treatment, giving

Y_1^{Total} = 13.41 evaporation particles/star

Of these (48), 24% will be ^3H, ^3He, or ^4He (i.e. $\alpha = 0.24$) giving

$Y_1^T \alpha$ = 3.22

But, in addition, there will be a further helium production associated with this "first star" due to the nuclear interaction of the "grey" protons and neutrons amongst the evaporation particles at a distance from the parent star of the order of one interaction length away. About one sixth of the protons(49) interact, while presumably all the neutrons do, so that we have seven twelfths of 5.36 evaporation particles/parent star(protons plus neutrons in Y_1^T) which will give rise to further stars, 24% of whose evaporation particles should also be ^3H, ^3He or ^4He, so that an additional Y_1^G of 7/12 x 5.36 x 0.24 will be associated with the parent star. This gives a total $Y_1 \alpha$ of 396.

Similarly, assuming the constant energy spectrum of the

FIG. 14

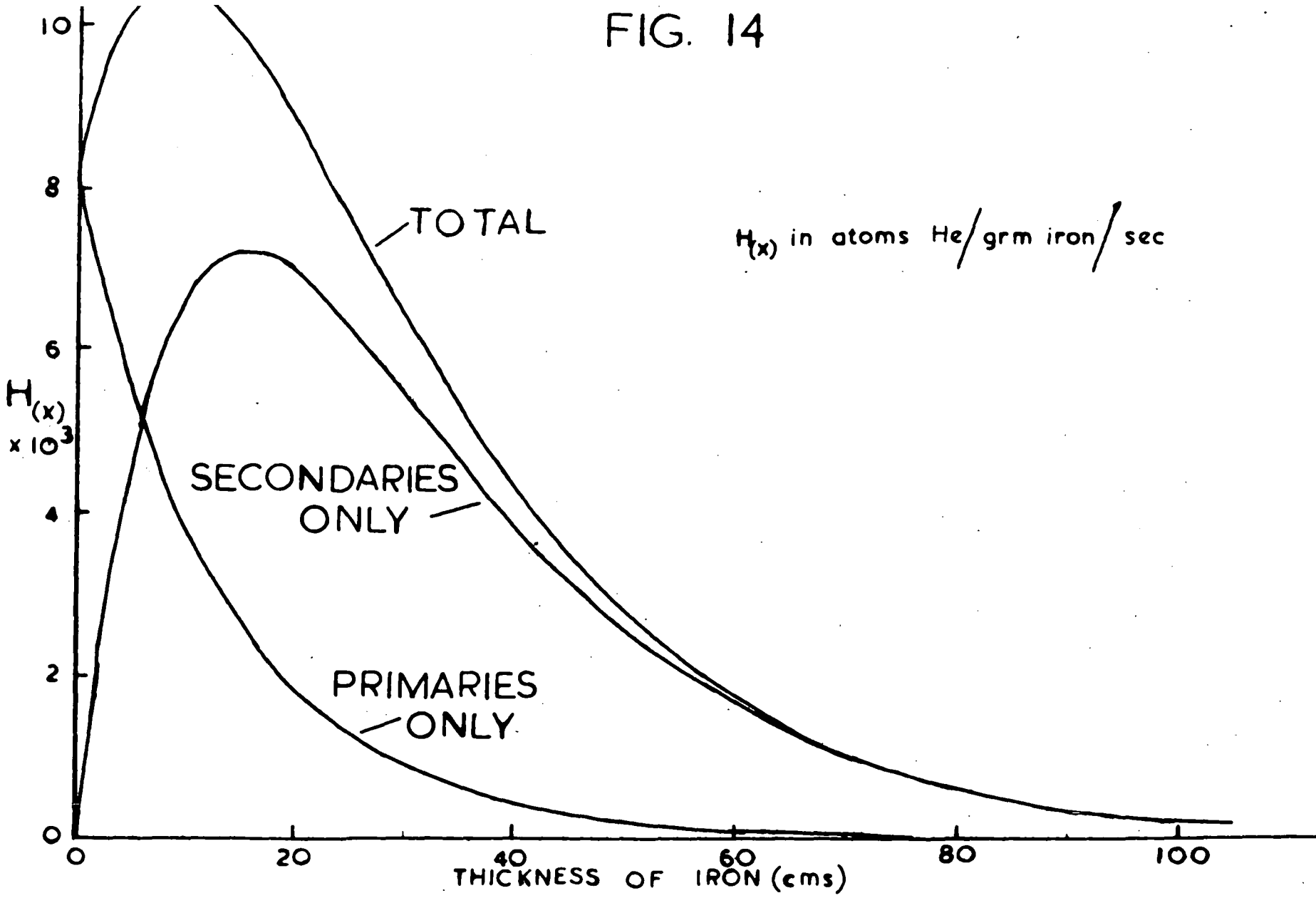
TOTAL
$H_{(x)}$ in atoms He/grm iron/sec
SECONDARIES ONLY
PRIMARIES ONLY
$H_{(x)}$ x 10^3
0
2
4
6
8
10
0
20
40
60
80
100
THICKNESS OF IRON (cms)

secondaries as before (32), the yield function of Camerini et al (46) is applied for particle energies greater than 1.4 B.e.v.sinc the interaction above this value may be regarded as essentially inelastic, but for particle energies lower than 1.4 B.e.v. which may be considered as giving rise to elastic interactions, the yield function of Le Couteur (50) is used. Further, on similar considerations to those in the preceding paragraphs of the additional star production by the protons and neutrons among the evaporation "tracks" of the "parent star" it may be deduced that

$$Yn\,\alpha = 2.89$$

that is, the yield of particles in the form ^{4}He, ^{3}He or ^{3}H per secondary induced star will be 2.89. All of these particles will of course, after the lapse of sufficient time to allow the ^{3}H to decay to ^{3}He be included in the total helium.

The numerical values for the various parameters can now be inserted into the equation (2) and give:

$$H_{(x)} = 203 \times 10^{-3}\, e^{-0.074x}\,(3.96 + 33.14(e^{0.0186x} - 1))$$ atoms of helium/grmFe/sec/sterad at depth x - - - - (1)

This relationship is shown grephically in Figure 14, together with the helium contribution from the primaries and secondaries respectively. Further, the rate of helium production at the centre of a spherical mass of iron, radius r, isotropically irradiated by cosmic rays, will show the same dependence on the radius of the mass, and hence the central helium yield will be :

$H_{(r)} \times 1.47 \times 10^{-11}$ ccs/He/gFe/year/4π solid angle.

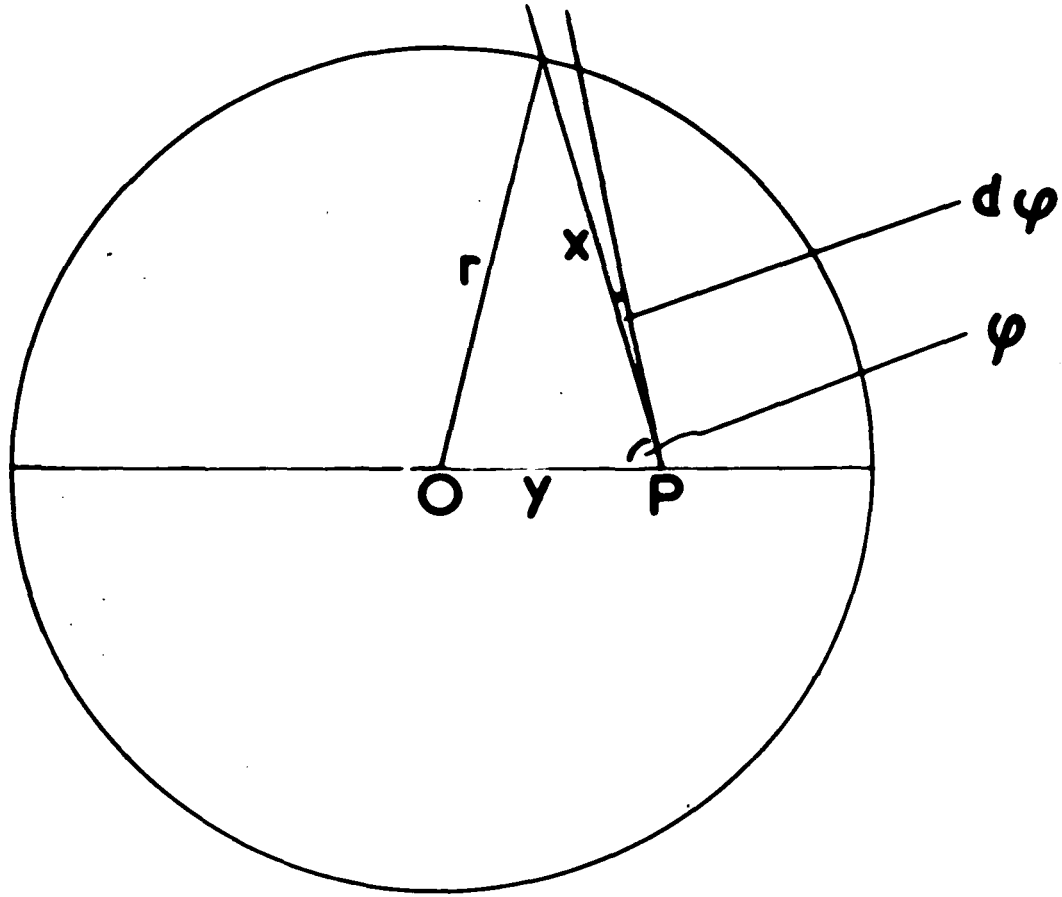

FIG. 15

(Iatom/sec/sterad = $\frac{3.15 \times 10^{7} \times 2.24 \times 10^{4} \times 4\pi \text{ cc/yr}}{6.02 \times 10^{23} \times 4\pi \text{ solid angle}}$

$= 1.47 \times 10^{-11}$)

To transfer the treatment from a plane slab of iron to a sphere, consider Fig. 15. A point inside the sphere and not at the centr will be subjected to different intensities of radiation, and also varying proportions of primary and secondary radiation according to the varying thickness of iron traversed by particles in approa ching the point from different directions.

The total intensity of radiation reaching the point P (and therefore the rate of He production at P) in the solid angle between φ and $\varphi + d\varphi$ will be given by :

$$\frac{2\pi r^2 \sin\varphi \, d\varphi \cdot H_{(x)}}{r^2}$$

$$= 2\pi \sin\varphi \, d\varphi \, H_{(x)}$$

$$= 2\pi d \, (\cos\varphi) \, H_{(x)}$$

And the total rate of production of helium at point P by radiatio from 4π solid angle will be :

$$-2\pi \int_{-1.0}^{+1.0} H(x) \, d(\cos\varphi) \quad \text{---- (ii)}$$

Also from Fig.15: $r^2 = x^2 + y^2 - 2xy\cos$

$$\frac{x}{r} = \frac{y}{r}\cos\varphi + \sqrt{1 - \frac{y^2}{r^2}\sin^2\varphi} \quad \text{---- (iii)}$$

From (iii) (ii) and (i) the value of the integral at (ii) can be obtained graphically for various values of y.

FIG. 16

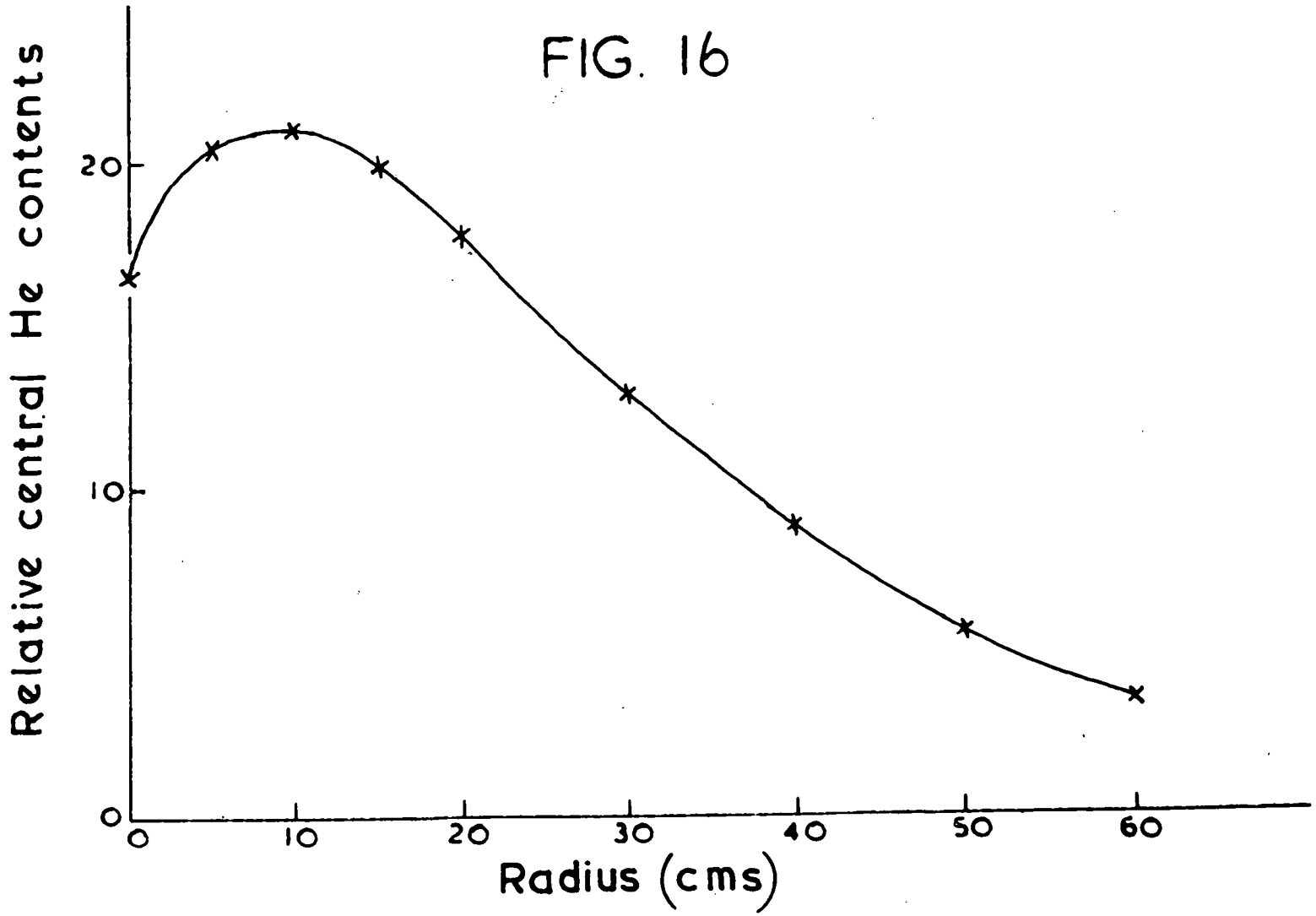
Relative central He contents
20
10
0
0
10
20
30
40
50
60
Radius (cms)

In this way, a complete table can be drawn up for $\int H_{(x)}\, d(\cos\varphi)$ for various radii of iron spheres.

T A B L E 19.

$\int H_{(x)}\, d(\cos\varphi)$ $\left(x \frac{10^3}{2\pi}\right)$

$\frac{y}{r}$	0	0.2	0.4	0.6	0.8	0.9	1.0
Radius (c.m.)							
0	16.29						
5	20.31						
10	20.94	20.87	20.74	20.43	19.85	19.17	17.84
15	19.72	19.71	19.69	19.66	19.30	18.52	17.18
20	17.62	17.54	17.78	18.18	18.15	17.52	16.17
30	12.72	12.52	13.58	14.73	15.82	15.90	14.42
40	8.60	8.94	9.79	11.44	13.59	14.47	13.11
50	5.52	5.91	6.90	8.86	11.79	13.32	12.18
60	3.50	3.83	4.82	6.79	10.33	12.06	11.52
80	1.296	1.58	2.32	4.03	7.64	10.57	10.66
100	0.46	0.617	1.080	2.42	5.97	9.28	10.15

These values for the helium content of irradiated iron spheres are relative values only since no figure has been inserted for the time of irradiation. To transfer them to absolute values, a known absolute helium content is inserted into the scale in the following way. An inspection of Table 19 shows that meteorites with radii of only a few cms. will be the ones with highest cosmic ray produced helium content. Further, plotting the values from the first column of Table 19 as in Fig. 16, shows that a meteorite of about 10 cms. diameter will have the highest possible central value for the cosmic ray helium content.

The meteorite "Morden" has the highest known helium content of 38.1×10^{-6} ccs/grm out of 70 different meteorites which have been investigated (51). Further, its post-atmospheric diameter of

FIG. 17

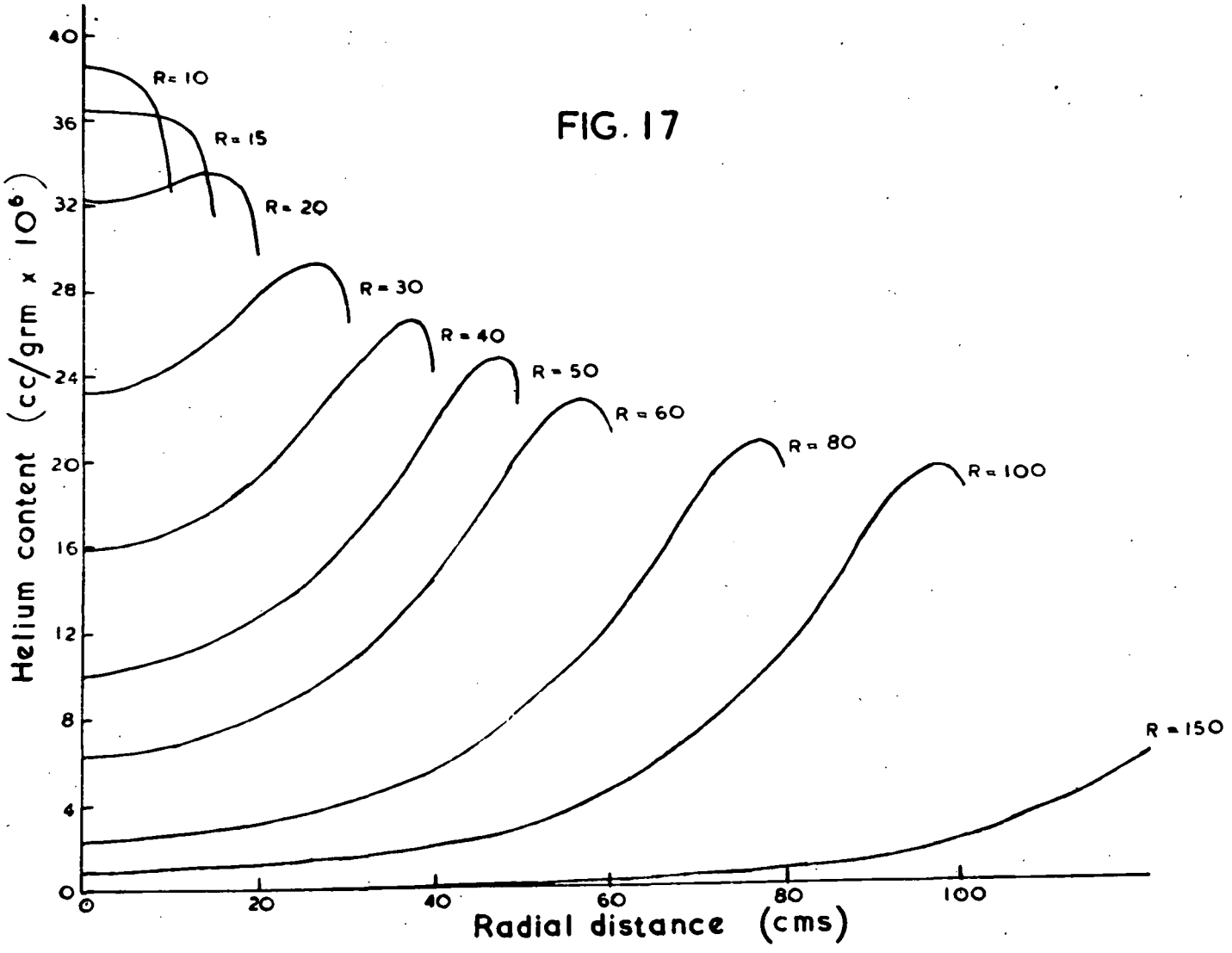
Helium content (cc/grm x 10^6)
Radial distance (cms)
R = 10
R = 15
R = 20
R = 30
R = 40
R = 50
R = 60
R = 80
R = 100
R = 150
0
4
8
12
16
20
24
28
32
36
40
0
20
40
60
80
100

8 cms. fits well, from the astro-ballistic considerations of Martin (52), with a pre-atmospheric diameter of about 10 cms.

Thus, the error involved in scaling up the relative values for Table 19 for a point 4 cms. distant from the centre of a sphere of 5 cms. radius to correspond to the absolute value of 38.1×10^{-6} ccs/grm. is probably not too serious, and involves the insertion of a scaling factor of 1.840×10^{-6} ccs/grm. From the values in Table 19, the lines in Fig. 17 can now be constructed.

Also, if all the helium in Morden is taken to be cosmic-ray produced helium, the time necessary to produce this helium content on the present day flux of cosmic rays, would be 2.52×10^{8} years. As will be shown later, it seems that the proportion of radio-genic helium in a meteorite so helium-rich as Morden will be extremely low, and thus not likely to alter significantly the above estimated time for helium production, calculated from the rate of production deduced earlier.

Conclusion.

When the experimental results for Treysa (central helium content 26×10^{-6} ccs/grm), Thunda (8) (central helium content 30.3×10^{-6} ccs/grm) and Carbo (Longitudinal hole) are superimposed, on the theoretical curves deduced by the above treatment from the central helium content of these meteorites, as in Fig. 18, it can be seen immediately why no clear radial variation in the helium content was observed with the first two meteorites, when only 8 cm. and 6 cm. radial distances respectively were available, whereas with Carbo, the variation is quite clear, and

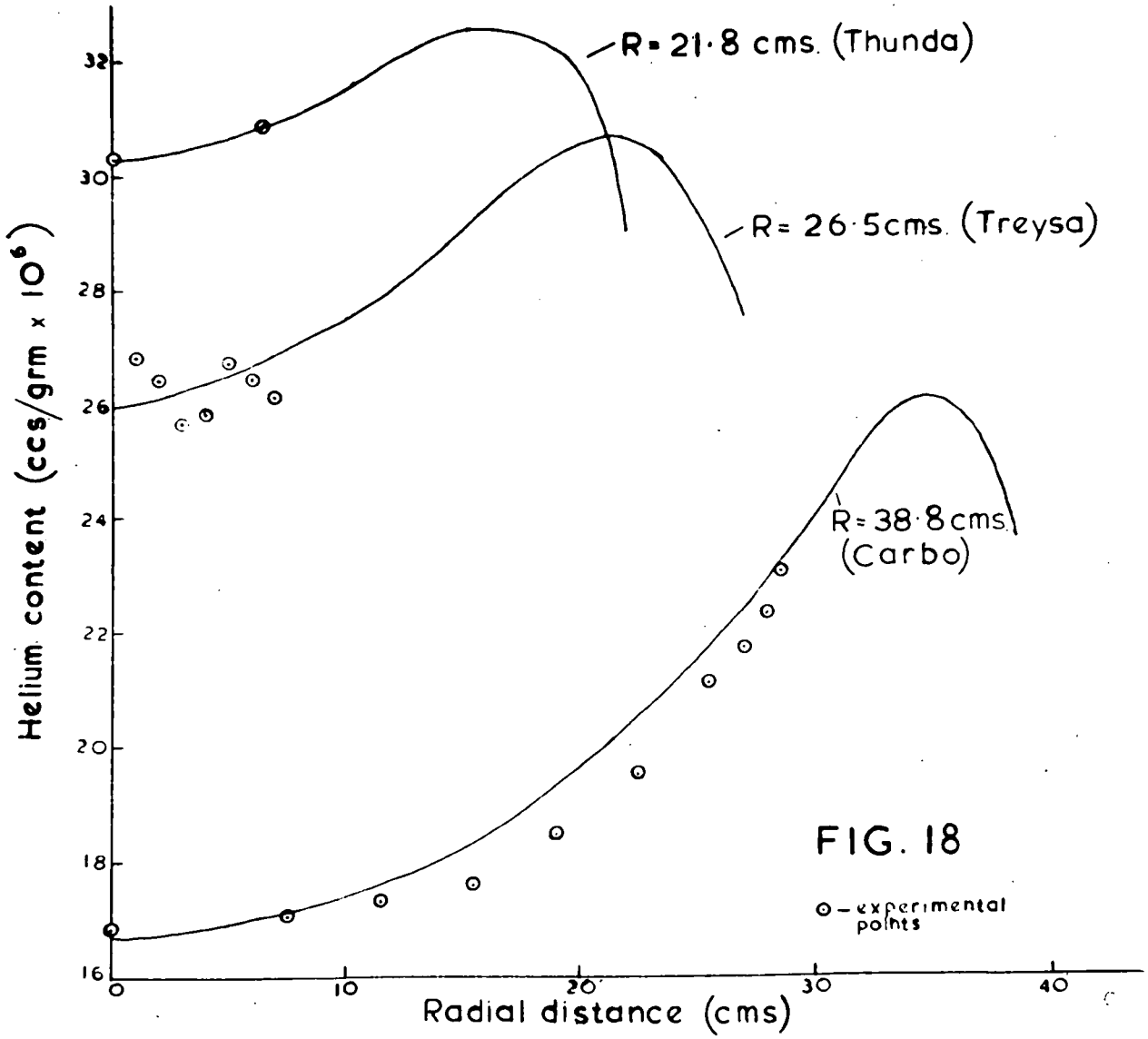
R = 21·8 cms. (Thunda)
R = 26·5cms. (Treysa)
R = 38·8cms. (Carbo)
Helium content (ccs/grm x 10⁶)
Radial distance (cms)
32
30
28
26
24
22
20
18
16
0
10
20
30
40
⊙ – experimental points

FIG. 18

furthermore, the experimental curve is as close to that derived by the foregoing theoretical treatment as could be expected. In fact, Carbo is not of a spherical shape, being nearer a conical form, and this has been allowed for as nearly as possible by the following method. The centre of the original mass has been taken to be at the point on the bore hole where the minimum helium content was found. (It will be noted that the helium content rises again between 29 and 37 centimeters depth along the bore hole). Distances from this centre point have been uniformly scaled down in the ratio (actual distance from this point to the present base of the cone; radius of a sphere of mass equal to the present mass) which involves a reduction in distances by a factor of about 0.86. In practice, this alters the conformity of the experimental curve with the theoretical curve very little.

With regard to the results for the transverse bore hole made in Carbo, it is felt that the "bump" in the curve is most probably explained by the fact that there is a large "hollow" in the meteorite, so that where the helium content would normally be decreasing with increasing depth, successive samples are in fact at decreasing depths from the nearest surface, until, the effect of the "hollow" is passed, and the helium content again decreased regularly.

Interpretation of $^3He/^4He$ ratio curves.

The figures for the $^3He/^4He$ ratio at various depths in Carbo are given in Table 20, and Fig.11.

T A B L E 20.

Longitudinal Hole.		Transverse Hole.	
Depth (cms)	$^3He/^4He$ Ratio%.	Depth (cms)	$^3He/^4He$ Ratio%
0.5	28.4	0.5	28.3
2.5-3	28.8	3	28.9
6	28.8	12	28.7
9.5	28.5	19.5	28.1
17	27.8		
28.5	27.7		

It was first suggested qualitatively by Dr. S.F.Singer, of the University of Maryland, that the rise in the first part of the curve in Fig. 14, Page 67 , for the total production of helium

by cosmic rays may be "filled in" by primary α particles stopping in the first few centimeters of iron.

Similarly, it seemed that the rise in the $^3He/^4He$ ratio curves over the first 5 cms. depth might be due to the stopping of primary α particles in the first few cms. of the meteorite, thus lowering the $^3He/^4He$ ratio in this range. As the flux of α particles decreases with depth, it is to be expected that the $^3He/^4He$ ratio will rise to a maximum, and then, as the mean excitation energy of the iron nuclei decreases with increasing depth, the $^3He/^4He$ ratio will decrease also, which would explain the shape of the curves.

To test this hypothesis, the attenuation of primary α particles in iron has been investigated quantitatively in the following way.

The Range versus Energy relation for α particles in iron can be deduced from the information in "Experimental Nuclear Physics" (53) and is given by :

$R = 6.7\,E^{1.69}$ or $E = 0.32R^{0.59}$

(R is range in g/cm^2, E in B.e.v.)

The Integral Energy spectrum for α particles in cosmic radiation is given by: $N(>E) = \dfrac{380}{\left(\frac{I+E}{4}\right)1.2}$ parts/m^2sec/sterad.

so that : $N(>R) = \dfrac{380}{\left(1+\frac{0.32\,R^{0.59}}{4}\right)1.2}$

$= \dfrac{380}{\left(1+0.08R^{0.59}\right)1.2}$

$$J_{(R)}\,dR = \frac{21.5}{R^{0.41}\left(1 + 0.08R^{0.59}\right)^{2.2}}\,dR \text{ particles/m}^2\text{/sec/sterad.}$$

$J_{(R)}$ will represent the number of α's stopping at depth R due to ionisation loss. Allowance is made for nuclear interactions of α particles as a cause of attenuation by multiplying the value of the number stopping at depth R by a factor

$$e^{-\frac{\mathcal{N}\varrho\sigma R}{A}}$$

where

$\mathcal{N}$ = Avogadro number.

ϱ = density.

A = At.wt.

σ = assumed interaction cross-section

This factor represents the proportion which have survived nuclear interaction in this distance.

Thus $J_{(R)}e^{-\mu R}$ $\left(\mu = \frac{\mathcal{N}\varrho\sigma}{A}\right)$

should give a measure of the ^{4}He production at varying depths for a beam of cosmic ray α particles, normally incident on a plane slab of iron, assuming that once an interaction between a primary α particle, and an iron nucleus has occurred, all trace of the incident particle is lost.

T A B L E 21.

R	$J_{(R)}e^{-\mu R}$ particle/grm/sec/sterad($\times 10^{-6}$)
5.	64. 3
10	27. 6
20	7. 6
30	2.6
40	0.95
50	0.36
60	0.15
70	0.057
80	0.024

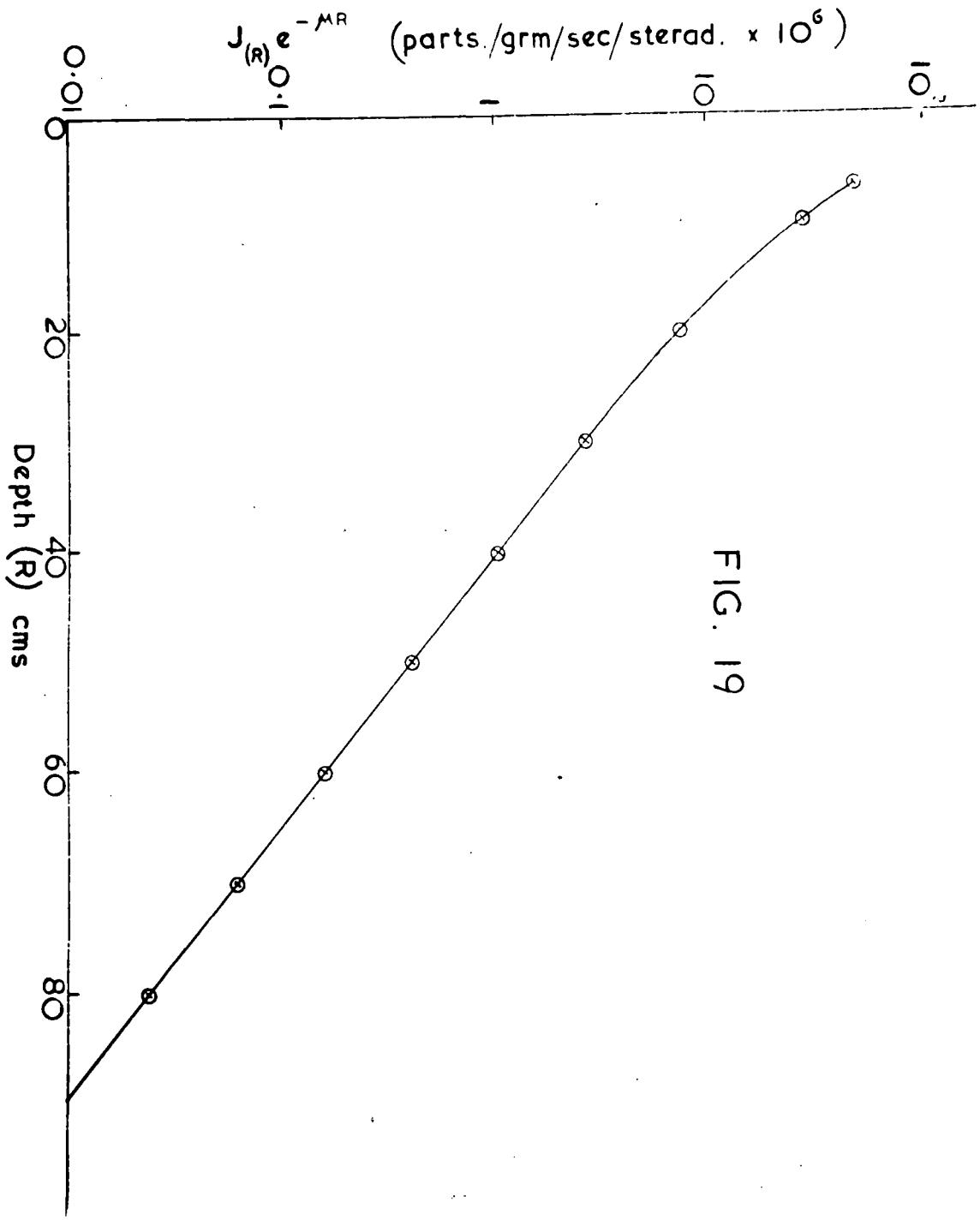
$J_{(R)} e^{-\mu R}$ (parts./grm/sec/sterad. x 10^6)
0·01
0·1
1
10
100
0
20
40
60
80
Depth (R) cms

FIG. 19

Due to the apparent existence of a sharp cut-off in the neighbourhood of 1 B.e.v. per α in the primary cosmic ray spectrum, it is to be expected that no α particles will be stopped in the first 6.7 cms. of iron by ionisation loss. Thus, a curve, as in Fig. 19, is obtained for the number of particles stopping at various depths in a plane slab of iron.

By integration of these values over a spherical body of radius 40 cms. (the apparent pre-atmospheric radius of Carbo (see Fig. 18)), for various points along a radius, Table 22 and Fig.20 is obtained.

TABLE 22.

Depth (cms).	Partic'e/grm/sec/4π solid angle x 10^{-6}
0	61.2
4	239.0
8	256.0
16	89.0
24	44.0
32	28.8
40	25.0

Now, since it appears from the previous section that about 8-10cms depth has been removed from the original meteorite, and that a good estimate of the time of irradiation of the meteorite is 2.52 x 10^8 years(or half this time at twice the average intensity)(as will be indicated later,which would give the same helium production)an estimate of the absolute amount of ^{4}He due to primary α

/particles

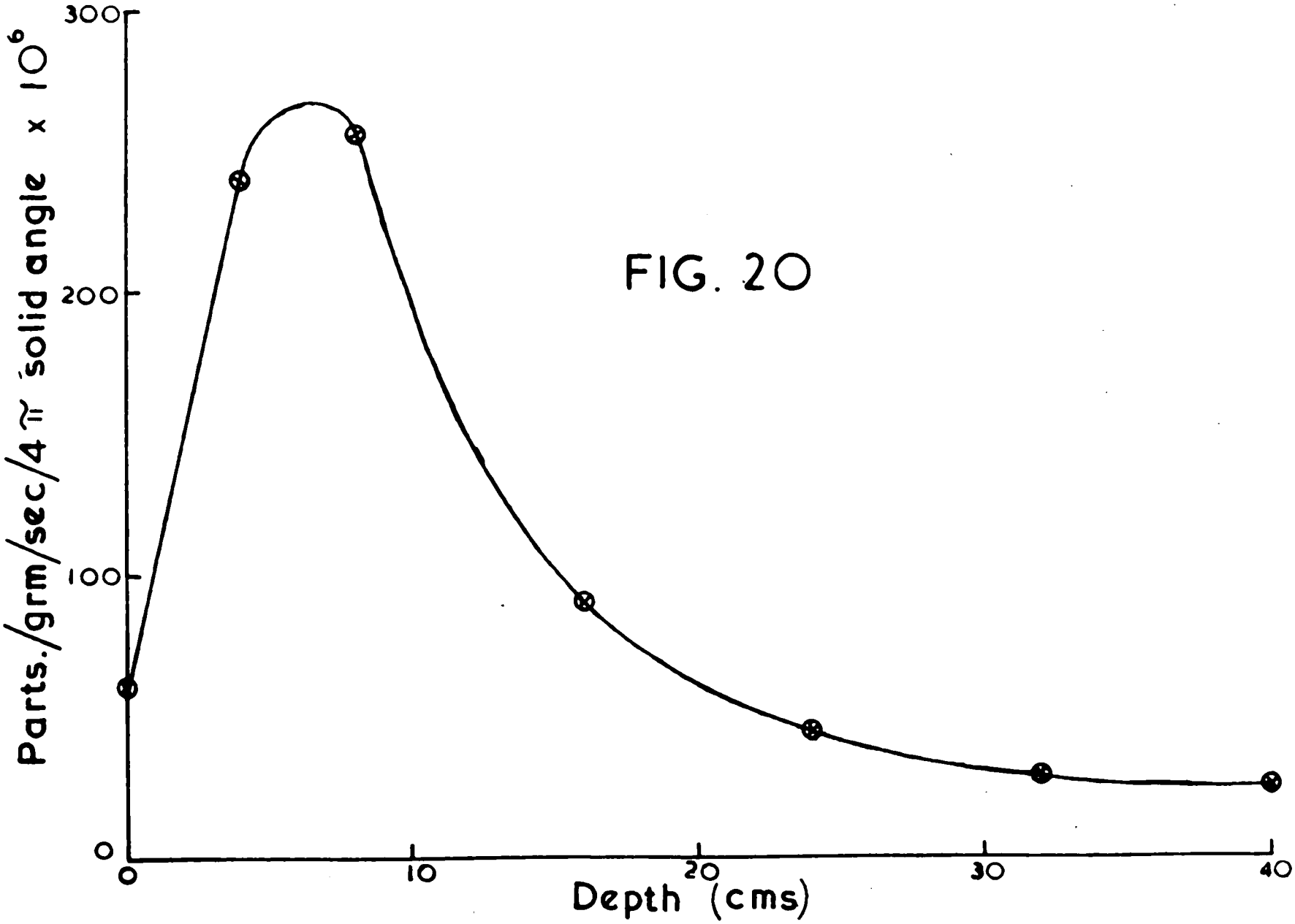
300
200
100
0
Parts./grm/sec/4π solid angle x 10^6
0
10
20
30
40
Depth (cms)

FIG. 20

stopping at the present surface can now be deduced.

At 8 cms. we have 256 particle/grm/sec/ $4\pi \times 10^{-6}$ which is equivalent to 7.54×10^{-8} ccs/grm in 2.52×10^{8} years.

From Fig. 20, the absolute amount of He from α's at various depths can now be obtained.

T A B L E 23.

Depth (cms).	^{4}He/ccs/grm/x 10^{-6}
0.5	0.075
2.5-3	0.046
6	0.034
9.5	0.022
17	0.012
28.5	0.008

If these amounts of ^{4}He are now subtracted from the total amounts of ^{4}He at corresponding depths, in order to obtain the true ^{3}He/^{4}He ratio produced directly by cosmic ray interactions with the iron nuclei, the following values are obtained:

T A B L E 24.

Depth (cms)	Recalculated ^{3}He/^{4}He Ratio.
0.5	28.8
2.5-3	29.0
6	29.0
9.5	28.7
17	28.0
28.5	27.8

FIG. 21

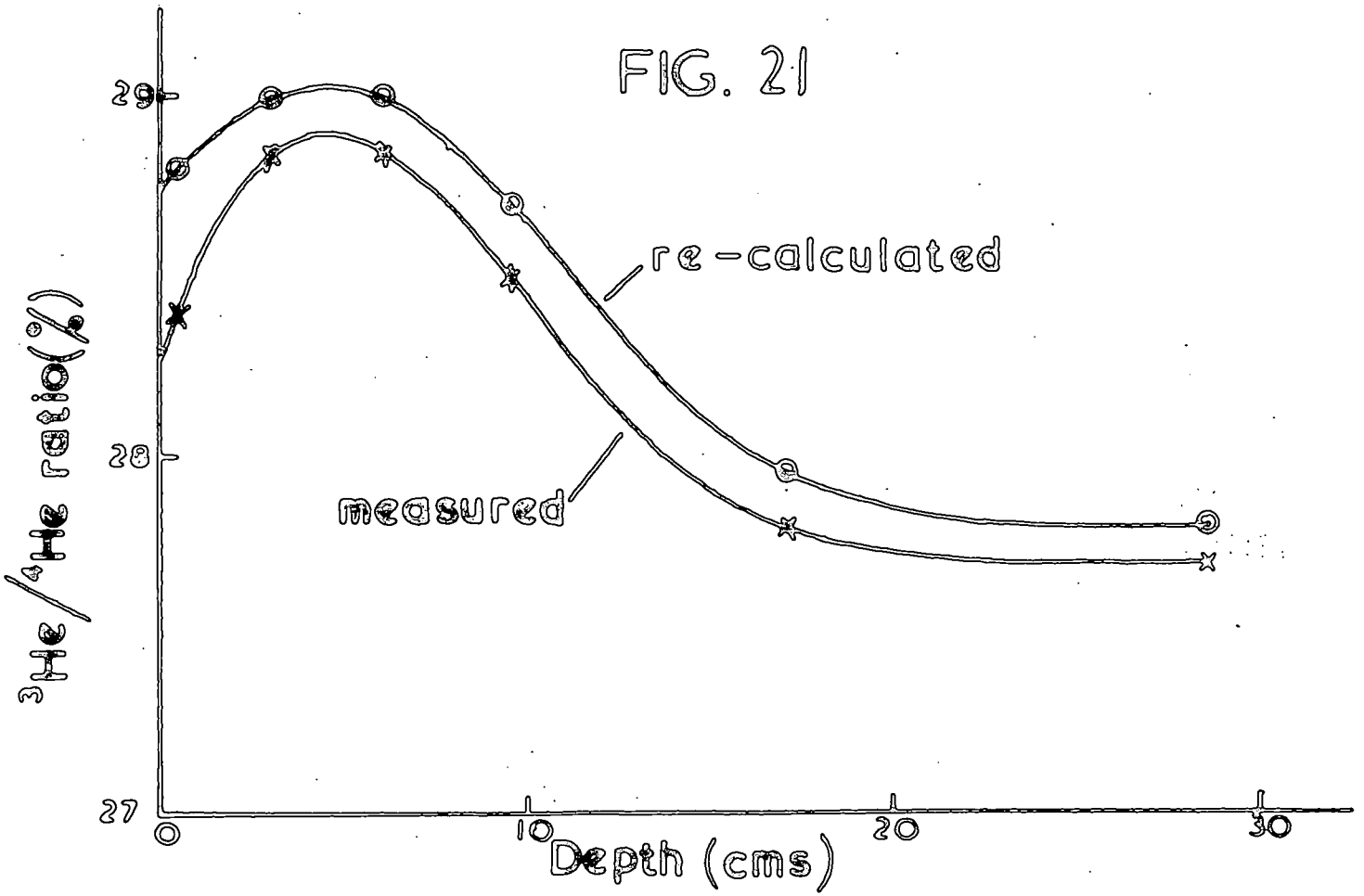
29
28
27
$^3He/^4He$ ratio(%)
re-calculated
measured
0
10
20
30
Depth (cms)

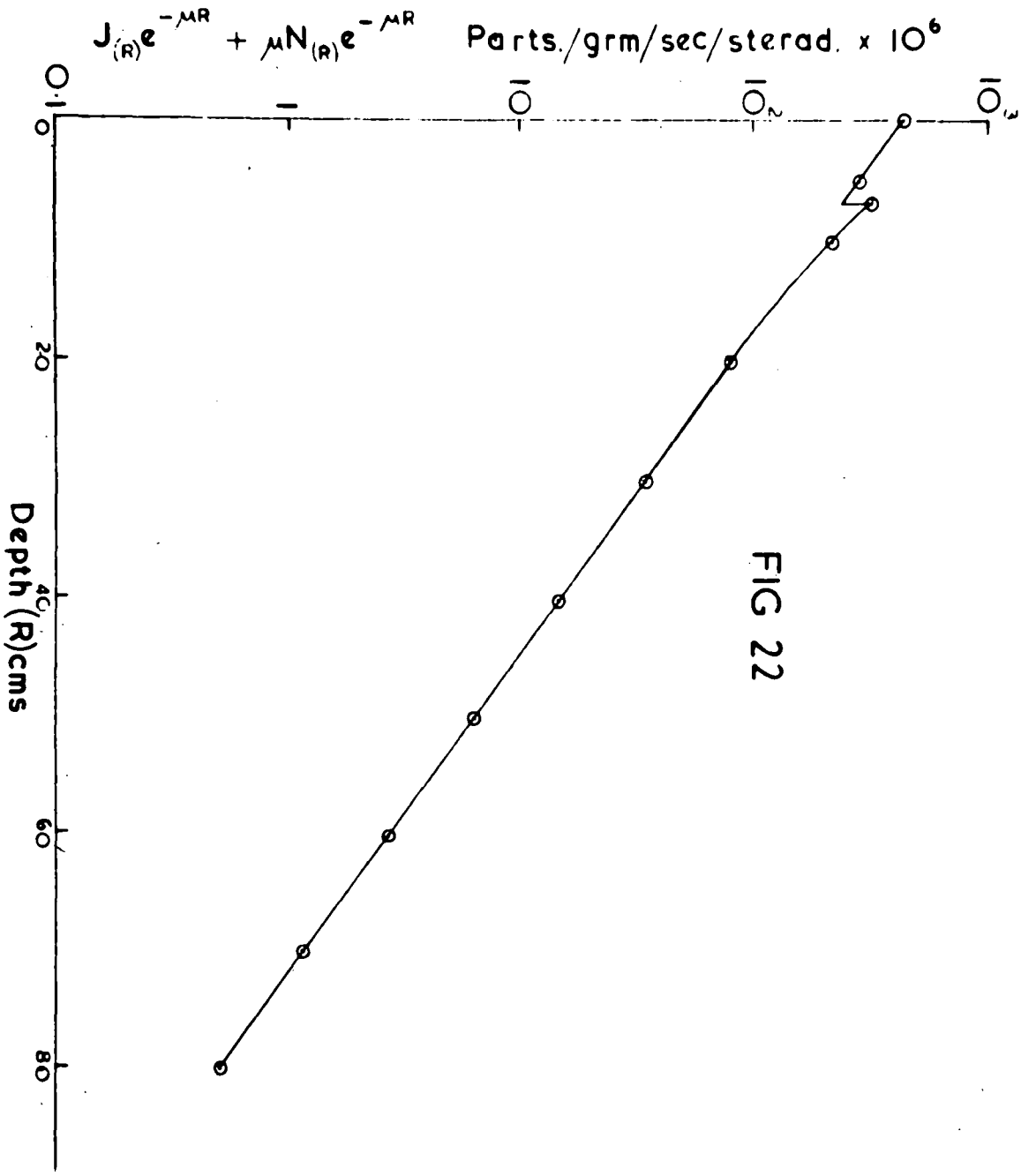
$J_{(R)}e^{-\mu R} + \mu N_{(R)}e^{-\mu R}$ Parts./grm/sec/sterad. x 10^6
0·1
0
20
40
60
80
Depth (R) cms

FIG 22

and it can be seen from Fig. 21 that the "dip" in the first part of the curve is not much affected by this allowance for the ionisation stopping of primary α particles.

α Particle Interactions with Iron Nuclei.

The calculation in the previous section was based on the assumption that once an α particle interacts with an iron nucleus all trace of the incident particle is lost. If, however, this is not true, and in fact, the excited nucleus tends to re-emit the α particle among the component fragments, a different picture emerges.

In this case, the helium production by primary α particles at any depth will now be given by:

$$He_{(R)} = J_{(R)}\, e^{-\mu R} + \mu\, W_{(R)}\, e^{-\mu R} \text{ parts/m}^2\text{/sec/sterad.}$$

which, making the appropriate correction gives the following values:

T A B L E 25.

R(cms).	He(particles/gm/sec/sterad x 10^{-6})
0.	424
5.	280.
6.7	305
10	205
20	70.
30	29
40	12.5
50	5.6
60	2.4
70	1.1
80	0.5

and Fig. 22.

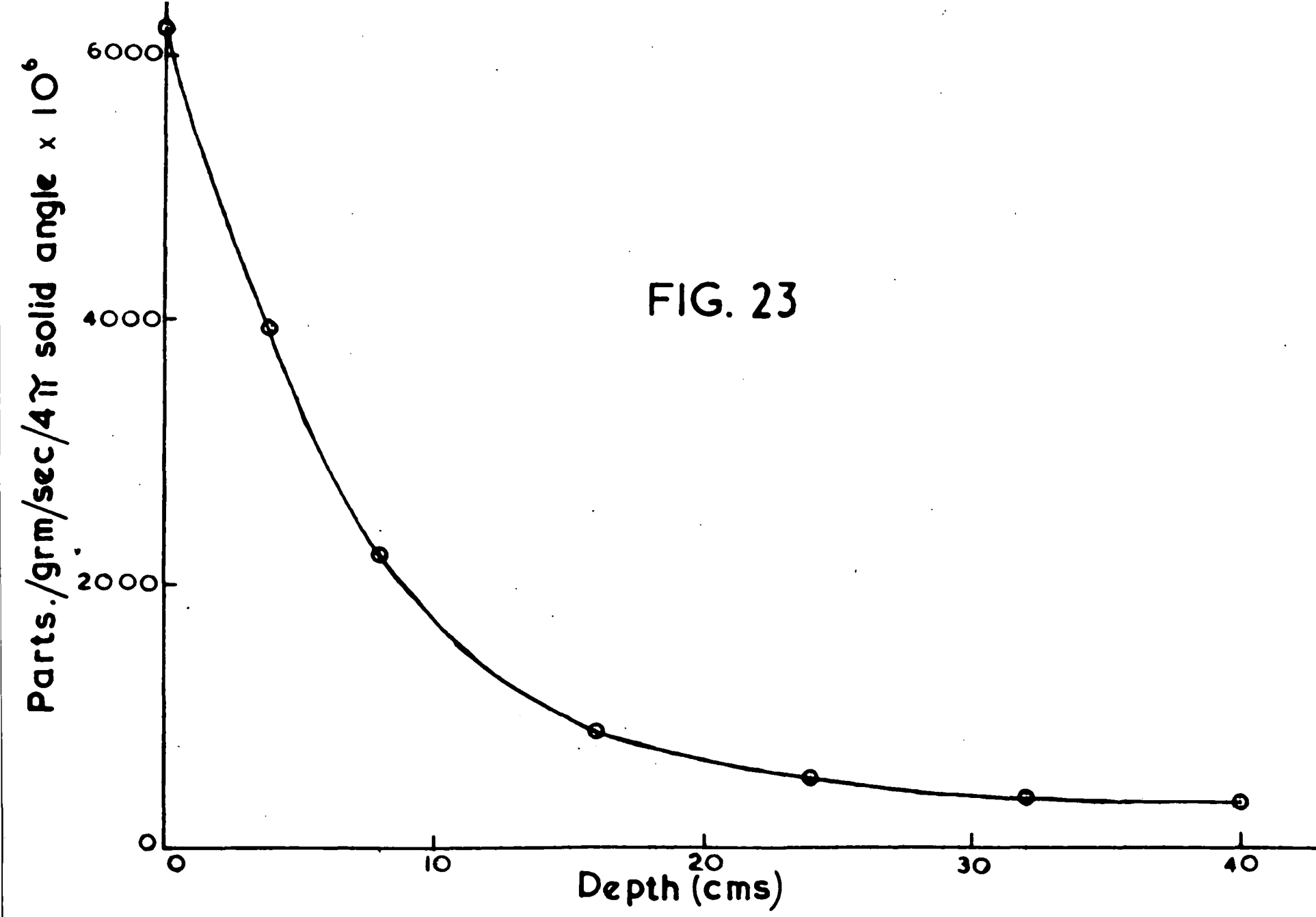
6000
4000
2000
0
Parts./grm/sec/4π solid angle x 10⁶
0
10
20
30
40
Depth (cms)

FIG. 23

Transfer to Spherical Body.

Again, by integration over a sphere, values can be obtained for the helium production at points along the radius of a sphere as before. Table 26 and Fig. 23.

T A B L E 26.

Depth (cms).	He(parts/grm/sec/ 4π solid angle x 10^{-6}
0	6150
4	3950
8	2200
16	870
24	510
32	364
40	326

which, again taking the time of irradiation as 2.52×10^8 years, and the present surface as about 8 cms. below the original one, gives the following values:

T A B L E 27.

Depth (cms).	^{4}He produc. by primary α's (ccs/grm x 10^{-6}
0.5	0.68
2.5-3	0.46
6	0.32
7.5	0.22
17	0.14
28.5	0.10

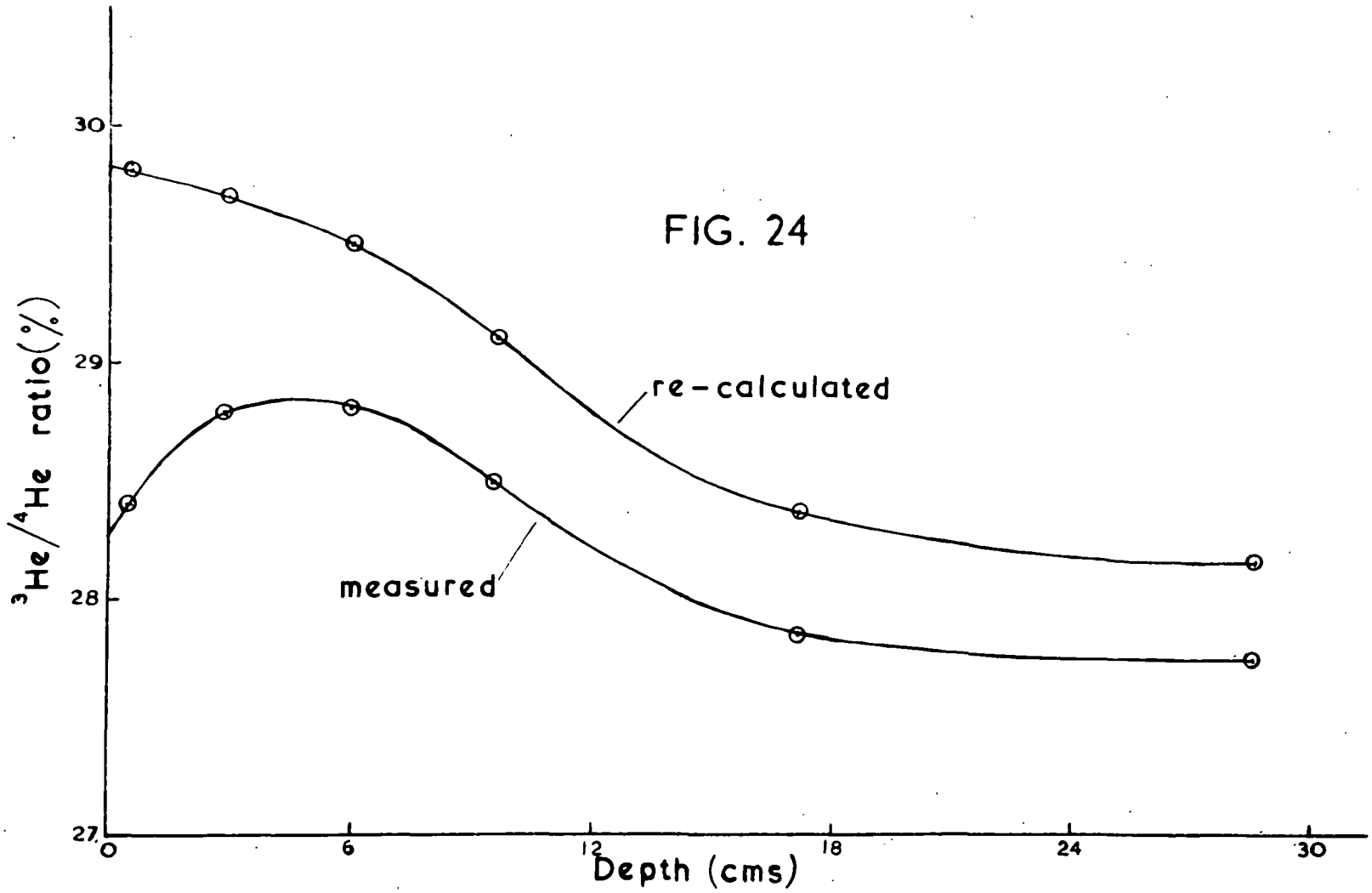
30
29
28
27
$^3He/^4He$ ratio(%)
re-calculated
measured
0
6
12
18
24
30
Depth (cms)

FIG. 24

For reasons given in the following section, it appears that the contribution of ^4He from Uranium and Thorium in the meteorite will be of the order of 0.12×10^{-6} ccs/grm (Table 32, column 3), so that now, subtracting the ^4He produced by primary α's and the radiogenic He from the total ^4He observed, the following treatment may be applied to give the true $^3He/^4He$ ratio produced by cosmic radiation.

T A B L E 28.

1	2	3	4	5	6	7	8	9
Depth (cms)	Total He Content ($\times10^{-6}$ccs/grm.	$^3He/^4$ He ratio	^4He ($\times10^{-6}$ ccs/grm)	^3He ($\times10^{-6}$ cc/g)	$^4/He\alpha$'s ($\times10^{-6}$cc/g)	^4HeRadiogen. ($\times10^{-6}$ cc/g)	True ^4He (cosmic ray prod.)	True $^3He/^4He$ ratio (cosmic ray prod.)
0.5	22.60	28.4	17.60	5.0	0.68	0.12	16.80	29.8
2.5-3	21.00	28.8	16.40	4.70	0.46	0.12	15.82	29.7
6	19.50	28.8	15.10	4.35	0.32	0.12	14.76	29.5
9.5	18.43	28.5	14.30	4.07	0.22	0.12	13.96	29.1
17	17.30	27.8	13.45	3.75	0.14	0.12	13.19	28.4
28.5	16.80	27.7	13.15	3.63	0.10	0.12	12.90	28.2

From Fig.24, it can now be seen that the decrease in the 3/4 ratio is removed, and, in fact, that the true 3/4 ratio is still increasing with decreasing depth, as would normally be expected.

Further, from the calculation of Le Couteur (50), it is clear that the true $^3He/^4He$ ratio is dependent to some extent on the mean energy of excitation of the nuclei involved, and this will depend on the relative contributions of primary and secondary particles to

the total helium production at the point in question. To test this, the relative proportion of helium produced by primaries to total helium produced by primaries and secondaries has been worked out. This has been done by taking values along the appropriate curves in Fig.14, and integrating them over a spherical body of 40 cms. radius.

T A B L E 29.

The following values are obtained:

Depth (cms).	$\frac{\text{He due to Primaries.}}{\text{He due to total radiation.}}$ (%)
0.5	28.5.
2.5-3	22.3
6	18.0
9.5	14.0
17	11.0
28.5	10.0

Now, if the true 3/4 Ratios are dependent on the mean excitation energies, there should be a direct relationship between the ratio -- $\frac{^3\text{He produced}}{\text{Total He produced}}$ obtained from the measured values in Table 28, and the ratio -- $\frac{\text{He produced by primaries}}{\text{Total He produced by primaries and secondaries}}$ deduced from cosmic ray theory, Table 29.

The appropriate values from Table 28 are given in Table 30.

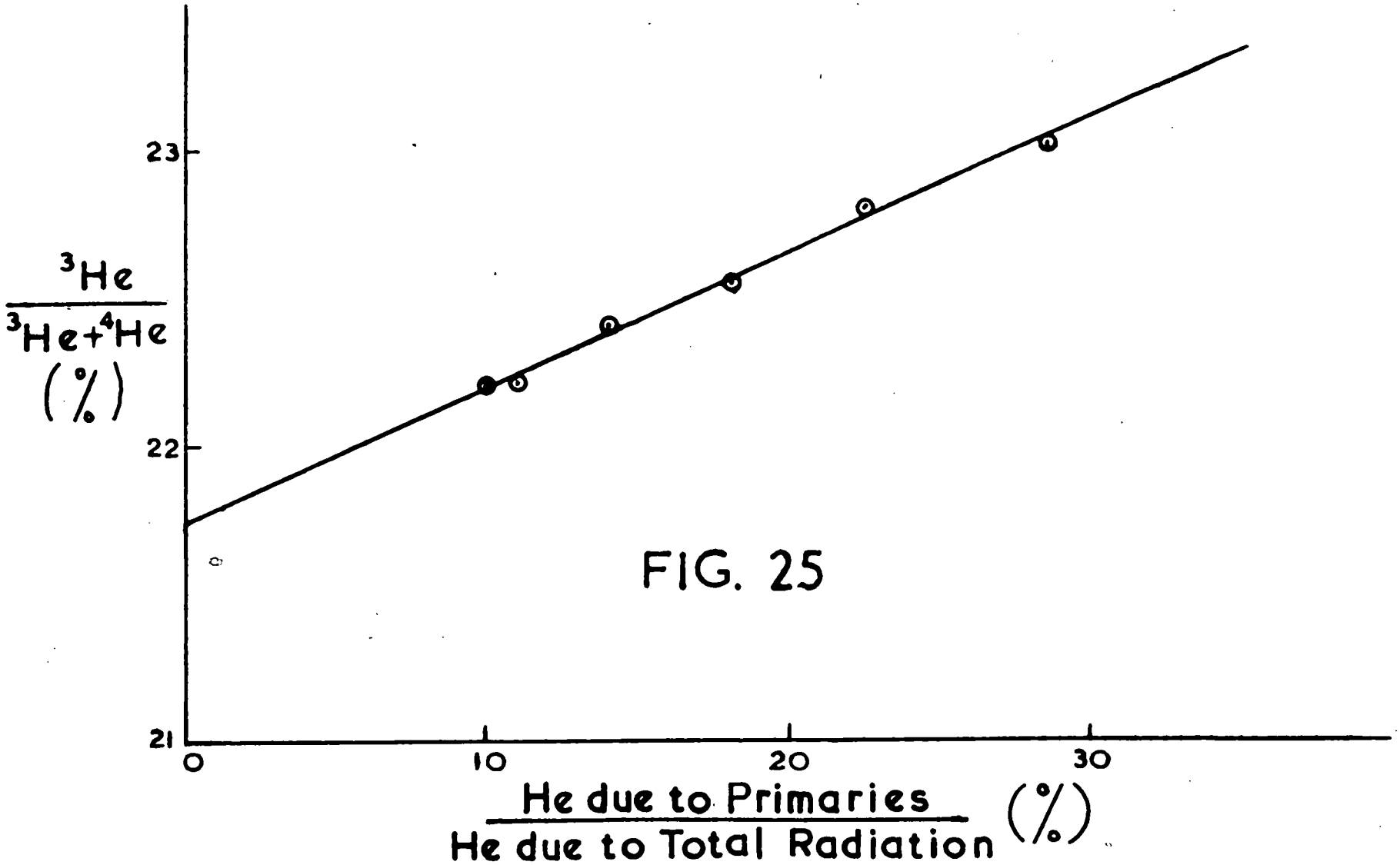
23
22
21
$\frac{^3He}{^3He+^4He}$ (%)
0
10
20
30
He due to Primaries / He due to Total Radiation (%)

FIG. 25

T A B L E 30.

Depth (cms)	$\frac{^3He^c}{^3He^c + {}^4He^c}$		
0.5	$\frac{5.0}{21.8}$	=	23.0
2.5-3	$\frac{4.7}{20.52}$	=	22.8
6	$\frac{4.35}{19.16}$	=	22.6
9.5	$\frac{4.07}{18.10}$	=	22.4
17	$\frac{3.75}{16.94}$	=	22.2
28.5	$\frac{3.63}{16.53}$	=	22.2

The values obtained are plotted in Fig.25, and it can be seen that the relationship is linear, as would be expected.

Conclusion.

From this, it seems that the "filling-in of the first part of the measured $^3He/^4He$ ratio curve is due to the effect of the primary α particles in cosmic radiation, but that, as well as the addition of ^4He from α particles stopped by ionisation loss, the above treatment suggests that for each nuclear interaction, the excited iron nucleus will tend to re-emit one particle in excess of those expected, or namely, that the incident particle tends not to lose its identity in the excited nucleus.

It should be pointed out here that the above treatment must necessarily be regarded as a "best approximation", in view of the inherent uncertainties in data on the size and shape of the

meteorites. Carbo is of a somewhat conical shape with the present base of the cone apparently the nearest surviving portion to the original surface. The apparent "centre" of the pre-atmospheric mass (deduced from the lowest helium value) is about 10 cms. below the apex of the cone. A consideration of Fig. 23 shows that the above treatment is quite sensitive to the assumed depth of the present surface below the original surface. Thus, if a depth of 4 cms. is taken, instead of the 8 cms. assumed, the ^4He contributio from primary α's will be doubled, and the $^3He/^4He$ curve will be raised and smoothed out even more. On the other hand, if the depth were taken as 12 cms. the ^4He contribution from primary α's would be almost halved, and the "bump" in the $^3He/^4He$ curve would be much less affected. Also, the effect of cavities in the original mass on the helium content and $^3He/^4He$ ratio at any given point cannot be estimated. However, it still remains that Carbo is by far the best approximation to the ideal spherical meteorite which has yet been investigated, and the only one known to exist which may perhaps throw further light on the "depth effect", namely "Hoba West", appears to present great difficulties in respect of obtaining any samples.

Investigation of the Helium, Uranium, and Thorium contents of a representative Range of Meteorites.

The Uranium and Thorium values for this work have been determined by Mr.J.C.Dalton, of these laboratories (55). Care has been taken to do the He, U, and Th, determinations on the same sample of a meteorite. The meteorites investigated were chosen to give the widest possible range of helium contents in order to see whether

any regularities could be detected in the variation of $^3He/^4He$ ratios with absolute helium content, and particularly to investigate as many as possible of the meteorites with low helium contents, since it is to be expected that these samples will give the best estimate of the true radiogenic helium content. The results for 14 meteorites are summarised in Table 31.

1 Name of Meteorite	2 He Content (in 10^{-6} ccs/grm)	3 $^3He/^4He$ Ratio %	4 ^4He Content (in 10^{-6} ccs/grm.)	5 ^3He content (in 10^{-6} ccs/grm.)	6 Uranium Content (10^{-8} g/grm.)	7 Thorium Content (10^{-8} g/grm.)	8 Diam. (cms) calculated from recovered masses, assumed spherical	9 Type of fall, single or multiple
Mount Ayliff	36.8	31.5	28.0	8.8	0.4	2	14.6	S.
Tamarugal	23.59	30.9	18.0	5.59	0.32	1.65	42	S
Carbo	22.0	28.6	17.10	4.90	0.51	0.65	48	S
Toluca (Durham)	18.9	29.7	14.60	4.30	0.58	0.60	51	M
Sacramento Mts.	11.21	30.75	8.60	2.65	-	-	38	S
Arispe	5.32	27.2	4.18	1.14	0.46	1.47	35	M
Bethany (Amalia)	3.4	27.8	2.67	0.73	0.53	0.92	150	M
San Martin	1.76	16.8	1.50	0.253	0.75	10.4	Not known	Not known
Henbury	0.88	25.4	0.70	0.18	1.07	2.96	very large (56)	M
Negrillos	0.46	19.0	0.387	0.73	-	-	150	M
Bethany (Harvard)	0.36	17.8	0.306	0.054	0.61	0.94	150	M
Coahuila	0.20	23.3	0.163	0.038	0.40	0.69	132	M
Toluca (Hamburg)	0.16	19.6	0.135	0.026	0.20	2.37	very large (28)	M
Uwet	0.17	11.0	0.153	0.017	0.31	0.46	23(?)	S(?)

TABLE 31.

It can be seen from Column 3 of this table that the measured $^3He/^4He$ ratios cover a wide range of values from 31.5 to 11.0.

Now, it seems likely that the large variation in the total helium contents of these meteorite samples can best be explained, not as previously by assuming very different ages up to a maximum of 7000 million years, but rather by suggesting that the majority of meteorite samples with low helium content have come from within meteorites with large pre-atmospheric masses, so that they have been well shielded from the effect of cosmic radiation, while the samples with large helium contents are from meteorites with small pre-atmospheric masses, so that they have been subjected to large cosmic radiation effects. A consideration of Fig.17 makes this clear.

Further, a consideration of the best available data, such as it is, set out in columns 8 and 9 of Table 31, tends to lend weight to this view. From column 8, it can be seen that the calculated diameters of the recovered masses of the high-helium-content meteorites are low, while the diameters of the low-helium-content meteorites are much higher. (The meteorite with the highest known helium content - "Morden", of helium content 38.1×10^{-6} ccs/grm has a post-atmospheric diameter of only 8 cms.) Column 9 shows that with the high-helium- content meteorites, the type of fall is preponderantly single so that the available samples would be from fairly near the surface, whereas, with the low-helium-content samples, the type of fall is predominantly multiple, so that the

samples could well be from the interior of a large mass which broke up on impact with the atmosphere or the ground, or alternatively from an agglomeration of iron masses which separated on impact.

Thus, since the total helium content of a meteorite cannot then be taken as a criterion of its age value, it is of interest to note the following considerations.

If the straight line obtained in Fig.25 is extrapolated back to the point where the helium contribution from the primary cosmic radiation is zero (i.e. the point beyond which only secondary radiation is left to produce helium), a value for the $^3He/^4He$ ratio of just over 27 % is obtained. A consideration of Fig.14 shows that a meteorite of diameter approaching already the largest given in Table 31 would be needed to attenuate the helium production due to primary cosmic radiation at its centre to zero. Further, since the energy spectrum of the secondary particles appears to be more or less dndependent of the energy of the incident particle (32), it would appear that a further large absorber thickness would be needed before the mean energy of the secondary particles would fall off sufficiently to produce a substantial decrease in the $^3He/^4He$ ratio, due to secondaries, of 27 %. Thus, it seems that the minimum $^3He/^4He$ ratio of the cosmic ray produced helium in the meteorite samples investigated should be about 27% Further, if the extrapolation is carried to 100% primary radiation, a maximum $^3He/^4He$ ratio of 36% is obtained, but this would only be realised in an extremely small meteorite, which might never succeed in traversing the atmosphere, or which might be too small to be found if it did.

The effect of fitting different assumed ages to the group of meteorites can now be tried, commencing with the age derived for Morden (2.5×10^8 years, if all its helium is taken to be cosmic ray produced, during which time its helium production from radio-active sources would be quite negligible by comparison).

The amount of helium from radio-active sources, using the measured uranium and thorium content, is calculated, and a correction applied to the amount of Helium in the sample, allowing a corrected $^3He/^4He$ ratio to be obtained.

The amount of helium generated during a given time is obtained by the following considerations.

One gram of uranium produces, per year, 1.202×10^{-7} ccs. of helium, one gram of thorium produces, per year, 2.88×10^{-8} ccs. of helium. If we denote by (U) and (Th) the grams of uranium and thorium per gram of sample, by He the ccs. of helium per gram of sample which have originated from these two radio-elements, then the age in years is given by the simple formula:

$$\text{Age} = \frac{He \times 10^{10}}{12.02\,(U) + 2.88(Th)} \text{ years.}$$

Table 32 can now be compiled.

(1). Name.	(2) Age 2.5×10^8 years. Ra.gen.He	New 3/4 ratio.	(3) Age 1.3×10^8 years. Ra.gen.He	New 3/4 Ratio.	(4) Age 0.2×10^8 years. Ra.gen.He	New 3/4 Ratio.
Mt. Ayliff.	0.265	31.8	0.138	31.6	0.074	31.55
Tamarugal.	0.236	31.4	0.122	31.2	0.06	31.22
Carbo.	0.234	29.0	0.120	28.9	0.058	28.8
Toluca(Durham)	0.224	29.9	0.118	29.8	0.060	29.7
Sacramento Mts.	-	-	-	-	-	-
Arispe	0.246	29.0	0.128	28.1	0.069	27.7
Bethany (Amalia)	0.226	30	0.118	28.7	0.063	28.0
San Martin	0.97	51	0.51	25.4	0.27	20
Henbury	0.55	120	0.28	42	0.15	33
Negrillos	-	-	-	-	-	-
Bethany (Harvard)	0.273	163	0.142	33	0.076	20
Coahuila	0.167	N.A.	0.087	50	0.047	33
Toluca (Hamburg)	0.22	N.A.	0.116	136	0.062	36
Uvet	0.123	57	0.064	19	0.035	14

N.A. Not applicable. The Radiogenic ^4He would be bigger than the total ^4He

TABLE 32.

He in 10^{-6} ccs/grm.

It can be seen from Table 32 that an age of about 1.3×10^8 years would be the best fit, if a common age value is to be applied at all, (bearing in mind the theory of a common catastrophic origin for meteorites), since an age of twice this value gives too many high $^3He/^4He$ ratios, and an age of half this value gives too many low $^3He/^4He$ ratios.

The reason for the low $^3He/^4He$ measured ratio (i,e. below about 2%) of the meteorites in the lower part of Table 31 can easily be seen. With these meteorites, the contribution of He from radio-active sources during 1×10^8 years, or even less, is a significant proportion of the total ^4He in the meteorites, and consequently has a large effect on lowering the $^3He/^4He$ ratios. With the meteorites at the top of the table, the radio-genic ^4He produced in such a time is insignificant compared with the total ^4He, and consequently barely alters the $^3He/^4He$ ratio.

Lastly, if the age of 1.3×10^8 years seems to be applicable to the majority of the samples, it is obvious that this value is now only one half of the age derived for "Morden" from cosmic ray considerations, and this would only need a value of the average cosmic ray flux over the past 10^8 years of about twice as high as the present day flux to bring the figures into direct agreement. Several theories suggesting this higher average value have been advanced (57(58(59).

Not all meteorites can be collected into the above mentioned category, however. Of the seventy different meteorites which have been investigated, it appears that five fall into a separate

class. The data on these five are set out in Table 33.

TABLE 33.

Name	He(in 10^{-6} ccs/grm.)	U(in 10^{-8} g/g).	Th(in 10^{-8}g/g).	Met.Age (Calculated from total He content) (in 10^{6} years).
Brenham Township	0.02	0.06	< 0.7	83
Muonionalusta (II)	0.013	0.20	< 1.1	25
Bethany (Lion River)	0.002	0.27	< 1.5	2.6
Cape York(Ahnighito)	< 0.001	0.56	0.77	< 1.1
Cape York (Savik)	< 0.0002	0.20	< 0.23	< 0.67

The five meteorites in this table could not treated in a similar manner to the meteorites in Tables 31 and 32, because their absolute helium contents were so low that insufficient material was available to produce large enough amounts of helium to be measured mass spectrometrically. For example, with Cape York (Savik) about 10,000 grms. would need to be dissolved. However, it might be possible to apply the "tritium method" to these samples.

There is no doubt that, even if all the helium in these samples is taken to come from radio-active sources alone, which is most probably a very gross exaggeration, the ages of these five are very much less than the ages of the majority. Here, one is forced to suggest some additional mechanism to account for the very low helium content, and a probable one would appear to be a re-melting by passing close to the sun.

Summary.

In the present work, the production of helium in meteoric irons by cosmic radiation has been clearly demonstrated, both by measurement of the $^3He/^4He$ ratios of fourteen different meteorite samples, and by the measurement of the expected "depth effect" on a large meteorite, Carbo. The experimental values for the "depth effect" curve in Carbo, and also figures for the two other meteorites are fitted into a theoretical estimation of the expected helium production by cosmic rays in meteorites of different masses, and good agreement is obtained. A calculation has been done to explain the shape of the $^3He/^4He$ ratio curves obtained for Carbo, and again, satisfactory agreement seems to have been achieved. Finally, an attempt has been made to derive some information about the probable age of the meteorite samples investigated, and certainly, the previously stated maximum value of 7×10^9 years (4) has been drastically reduced. It is of interest to note that, until a few months ago, astronomical evidence seemed to suggest a value for the age of the universe of about 2×10^9 years, while the age of the earth seemed to be about 3.5×10^9 years, and previously mentioned work gave an age for the higher helium-content meteorites of 7×10^9 years. Recently, however, new results (60), indicate a doubling of the age of the universe to 4×10^9 years, and the present work lowers the age of meteorites to well below the accepted age of the earth, so that the three previously discordant values are now brought into very satisfactory agreement.

- Chapter IV -

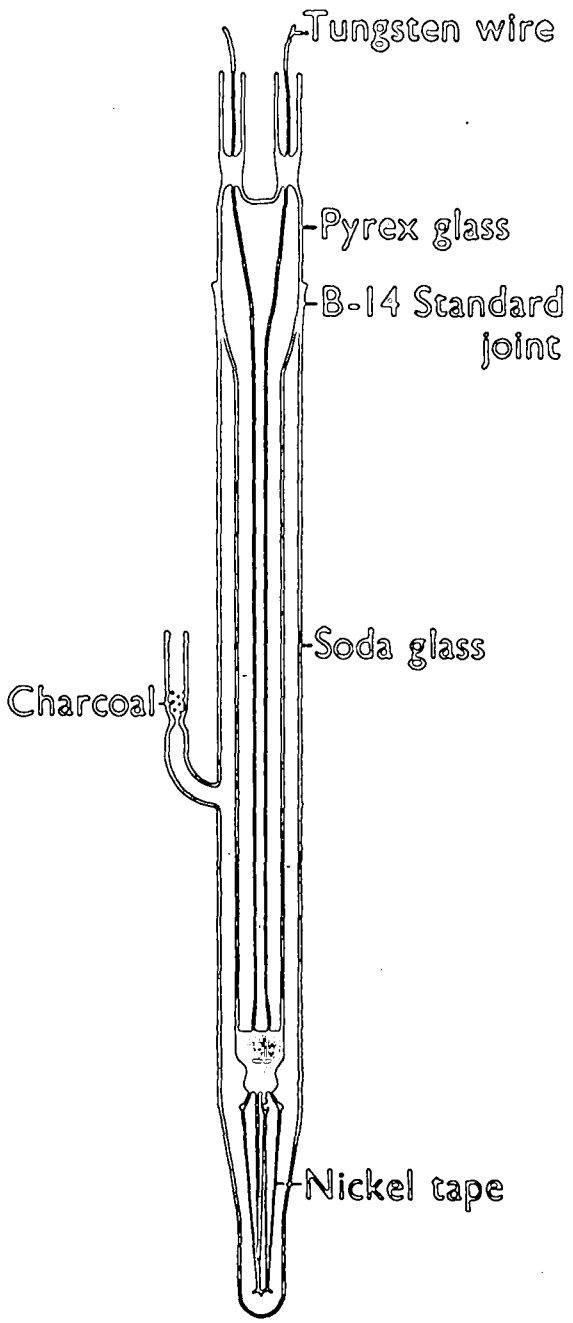

Pirani gauge.

FIG. 26

C H A P T E R IV.

Section 1 - The Helium Apparatus.

Introduction.

(1) The Measurement of Helium and Neon Volumes.
(2) The Fractionating Column.
(3) The Circulating System.
(4) The O_2 Reservoir.

The modern helium apparatus, as described in this chapter, is the result of gradual development and improvement over a period of a quarter of a century. The present apparatus, which was built for the work described, is capable of handling and measuring amount of helium and neon of the order of 1×10^{-8} ccs N.T.P. with an accuracy of about 1% to 2%, and amounts of Argon of about 10^{-4} ccs with an accuracy of ½%.

(1) Pirani Gauges.

The helium and neon were measured in a Pirani gauge, the design of which is indicated in Fig.26. It is an improvement on the previous design in so far as the centrepiece is demountable to allow the filament to be replaced when necessary.

For high sensitivity and stability, it is necessary to have the gas space as small as possible, and to maintain the outer jacket at a low temperature; this is achieved by having the outer jacket close fitting, with the filament in the small space at the bottom, covered to a depth of about 15 cms. in a liquid nitrogen bath. The leads to the Wheatstone net circuit are carried through the central tube, which is previously evacuated and sealed off, to prevent spurious temperature effects which would be given by convection and

conduction if air were present.

The filament itself is very fine Nickel tape, which was found to have the best temperature coefficient of resistance for the purpose.

It is about 30 cms. long and is in the shape of a W, being held taught on a glass former by means of a tungsten spring. A small amount of charcoal is placed in the side arm to protect the gauge from gases released during use by the glass walls and the stopcock grease.

In practice, two identical gauges are used in the same low temperature bath, one forming a compensating arm in the bridge, being kept permanently evacuated, and the other being the working gauge and the second arm. The other two arms are provided by a resistance box and a fixed resistance, and a sensitive moving coil galvanometer is mounted across the bridge.

A potential of exactly 1 volt is applied across the gauges when in use, and the sensitivity of the gauges to varying amounts of helium and neon is adjusted by varying the galvanometer shunt.

By means of this arrangement, it is possible to measure amount of helium and neon between about 1×10^{-9} ccs.N.T.P. up to 1×10^{-4} ccs. N.T.P.

When gas enters the gauge the heated filament loses energy due to the impact of "cold" gas molecules upon its surface, consequently its resistance falls, and the increase in current

FIG. 27

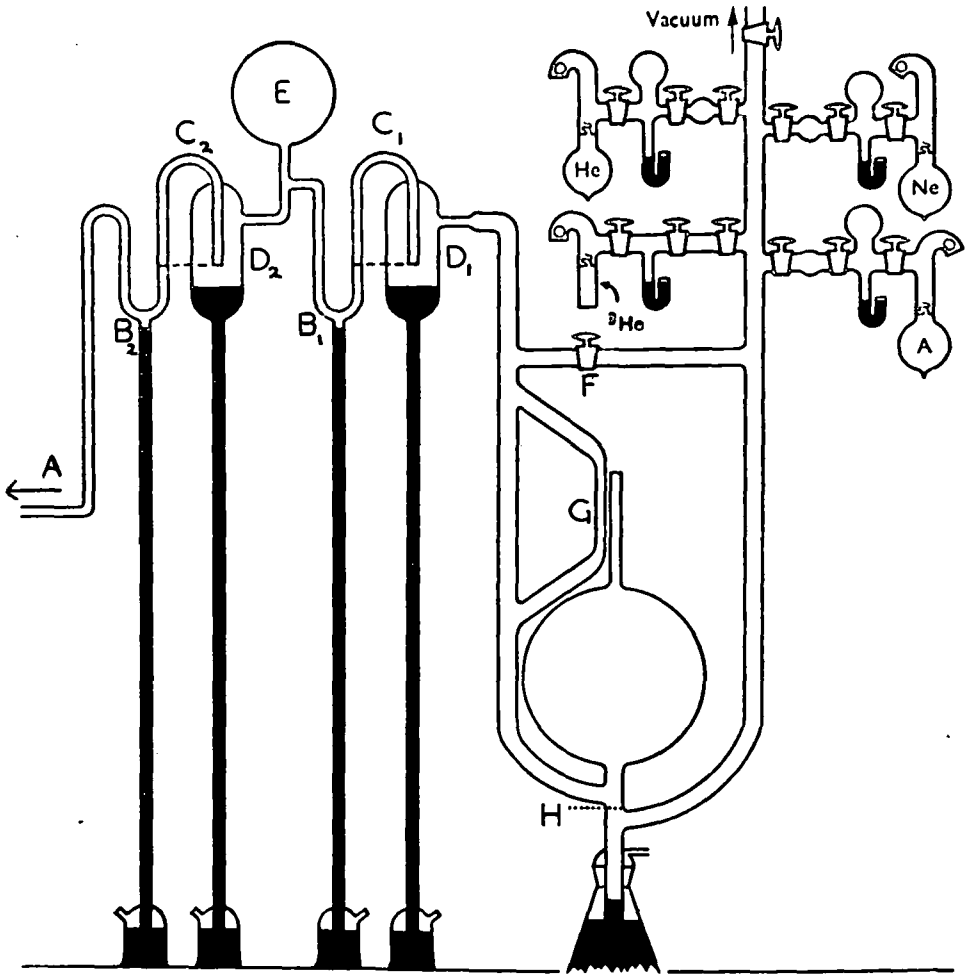

McLeod gauge for calibration and expansion system.

produces a deflection of the galvanometer spot. The Thermal conductivity of the gas is proportional to its pressure when this is small, and consequently, the galvanometer deflection bears a linear relationship to the pressure of gas introduced.

Gauge sensitivity naturally varies with the gas employed, so that the gauges were calibrated with both helium and neon.

Calibration.

The Pirani gauges were calibrated during each experiment to obviate small fluctuations in sensitivity due, for example, to varying bath temperatures, slight changes in voltage applied to the filaments from day to day, etc. This was done by introducing into the gauges, immediately after the unknown amounts of helium and neon had been measured, accurately measured amounts of helium and neon respectively from the calibration apparatus.

First of all, an amount of spectrally pure helium or neon from a reservoir was measured in the McLeod gauge, Fig.27, after pumping out the side arm G through tap F. Tap F was then shut, the mercur lowered just to the mark at H, which allowed the gas to expand into a known volume (883.875 ccs). defined by the mercury meniscus, tap F, and the mercury in the left hand side of the pipette C_1, which was brought exactly to an etch mark. Since the volume of pipette C_1 was accurately known (2.947ccs) raising the mercury in vessel D_1 above the right hand end of the pipette C_1, cuts off in C_1 a known proportion of the original gas volume, $\frac{2.947}{883.875}$ ths. By lowering the mercury in the inverted U tube B_1, to a mark at the top of the

vertical tube, this fraction of the original gas was then expanded into a known volume (166.383 ccs) comprised of the pipettes C_1, and C_2, and the expansion bulb E, with the mercury in the second pipette C_2 just at an etch mark on the left hand side.

The mercury in the vessel D_2 was then raised above the cut off of the right hand end of the pipette C_2 (vol.3.283 ccs), and the mercury in the second U tube B_2 lowered just to the top of its vertical tube, so that $\frac{3.283}{166.383} \times \frac{2.947}{883.875}$ ths of the original gas volume was allowed to expand into the large compression bulb A. The mercury in the compression bulb A was then raised up to a ball valve at the top, so that the gas was compressed into the Pirani gauge with very little dead space due to side tubing.

Hence, since the original gas volume in the McLeod limb was defined by $\frac{P}{760} \times V \times \frac{273.}{273 + T^{o}C}$ ccs. N.T.P. where P is the pressure in mms., V is the volume in ccs. of the gas in the McLeod limb from the volume calibration curve previously determined, T is the room temperature ^{o}C., the amount of gas introduced into the Pirani gauge was given by:

$$P \times V \times 8.6567 \times \frac{273}{273 + T} \times 10^{-7} \text{ ccs. N.P.T.}$$

By this means, amounts of gas varying from 3×10^{-8} ccs to 1×10^{-3} ccs. could be introduced into the gauge.

Scale Calibration.

Since the galvonometer scale was straight, it was found that, for equal angular deflections of the galvonometer (i.e. for equal amounts of gas introduced into the Pirani gauge) readings taken nea

the ends of the 50 cm. scale were considerably greater than those taken near the centre, thus introducing an error into the readings corresponding to the position on the scale over which the deflecti was measured.

The correction calibration was made by installing a megohm resistance across one of the Pirani gauges, with a mercury-switch in circuit. By adjusting the galvo shunt to the correct value, throwing the mercury switch gave a deflection of the required order analogous to admitting helium into the gauge. Deflections were taken over all ranges of the scale, and it was discovered that with a deflection of about 6 cms. on a 50 cm. scale, the readings at either end were about 10% greater than in the centre.

A graph was therefore drawn of size of deflection against range on the scale, a parabolic curve fitted, and a comprehensive correction table calculated which gave the correction to be applied to any reading between given range limits on the scale.

It was thus possible to reduce any reading to what would have been read on a perfectly circular scale.

In practice, also, the actual deflections given by the unknown amounts of helium and neon were as far as possible taken over the same range as the deflections given by the known calibration amounts of helium and neon, which could usually be ensured by a rough calculation beforehand, so that any error due to this "non-linearity" affect of the scale was reduced to negligible proportions.

(2) Separation of Helium and Neon and Purification from other Gases

The separation of helium and neon is effected by means of a fractionating column which utilises the fact that these two gases are adsorbed to a markedly different extent, under the right conditions, on activated charcoal cooled in liquid nitrogen.

A full theoretical discussion of the fractional adsorption and desorption as well as the practical consideration of helium and neon separation has been given by Glückauf (5). Consequently, only an outline of the theory, and an account of the operation of the modern fractionating column is called for here.

A gas will distribute itself between an adsorbent and a gas space, the quantity of gas adsorbed being determined by:-

1. The quantity of adsorbent.
2. The volume of the gas space.
3. The temperature of the adsorbent.
4. The adsorption coefficient of the particular gas.

Quantity S of charcoal.

Volume of Gas space V.

Helium - Gas A.

Neon - Gas B.

The ratio of the concentrations Cs and Cv in the solid and volume phases respectively is governed by an equation of the Langmuir type:

$$C_s = \frac{k_1 C_v}{1+k_2 C_s} \quad \text{----- (1).}$$

The concentration of the adsorbate encountered during micro-analysis is so small that k_2C_s is $\ll 1$

and may be neglected in comparison with 1, so that (I) reduces to $C_s = \alpha C_v$ where α is the adsorption coefficient for A. The distribution of a quantity A_o of the gas A at equilibrium between two phases leaves in the volume phase the quantity

$$A_1 = \frac{VC_v}{VC_v + SC_s} \cdot A_o = \frac{1}{1 + \alpha\frac{S}{V}} \cdot A_o = aA_o$$

and in the solid phase $\bar{A}_1 = (1 - a)\, A_o$.

The expression $a = \frac{1}{1 + \alpha\frac{S}{V}}$ is called the distribution factor of the adsorption unit for the gas A.

The second gas B has a distribution factor $b = \frac{1}{1 + \beta\frac{S}{V}}$

Now, since the distribution factor "a" may be regarded as the fraction of Gas A in the volume phase, and "b" the fraction of the gas B in the volume phase, the condition for the best separation will be obtained when (a-b) is a maximum.

Thus $(a-b) = \frac{1}{1 + \alpha\frac{S}{V}} - \frac{1}{1 + \beta\frac{S}{V}}$

$$= \frac{V}{V + \alpha S} - \frac{V}{V + \beta S}$$

$$= \frac{VS(\beta - \alpha)}{(V + \alpha S)\ (V + \beta S)}$$

$$= (\beta - \alpha) \left[\frac{VS}{V^2 + \alpha VS + \beta VS + \alpha\beta S^2}\right]$$

$$\therefore \frac{1}{(a-b)} = \frac{1}{(\beta - \alpha)} \left[\frac{V^2 + \alpha VS + \beta VS + \alpha\beta S^2}{VS}\right]$$

$$= \frac{1}{(\beta - \alpha)} \left(\frac{V}{S} + \alpha + \beta + \frac{\alpha\beta S}{V}\right)$$

$$\frac{d\left(\frac{1}{a-b}\right)}{d\left(\frac{S}{V}\right)} = \left(\frac{1}{\beta - \alpha}\right) \left[-\frac{1}{\left(\frac{S}{V}\right)^2} + \alpha\beta\right]$$

when (a-b) is a maximum, i.e. $\left(\frac{1}{a-b}\right)$ is a minimum,

$$\frac{1}{\left(\frac{S}{V}\right)^2} = \alpha\beta$$

$$\frac{V}{S} = \sqrt{\alpha\beta}$$

Also, $a + b = \frac{V}{V + \alpha S} + \frac{V}{V + \beta S} = \frac{V^2 + V\beta S + V^2 + \alpha SV}{V^2 + V\beta S + V\alpha S + \alpha\beta S^2}$

$$= \frac{2V^2 + V\beta S + V\alpha S}{V^2 + V\beta S + V\alpha S + \alpha\beta S^2}$$

$$= 1.$$

Now, experiment has shown that 2.5 grms. (S) of hard nut charcoal at liquid nitrogen temperature, adsorbed 26.5 ccs. (α S) of helium (measured at 20°c), and 293 ccs (β S) of neon.

This gives $\alpha = 10.60$

$\beta = 110.72$

Since the volume (V) of the bulbs to be used are approximately 25 ccs. volume, this gives, from $\frac{V}{S} = \sqrt{\alpha\beta}$

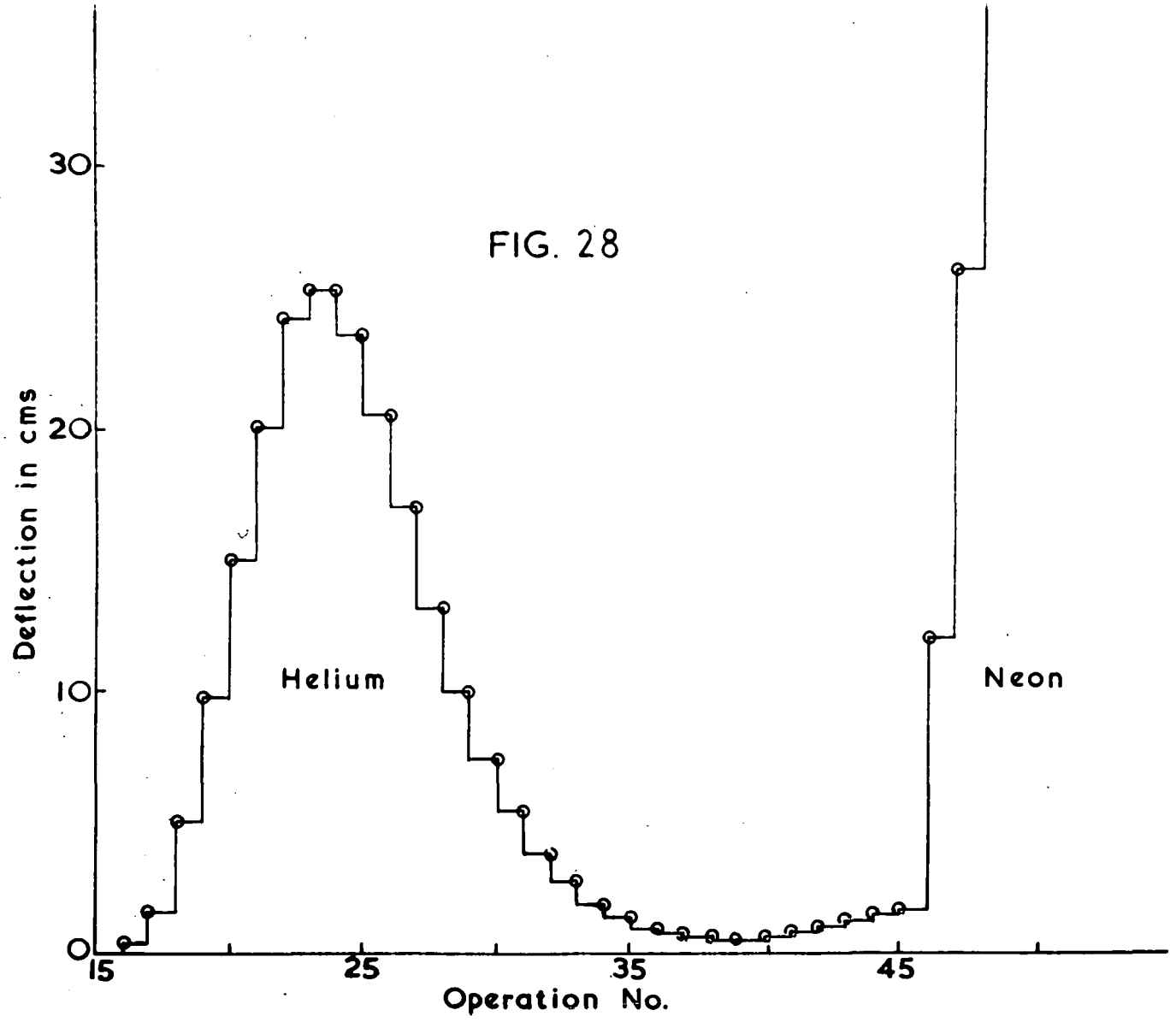
30
20
10
0
Deflection in cms
Helium
Neon
15
25
35
45
Operation No.

FIG. 28

A similar table can be developed for gas B. Thus, for any given number of fractionation units in the column, the amounts of gas which are removed from the end of the column at any given operation number can be obtained, and a distribution curve of gas yield against operation number can be plotted.

For example, with a 3 unit column, from the above table, the fractions of gas A which come through at operations 3, 4, 5, 6, ... are a^3, $3a^3(1-a)$, $6a^3(1-a)^2$, $10a^3(1-a)^3$ ---- respectively, and similarly with gas B.

This can be expanded to include a fractionating column of any number of units, and thus it is possible to determine the number of units necessary to obtain Gas A of the required degree of purity, with contamination by gas B reduced to a minimum. In practice, the gas in the storage bulb at the end of the new fractionating column after 36 operations was found to be 99.3% helium plus 0.7% neon. Figure 28 shows a typical helium and neon distribution curve obtained on the fractionating column.

Operating Procedure.

The operation of the fractionating column is as follows. (See Fig.29). The mercury in the front and back sections of the column is raised to just above the ring seals in the bulbs. The helium and neon plus the carrier gas, pure oxygen and sometimes traces of argon and nitrogen are toppled from the circulating system in to the first charcoal tube C_1 where all the gases except the helium and neon are completely adsorbed. When the mercury

FIG. 29

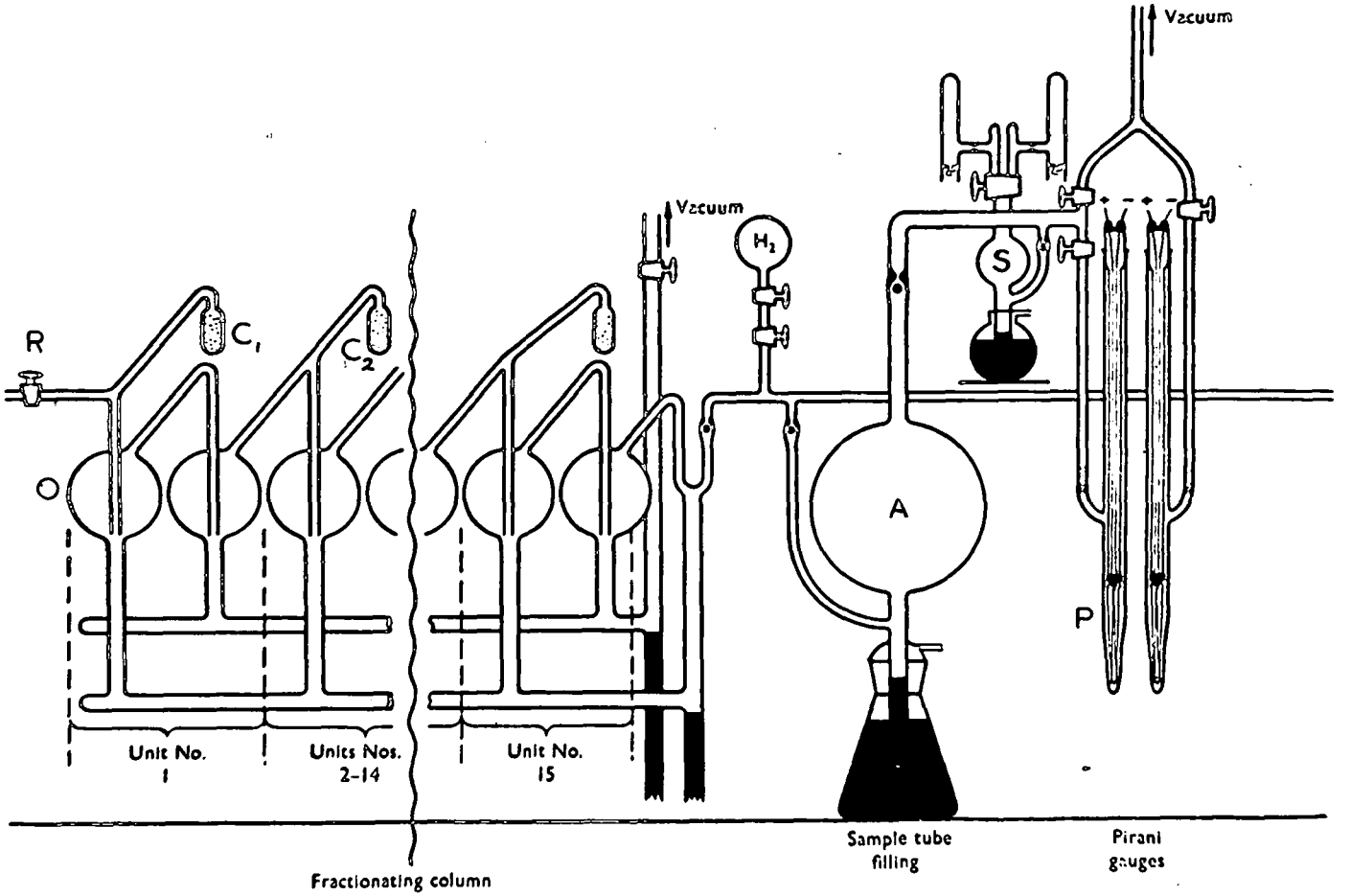

Fractionating column and Pirani gauges.

in the front of the column is lowered just into the neck of the bulbs, the tube down the centre of the bulb is opened to the bulb and the helium and neon present equilibrate themselves between the gas phase and the solid phase --- about 75% helium in the gas volume, about 25% on the charcoal, with about 25% neon in the gas space and about 75% on the charcoal. The mercury in the front of the column is then raised, compressing the helium and neon into the side tube, and the mercury in the back of the column lowered, allowing the gas to expand into the first of the rear bulbs. The back mercury is then raised, compressing the gas into the second side tube and bringing it into contact with the second charcoal tube C_2.

This is one complete operation. When the front mercury is lowered again, the gas in the second charcoal tube again equilibrates itself with the gas volume so that 75% of the neon is retained, while only 25% of the helium is held, and the cycle is repeated.

However, on the second lowering of the front mercury, the helium and neon which was left behind on the first charcoal will again distribute itself between the volume space and the charcoal, so that 75% of the remaining neon is retained and only 25% of the remaining helium. This gas is then transferred to the second charcoal and combined with the gas remaining there. Thus, as the column is continuously operated in this fashion, the total effect is that the helium is progressively taken forward through the column, while the neon is retained. The first amount of helium

expands past the ventil into the large storage bulb^{A} at the 16th operation, gradually rises to a maximum amount at the 23rd operation, and then tails off, as shown in Figure 28, so that 99.3% helium and 0.7% neon is collected up to operation 36. This is stored in the large bulb at the end of the fractionating column, of volume more than one litre, so that, when the mercury is raised to compress the gas into the pirani gauge, only about ½% of the gas is left in the dead space tubing.

To save unnecessary operations in fractionating the neon, the first Dewar flask on the column is lowered so that only the first charcoal tube, which is lower than the other three in the group, is immersed in the liquid nitrogen after operation 25, the last batch of helium having passed the fourth charcoal tube by this time. After the 29th operation, the second Dewar flask is removed altogether, the third after operation 33, and the last after operattion 36. This progressively releases the neon from the charcoal, so that a further 25 operations suffice to bring the neon through into the compression bulb.

For convenience, the fractionating column was made to operate automatically, so that it could be set to do any number of operations up to 27, and then switch itself off. This was achieved by having the air inlet and vacuum lead to the mercury reservoirs controlled by fine jets, opened or shut off by a rubber gasket attached to the bottom of a steel slug. The slugs could be lifted or lowered by means of solenoids, and the solenoids were coupled in pairs so that when the vacuum jet was open, the air jet

FIG. 30

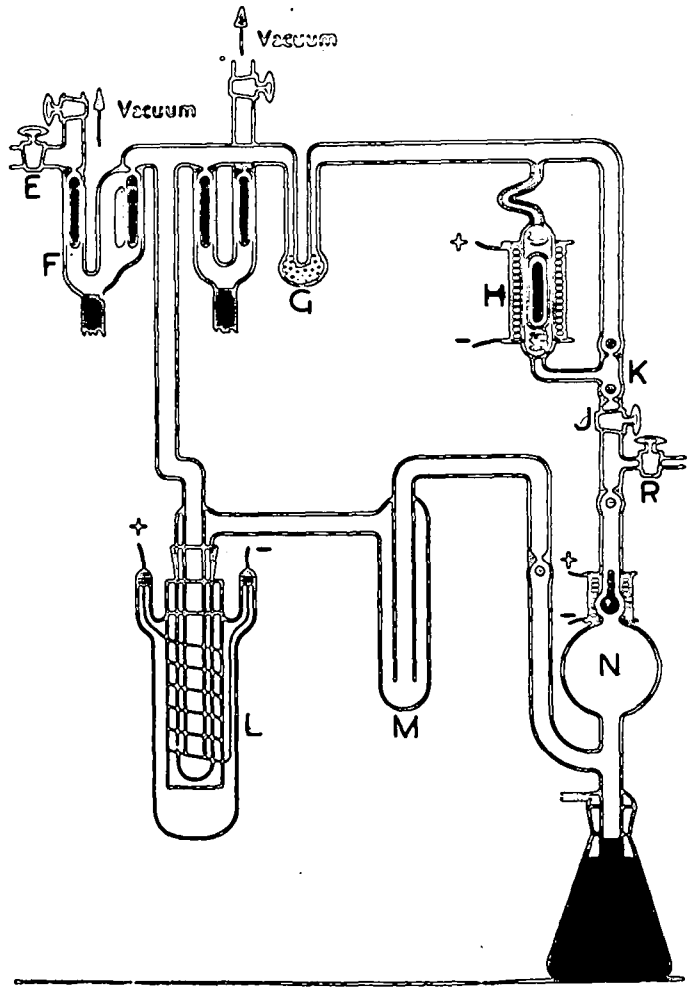

Palladium furnace and circulating system.

was closed, and vice versa. By controlling the two pairs of solenoids by means of two relays con-operated by a synchronous motor, which also drove a dial indicating the number of operations done, the column operation was made fully automatic.

(3) - The Circulating System (Fig.30).

The helium which is liberated from meteorites by acid dissolution will be accompanied by varying amounts of water vapour and hydrogen as well as other gases. The water vapour must be removed before passing the gases into the column, otherwise the narrow bore tube leading to the first charcoal unit would become blocked with ice, and the hydrogen must be removed, as this comes through the column almost as soon as the neon. The other gases, with the exception of helium and neon, will be retained at the first charcoal tube, together with the pure oxygen carrier.

Thus a few mms. pressure of pure oxygen are let into the dissolving vessel from a reservoir, and this is flushed onto the charcoal tube G (Fig.30) which is cooled in liquid nitrogen, carrying the major part of the helium and other gases with it. The mercury in the ventil F is kept raised just above the bend to act as a non-return valve to prevent back diffusion of helium. This process is repeated six times, which is sufficient to carry the helium quantitatively into the circulating system. The water trap M is kept cooled all the time. The ventil F is then closed, and the liquid nitrogen removed from the charcoal U tube.

The Palladium furnace L is then heated, and the gases circulated past it for 30 minutes by means of the circulating

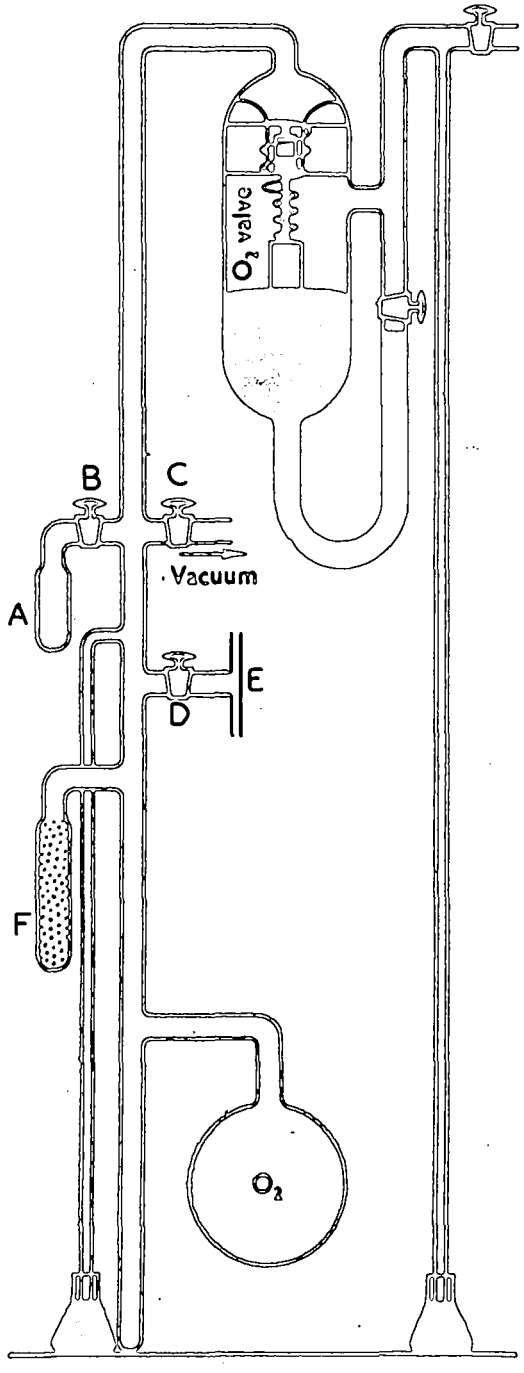

Oxygen reservoir.

FIG. 31

pump H to remove the last traces of hydrogen.

The circulating pump is comprised of a small steel slug encased in a glass jacket, which fits inside the outer tubing with the minimum of clearance. The steel slug and jacket are made to rise and fall by means of the solenoid, so that the gases are drawn steadily past the two non-return ball valves K. The water vapour is trapped out at the same time. The tap J is then closed and the tap R opened, and the gas from the circulating system is toplered into the first charcoal tube of the fractionating system (Fig. 29).

(4) Production of Pure Oxygen.

Oxygen gas, free from helium and neon, is needed to act as a carrier gas for the small amounts of helium and neon involved in meteorite analyses and stratospheric air investigation, and also to burn the last traces of hydrogen when acid dissolution of iron meteorites is used.

Originally, the gas was prepared by decomposing hydrogen peroxide by means of platinum black, but the reaction is not controllable, since the peroxide decomposes spontaneously under vacuum, and more important, in the presence of the hydrogen peroxide solution, the vapour pressure in the system cannot be reduced below a few mms. of mercury, so that the air adsorbed on the glass wall cannot be rigorously pumped away, even over a long period.

Instead, commercial cylinder oxygen was used and purified in the system shown (Fig.31).

The whole system is first rigorously evacuated, and the charcoal in the tube F baked for about one hour at 200°C. The oxygen cylinder is then connected to the T piece E by rubber tubing, a glass tube dipping into the flask of mercury connected to the other limb and the oxygen turned on so that the T piece is well flushed out and the oxygen bubbles continuously past the mercury. After a few minutes the tap D is cautiously opened, so that oxygen passes slowly into the reservoir system, maintaining the oxygen pressure in the rubber tubing to prevent air leaking in When the system contains oxygen to atmospheric pressure, the tap D is closed, the major part of the oxygen is liquified in the trap A by means of liquid nitrogen, the tap B is closed and most of the remainder of the oxygen is adsorbed on the charcoal, using liquid nitrogen, until a pressure of only a few mms. mercury is left in the system. The tap C to vacuum is then opened, and the residual gas, containing the major part of the helium and neon is pumped away for about 5 minutes. The tap C is then closed, the liquid nitrogen removed from the charcoal tube, and when this has warmed up the tap B is opened and the liquid oxygen allowed to boil off. The whole process is repeated about six times, and the helium and neon are thus fractionated away, leaving the reservoir full of helium-and-neon-free oxygen at a pressure of only two or three centimeters below atmospheric pressure.

A sample of the purified oxygen is then passed through the fractionating column, about ten times larger in quantity than is actually used in an experiment, and if any trace of helium or

neon is found, the process is repeated again until the oxygen in the reservoir is of satisfactory quality.

It was also found that once the oxygen was freed from helium and neon to this extent, it would remain pure for several months at least, contrary to previous information (8).

Section 2. - Specimen Experimental Calculation.

A typical experimental calculation for a stratospheric air experiment is given below.

Bottle B - 8.

1. Original air volume in air pipette. Pressure:0.610cms.T.19.1°C. (pipette volume 8.349 ccs).

2. After 1st heating of copper spiral. Pressure:0.562cms.T.19.1°C. (20 mins.)

3. After 2nd heating of copper spiral. Pressure:0.562cms.T 19.1°C. (5 mins.)

Therefore: O_2 % is 7.70.

Nitrogen plus Argon volume left = $\frac{0.562}{76} \times 8.349 \times \frac{273}{292.1}$

= 0.05772 ccs N.T.P.

Pure helium from calibration pipetting system.

McLeod pressure 2.566 cms. at volume Mk. II (0.3677 ccs).

This means that $2.566 \times 0.3677 \times 8.6567 \times \frac{273}{294.3} \times 10^{-7}$ ccs N.T.P.

of helium will be delivered by the pipette,

= 7.550×10^{-7} ccs N.T.P.

Galvanometer Deflections.

Reading I (Δ_{c_1})	8.97 cms.	Average + 1% = 9.00 cms.
Reading II (Δ_{c_2})	8.85 cms.	

Therefore sensitivity of gauges to helium (on sensitivity range 10) $= \frac{2.550 \times 10^{-7}}{9.00}$ ccs/cms

$= \underline{8.389 \times 10^{-8} \text{ccs/cms.}}$

Galvanometer Deflection from Operations 16-36 (Δ_{16-36}) = 927 cms.

∴ Helium amount $= 9.27 \times 8.389 \times 10^{-8}$ ccs.

B-8 Helium in % of Nitrogen plus Argon volume $= \frac{9.27 \times 8.389 \times 10^{-6}}{0.05772}$

$= \underline{13.47 \times 10^{-4}\%}$

Ground level Helium in % of Nitrogen plus Argon volume $= \underline{6.636 \times 10^{-4}\%}$

Therefore, ratio $\frac{(He)}{(N_2+A)}$ Strat. / $\frac{(He)}{(N_2+A)}$ ground level $= 2.029.$

=====

Pure Neon delivered from calibration pipetting system. =

$2.586 \times 5902 \times 8.6567 \times \frac{273}{294.1} \times 10^{-7}$ ccs.

$= \underline{12.27 \times 10^{-7} \text{ccs N.T.P.}}$

Calibration Deflection (Neon).

(Δc_1)	10.495 cms.	Average * 2% = 10.471 cms.
(Δc_2)	10.275 cms.	
(Δc_3)	10.030 cms.	

∴ Sensitivity of Gauge to Neon (sensitivity range 10) $= \frac{12.27 \times 10^{-7}}{10.471}$ ccs/cms.

$= \underline{11.71 \times 10^{-8} \text{ccs/cms.}}$

Galvanometer Deflection for Operations 37-6I ($\Delta_{37\text{-}6I}$) = I3.44 cms.

$\therefore$ Neon amount = $I3.44 \times II.7I \times I0^{-8}$ ccs

= $I57.5 \times I0^{-8}$ ccs N.T.P.

$\therefore$ Neon to Nitrogen plus Argon % (B-8) = $\frac{I57.5 \times I0^{-4}}{5.772}$

= $27.29 \times I0^{-4}$ %

Ground level Neon to Nitrogen plus Argon ratio: = $22.94 \times I0^{-4}$ %

$\therefore$ Neon ratio $\left(\frac{\text{Stratosphere}}{\text{Ground level}}\right)$ = I.I86

Argon.

Pressure of original air sample in pipette. = 0.695 cms. T. I9.2°C.

Air vol. = $\frac{0.695}{76} \times 8.349 \times \frac{273}{292.2}$

= 7I.36 μLitres.

Pressure after O_2 removal = 0.649 cms. T. I9.2°C.

Vol. after O_2 removal = 66.62 μLitres.

i.e. O_2 % is 6.7

Measuring McLeod reading of Argon. = 0.695 cms. P at 2I° C.

0.695 x I.005 = 0.698

(The I.005 is the correction applied for pressure in the open limb of the McLeod gauge due to Argon left in the dead space.)

Now, from the calibration curve of the McLeod gauge closed limb, 0.698 cms. press., is equivalent to 0.695 μLitres volume.

∴Argon % of Nitrogen plus Argon volume (B-8) $= \frac{69.5}{66.62}$

$= \underline{I.043\ \%}$

Argon % of Nitrogen plus Argon volume(Ground level) $= \underline{I.I79\ \%}$

Argon ratio $\frac{\text{Stratosphere}}{\text{Ground level}} = \underline{0.886}$

*N.B. The I% addition for two readings, or the 2% addition for three readings, is made to allow for the small decrease in the amount of helium or neon delivered from the pipetting system with each successive delivery. This correction has been worked out from the known volumes of the pipette components.

In addition, it will be noted that the above readings for sample B-8 were worked out using the ratios of He, Ne, and A respectively to (N_2 + A). When it was observed with the first two samples, B-6 and B-8, that some depletion of Argon was occuring, the results were corrected to give He, Ne, and A ratios to N_2 only, and subsequent results were worked out on this basis.

- Appendix -

A P P E N D I X

+=+=+=+

Special Investigation of the Beddgelert Meteorite.

(a) Introduction.

The Beddgelert meteorite was one of special interest, since it was the most recently observed fall in this country. Details of its fall are given in a published paper (6I). Before entering the Earth's magnetic field, a meteorite will be exposed to the full force of the cosmic radiation; it is to be assumed that under its impact a certain number of atoms in the meteorite will

be disintegrated, with the production of some radio-active nuclides. A rough calculation shows that any radio-activity thus produced can only be feeble, but it did seem worth while testing a meteorite shortly after its fall to find whether it displayed a measurable activity additional to that due to its uranium and thorium content.

The first measurements were made with a β-ray Geiger-counter elevn days after its fall, with the following results:-

Background. 13.2, 13.6 c.p.m.

Meteorite. 14.2, 13.6, 14.5 c.p.m.

The following day a piece of magnetite of similar shape and size was measured for activity and gave:

14.2, 14.5, 14.2, 13.8 c.p.m

The next day we repeated the meteorite measurements with greater precision:-

Background	12.3± 0.5	c.p.m.
Meteorite	13.7± 0.3	c.p.m.
	13.7± 0.5	c.p.m.
Background	13.7± 0.5	c.p.m.

The figures show that 11 and 13 days after its fall no detectable β-activity was present.

(B) Separation of Stone and Iron Phases.

The meteorite is classed as a black, crystalline chondrite, the small iron inclusions forming 18% by weight of the meteorite, the rest being stone. It was decided to do independent age determinations on the two phases, and for this reason, the stone and iron phases had to be separated.

First of all, preliminary experiments were carried out to see how much helium was released from the stone phase by heating alone in vacuo at about 400°C. From later results, it was found that only about 10% of the helium was released by this method.

The separation of the stone and iron phases was achieved by taking about 2 grms. of Bethlegert and crushing it thoroughly in an agate mortar and pestle. The powder and small iron nodules were then sieved in a geological sieve, when it was found that various sizes of iron nodules were separated out by the different sieves, and a very fine powder, with extremely small iron fragments, was left. The iron nodules were retained for measurements of the helium content of the iron phase, and the powder was subjected to magnetic separation, which extracted a small quantity of iron particles and left an entirely non-magnetic stone phase for helium determinations.

(c) Helium Determination on Iron Phase.

The method of acid dissolution of the iron nodules was exactly the same as that used before. Any small grains of silicate phase which had been ground into the iron nodules during the powdering process were washed out of the flask after the dissolution of the iron, and were weighed so as to allow a correction to be applied to the weight of iron initially taken

(d) Helium determination of Stone Phase.

The method of releasing the helium first tried was to break off a small piece of the meteorite, powder it in an agate mortar and pestle, sieve out the iron pieces, and heat the powder alone

to 800°C in a platinum furnace in vacuo.

The first two results obtained were :

5.36 x 10^{-6}ccs/grm heated for one hour.

4.450 x 10^{-6}ccs/grm heated for 3½ hours.

Since these two figures were not in good agreement, it was thought that some helium might be leaking away during the powdering process, so that next, helium determinations on small solid pieces were tried, without powdering.

Results.

Sample 1.

(a) 1.258 x 10^{-6}ccs/grm - heated for 8 hours at 800°C.

(b) same sample reheated for another four hours gave 0.684 x 10^{-6} ccs/grm.

(c) same sample heated for another 4½ hours at 850°C gave 0.47 x 10^{-6} ccs/grm.

(d) same sample reheated at 850°C for 3 hours gave no more helium.

This brought the total of helium for this sample after 19½ hours heating to: 2.413 x 10^{-6}ccs/grm.

Sample 2.

(a) 1.535 x 10^{-6} ccs/grm - 3 hours heating at 900°C

(b) 0.538 x 10^{-6} ccs/grm - 2 hours more at 900°C

(c) no more helium after 1 hour more at 900°C

Total: 2.073 x 10^{-6} ccs/grm.

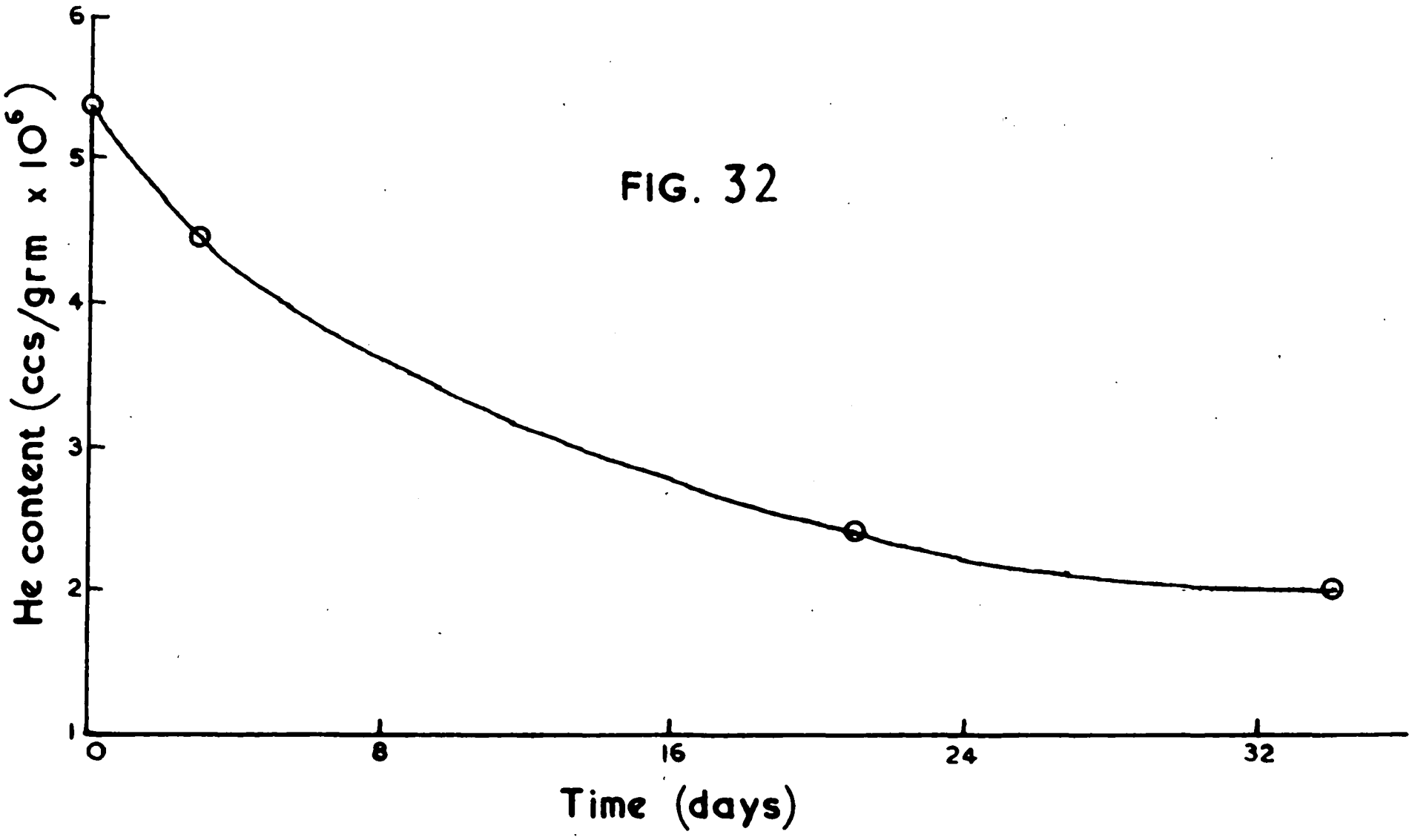

FIG. 32

Since these four results were progressively lower each time, it seemed that the meteorite might be losing helium fairly quickly, as the above series of determinations were done within four weeks. Moreover, plotting the results, a graph of the form given in Figure 32 was obtained.

It was therefore decided to find out if the meteorite was losing helium. Two bulbs with a tap and ground glass cone so that they could be fitted straight on to the apparatus, were made as nearly alike as possible. A quantity of the meteorite composed of several small fragments and about four times as much as normally used, for a determination, was introduced into one bulb, which was then rigorously evacuated for ½ hour, the tap closed, and a quantity of mercury poured down into the tube above the tap to prevent the tap leaking air across it. The other bulb was left empty, evacuated and sealed in exactly the same manner. Both bulbs were left to stand for 14 days. On determining the amounts of helium in both, the results were:-

(1) Bulb containing meteorite sample, 2.5×10^{-8} ccs helium.

(2) Empty bulb 3.8×10^{-8} ccs helium.

Thus, it seems that the meteorite could not be leaking helium at room temperature, and the larger figure for the blank bulb is probably due to the fact that it was a little larger than the other one with therefore a larger surface area.

It was now decided to try the effect of using a flux to bring the stone phase into solution. A small platinum thimble was made with a long platinum wire attached, so that the meteorite sample

and flux could be put into the thimble and lowered into the bottom of the platinum furnace as shown in Fig.33.

A.R. Potassium hydroxide pellets were used as flux, and a preliminary experiment on the flux alone showed that it contained no helium. About 0.05 grms. of powdered meteorite was used for each determination, with 4 pellets of KOH as flux, and was heated for 3 hours at 850°C.

Results. He content in 10^{-6} ccs/grm.

(1) 75.740

(2) 4.837

(3) 17.230

(4) 16.010

(5) 14.210

(6) 30.720

Average: 26.8 x 10^{-6} ccs/grm.

It was obvious that there was some inhomogeniety of sampling with the method so far used, which was just to use a small chip of the meteorite, taken at random from any part of the meteorite -- about 0.05 grms., powder it, and use it for a determination. It was thus decided to take the residual powder from the method used to separate the iron and stone phases, and do a determination on this.

About 1.5 grms. of powder, entirely non-magnetic, and finely ground, was left, so a portion of this was taken by the "coning and quartering" method, and gave the following helium content: 40.26 x 10^{-6} ccs He/grm.

Parts of the work for this thesis have already been published in the following papers.

1. Chackett, K.F., Golden, J., Mercer, E.R., Paneth, F.A., and Reasbeck, P., Geochim. et Cosmochim. Acta, 1950, 1, 3.

2. Chackett, K.F., Paneth, F.A., Reasbeck, P., and Wiborg, B.S., Nature 1951, 168, 358.

3. Paneth, F.A., Reasbeck, P., Mayne, K.I., Geochim. et Cosmochim. Acta 1952, 2, 300.

4. Paneth, F.A., Reasbeck, P., Mayne, K.I., Nature 1953, 172, 200.

5. Chackett, K.F., Reasbeck, P., Wilson, E.J., Geochim. et Cosmochim. Acta 1953, 3, 261.

6. Reasbeck, P., Wiborg, B.S., Report of the Oxford Conference on upper atmospheric rocket exploration Aug. 1953 (Pergamon Press) In the press.

7. Dalton, J.C., Reasbeck, P., Thomson, S.J., and Mayne, K.I., Nature. In the press.

FIG. 34

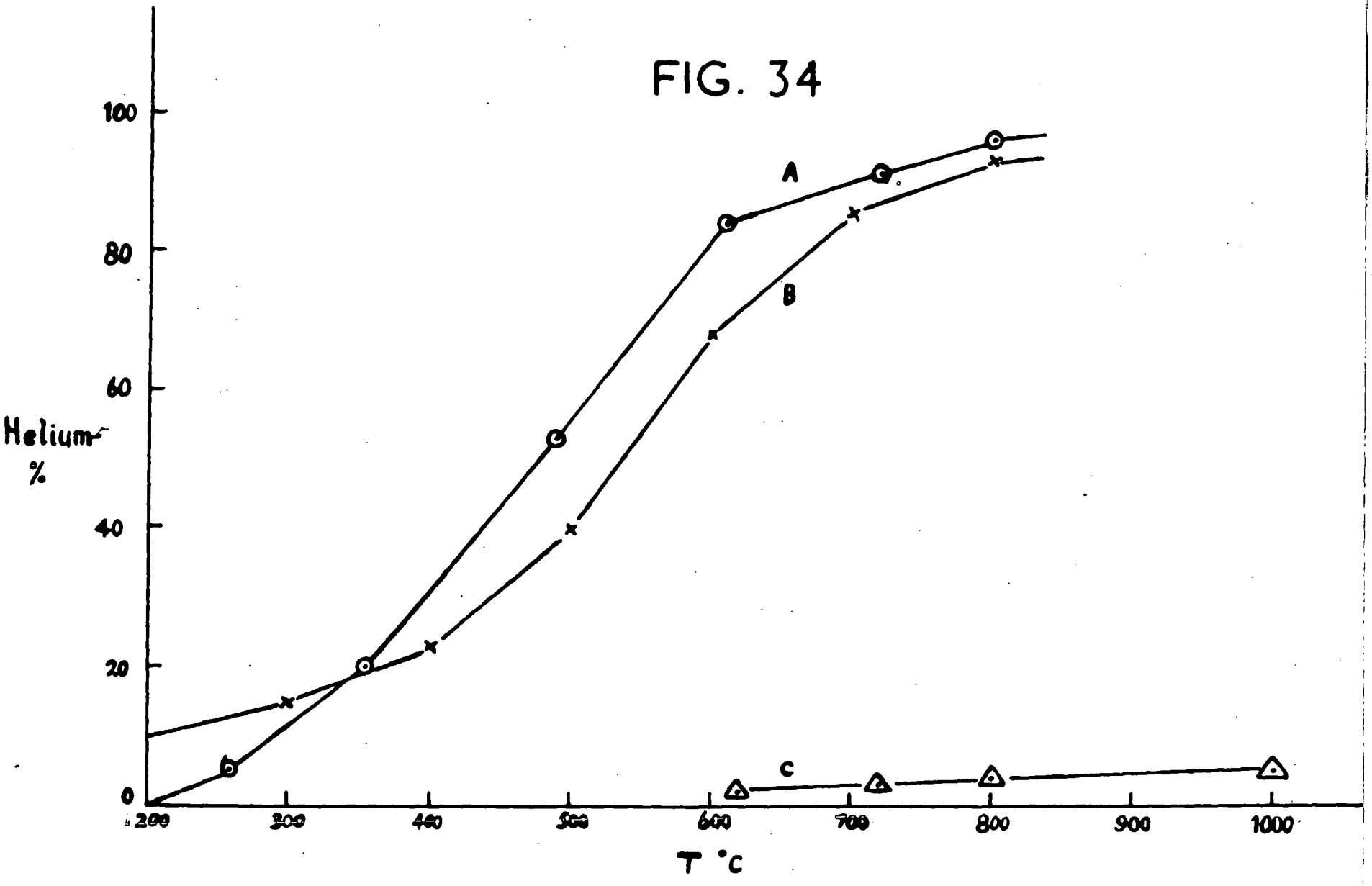
100
80
60
40
20
0
Helium %
A
B
C
200
300
400
500
600
700
800
900
1000
T °C

The next experiment undertaken was to investigate how the helium release with rise in temperature compared with that for a stone meteorite, and an iron meteorite. Accordingly a sample of 0.15 grms. weight was broken off the meteorite, crushed up, though not too finely powdered, and inserted into the furnace. It was then heated in stages of 100°C difference in temperature for three hours at a time, with no flux, to find out what % of helium is released at each temperature up to 800°C. Finally six KOH pellets were introduced, and the whole heated for two hours at 800°C to release the last traces of helium.

Results. T A B L E 34.

Temp.°C.	He in 10^{-6} ccs/grm	% at Temp. concerned	Total %.
300	2.202	14.890	14.890.
400	1.186	8.026	22.916
500	2.487	16.830	39.746
600	4.193	28.360	68.106
700	2.570	17.390	85.496
800	1.140	7.713	93.209
Flux 800	1.000	6.766	100.
Total:	14.778		

The results are plotted in Figure 34.

Explanation of Fig. 34.

Percentage loss of helium. (3 hours heating at each stage).

Curve A: Stone Meteorite - Pultusk.

Curve B : Stone Meteorite - Beddgelert.

Curve C : Iron Meteorite - Mount Ayliff.

It is obvious that the curves A and B are closely similar, so that Beddgelert loses helium at about the same rate as Pultusk, although the former is much harder than the latter. The higher helium loss for Beddgelert at low temperatures may be due to the differential expansion of the iron and stone opening up micro-cracks which allow some of the helium to escape more readily.

Summary of Results.

Iron Phase.

The iron nodules were graded into five different sizes by the five different meshes in the geological sieve, and there seemed to be some difference in helium content between the various sizes of nodules. Thus, for example, the results obtained were:

	He content in 10^{-6} ccs/grm.
1. Largest size nodules	1.90
2. Largest size nodules.	2.02
(3) Second size nodules	5.30
(4) Second size nodules	4.20
(5) Third size nodules	1.65

Lack of time prevented any further experiments being done on the different sized nodules, and the helium figure was averaged out over the whole weight of the separated iron phases, giving 2.86×10^{-6} ccs/grm as the helium content of the iron phase. It may be that the variation in the helium content of the different

sized iron nodules represented a different concentration of Uranium and Thorium in the various nodule sizes but more work would have to be done before the apparent variation could be confirmed.

Stone Phase.	He content in 10^{-6} ccs/grm.
Experiment 1 ;	75.740
" 2:	4.837
" 3 :	17.230
" 4 :	16.010
" 5 :	14.210
" 6 :	30.720
" 7 :	40.260
" 8 :	14.778

Avcrage: 26.7×10^{-6} ccs He/grm.

Table 35 gives the values of the helium, uranium and thorium contents for both the phases, and the derived ages, assuming all the helium to be radiogenic.

T AB L E 35.

	He in 10^{-6} ccs/grm	U in 10^{-8}g/g.	Th in 10^{-8}g/g	Ages (calculated from total He) in 10^{8} years.
Metal Phase	2.8	9.1 ± 1	8.5 ± 4.9	2
Silicate phase	26.7	10.8 ± 2.7	39 ± 8	10

While the helium determinations were done on samples of 30 or 40 milligrams, and the uranium and thorium analyses on 20 or 30 gram samples, the helium results are averages of several

determinations, and it is therefore fairly safe to use the figures for age calculations. Ideally, it would be best to determine the helium, uranium and thorium contents of one and the same sampl but this presents difficult problems from the point of view of dissolving agents in the case of iron meteorites, since acid dissolution of the large amounts of irons necessary for thorium analyses would require a very large dissolving vessel and would also generate many litres of hydrogen which would be troublesome to remove; and potassium-cupric chloride, which generates no hydrogen, is not satisfactory from the point of view of radio-chemical purity. However, from the above figures, it seems that the ages of the two phases are widely different: the age of the silicate phase being about five times the age of the iron phase. This calculation neglects the cosmogenic Helium production found later, but this factor will merely alter the absolute age values, while the large difference will still be present, since the production of helium in stone and iron by cosmic rays is thought t be very much the same.

Further, work is at present under way on the pallasite "Brenham Township", the age of the silicate phase is being determined independently with the "Potassium-Argon" method by Dr. E.J.Thomson, of this laboratory, and the ages of the silicate and iron phases are being determined with the "Helium Method" by the writer. Preliminary results seem to indicate that in this meteorite, also, the stone phase is considerably older than the iron phase.

+=+=+=+=+=+

B I B L I O G R A P H Y

1. Paneth, F.A., and Peters, K. - Z.Phys.Chem. 1928. 34. 353.

2. Paneth, F.A., and Urry, W.D. - Mickrochem. Emich Festschrift. 1930. 233.

3. Paneth, F.A., and Urry, W.D. - Z.Phys.Chem. A. 1931. 152. 110 and 127.

4. Arrol, W.J., Jacobi, R.B., Paneth, F.A. - Nature. 1942. 149. 235

5. Glückauf, E., Paneth, F.A., -Proc. Ray.Soc. A.1945. 185. 89

6. Chackett, K.F., Paneth, F.A., Wilson, E.J., - Nature. 1949. 164. 128.

7. Chackett, K.F., Paneth, F.A., Wilson, E.J., - J.Atmos. & Terr. Phys. 1950. 1, 49.

8. Wilson, E.J., - Ph.D.Thesis. Durham. 1950.

9. Jacobi, R.B., - Ph.D.Thesis. Durham. 1942.

10. The Rocket Panel - Phys.Rev. 88, 1027. 1952.

11. Chapman, S. - Compendium of Meteorology, American Meteorological Society. 262. 1952

12. Hermann, R. - Comptes Rendus. 1948. 226. 1712.

13. Epstein, P.S. - Gerl.Beitr.Z. Geoph. 35. P.153. 1932.

14. Frieke, R., and Kubach, J. - Z.Electrochem. 1949. 53. 76.

15. Gunther, P.L., Paneth, F.A., - Z.Phys.Chem. A.1935. 173. 401.

16. Progress Report No.5 - U.S.Army Signal Corps., Engineering Research Institute, University of Michigan. Sept.1950 - Dec.1951 - P.11.

17. McQueen, J.H., - Phys.Rev. 80. 100. 1950.

18. Armbruster, M.M., Austin, J.B., - J.A.C.S., 66. 159. 1944

19. Paneth, F.A., - J.C.S. Sept, 1952. 3651.

20. Halstead, R.E., Nier, A., - Rev.Sci.Instr. - 28. 1019. 1950.

21. Barnard - Modern Mass Spectrometry. P.112-115.

22. Paneth, F.A., - Occ.Notes. Ray.Astron.Soc. 5. 57. 1939.

23. Paneth, F.A., - Gehlen, M., Peters, K., Z. A_{norg} .Chem. 175. 383. 1928.

24. Chlopin, V., Herling, E., Joffe, E., - Nature (1934). 133. 28.

25. Bauer, C.A. - Phys.Rev. 72. 354. 1947.

26. Bauer, C.A., - Phys.Rev. 74. 225. 501. 1948.

27. Huntley, H.E., - Nature. 151. 356. 1948.

28. Prior, G.T., - Catalgue of Meteorites, British Museum. 1923. p.177.

29. Treadwell, F.P., - Analytical Chemistry. Vol.2. p.363.

30. Lattes, C.M.G., - Occhialini, G.P.S., - Powell, C.F., - Nature. 1947. 160. 453.

31. Martin, G.R., - Geochimica et Cosmochimica Acta. 1953. 3. 288.

32. Camerini, U., Fowler, P.H., Lock, W.O., Muirhead, H., - Phil.Mag. 1950. 41. 413.

33. Jacobsen, M., Schulz.A., Steinberger, J., - Phys.Rev.1951. 81. 89

34. Ney, E.P., Thon.O.M., - Phys.Rev. 1951. 81. 1069.

35. Peters, B., -"Progress in Cosmic Ray Physics." p.232. 1952.

36. Hilberry, N., - Phys. Rev. 1941. 60. 1.

37. Haber-Schaim, U., - Phys.Rev. 1951. 84. 1199.

38. Van Allen, J.A., - Singer, S.F., - Phys.Rev. 1950. 78. 819.

39. Neher, H.V., in "Progress in Cosmic Ray Physics." p.301 (North Holland Pub.Co., Amsterdam. 1952).

40. Winckler, J.R., Stix, T., Dwight, K., Salim, R, -Phys.Rev. 1950 79. 656

41. Jánossy, L., - Z.Phys. 1937. 104. 430.

42. Von Klüber, M., - Mon.Not.Ray.Astr.Soc. 1951. 111. 2.

43. Brown, R.R, - Phys.Rev. 1952. 87. 999.

44. Cool, R.L., Piccioni, O., - Phys.Rev.1952, 87. 531.

45. Camerini, U., Fowler, P.H., Lock, W.O., Muirhead, H. Yekutieli, G., - Rep.Prog.Phys. 1951. 14. 247.

46. Camerini,U., Lock,W.O., Perkins,D.H. - Progress in Cosmic Ray Physics. 1952. p.11

47. Wilson,I.G., - "Progress In Cosmic Ray Physics". Fig. 4. p.11. 1952.

48. Le-Couteur,K.J., - Proc.Phys.Soc. A.63 259. 1950.

49. Brown,R.M., Camerini,U., Fowler,P.H., Meitler,H., - Phil.Mag. 40. 862. 1949. King,D.T., Powell,C.F.

50. Le Conteur,K.J., - Proc.Phys.Soc. - 1950. A.63. 259.

51. Chackett,K.F., Reasbeck,P., Wilson,E.J., - Geochimica et Cosmochimica Acta. 1953. 3. 261.

52. Martin,G.R., - Geochimica et Cosmochimica Acta. 1953. 3. 304.

53. Experimental Nuclear Physics - 1. 222. 1953.

54. Wilson,J.G., - Prog. in Cosmic Ray Physics - p.223. 1952.

55. Dalton,J.C. - Ph.D.Thesis - Durham - 1953.

56. Hey,M.H. - 2nd Appendix - British Museum Catalogue of Meteorites. 1940. p.50.

57. Ready,J., - Nature, 1939. 44. 1046.

58. Baade,W., Zwicky,F., - Phys. Rev. 1934. 45. 138.

59. Hoyle, F. - Mon.Not. Roy.Astr.Soc. 1946 - 106. 384.

60. Science News Letter - 63. 19. 242. 64. p.p.147. 166. 1953.

61. Chackett,K.F., Golden,J., Mercer,E.R.,Paneth,F.A.,Reasbeck,P., - Geochimica et Cosmochimica Acta. 1950. 1. 3.

62. Wylie,C.C., - Pop. Astron. 47. 291. 1939.

63. Goldschmidt, V.M., - Det. Vidonskaps.Akad. i Oslo. 1. Mat - NaturV. Klasse. 1937. No.4

64. Brown,H.S., Patterson,C., - J. Geol. 56. 85. 1948.

65. Brown,H.S. - Rev.Mod.Phys. 21.625. 1949.

66. Urey,H.C. - Geochimica et Cosmochimica Acta. 2. 269. 1952.

+=+=+=+

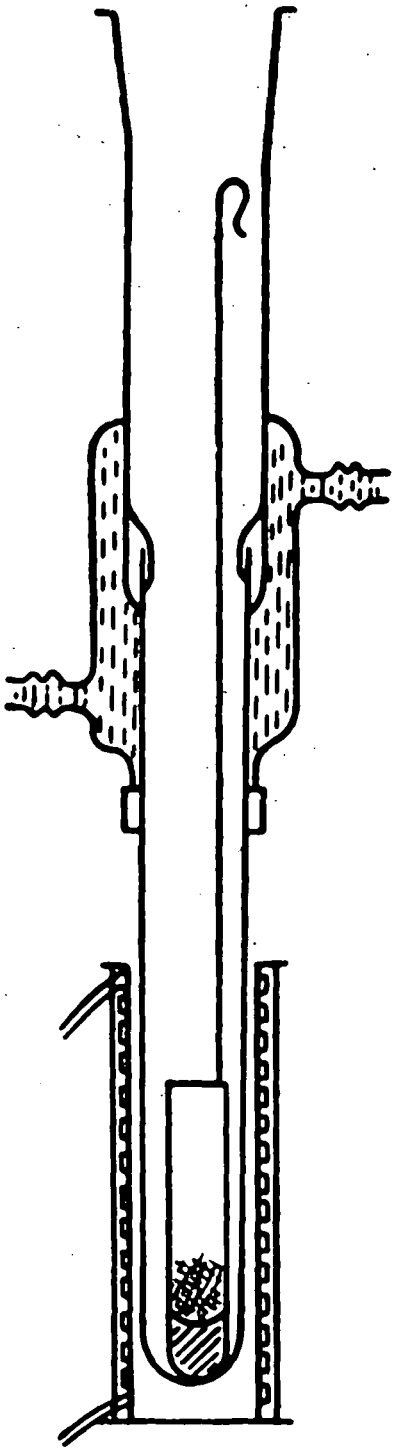

FIG. 33